ABSTRACT

MULLA, MOHAMMED A. Development of a Portable Mini Dynamic Penetration and Torque Devices (MDPT and MDPT-t) and its Application to Estimate Engineering Properties of Soils. (Under the direction of Dr. Mohammed A. Gabr and Dr. M. Shamim Rahman)

Understanding soil strength and other engineering properties are essential for the adequate design and analysis of foundations, particularly when assessing the load-carrying capacity of the underlying in-situ soil during design and construction. The engineering foundation design relies primarily on in-situ and laboratory soil testing to determine soil properties. Currently, no portable, manual or automatic, economical, and easy-to-use field device exists that can measure these properties to depths of 45 ft (13.7 m) and verify bearing capacity during construction without auguring holes. This paper presents the development of a new and portable Mini Dynamic Penetration Test (MDPT) and examines the direct and indirect relationship between the penetration resistance MDPT-n value and the standard penetration test SPT (N), cone penetration test (CPT), tip resistance (q_t), and dry density γ_d. This paper also evaluates the relationship between the MDPT-n blows per ft, the MDPT-t torque generated from the rotation of the cone using a torque wrench with soil shear strength, and CPT sleeve friction (*fs*).

The MDPT was tested in 14 counties from the Coastal region (CR) and the Piedmont region (PR) of the state of North Carolina. The analyses of the data collected show a strong correlation between the measurements from the SPT (N), CPT q_t, and *fs*, dry density, and the MDPT-n blows per ft and MDPT-t measured torque. In addition, in-situ test results from the MDPT indicate that soil properties can be estimated from portable dynamic penetration test data without the use of heavy and costly drill rigs or trucks. The MDPT can also be used to evaluate

subgrade and soil-layer strength and estimate soil properties using correlations with other in-situ testing methods.

Comprehensive testing was conducted to evaluate the MDPT's correlations and to estimate the reliability and repeatability of the soil properties. The CPT, SPT, unit skin friction *fs,* and dry density γ_d correlations were analyzed and the results were encouraging, demonstrating reliable MDPT correlations. The test results show that the MDPT-n will produce three to five blows/ft for each SPT (N) blow/ft. On average, the correlation shows that MDPT-n approximately = SPT (N)*4. The correlation results, data analysis, and related information are presented in this study.

Overall, the results indicate the MDPT is a very useful device for design engineers and is capable of providing valuable soil properties quickly and more economically. Due to its behavior (generating skin and tip resistance) and its multiple applications, the MDPT tool is superior to similar devices that can quickly verify the accuracy and quality of the in-situ SPT and CPT results.

Development of a Portable Mini Dynamic Penetration and Torque Devices (MDPT and MDPT-t) and its Application to Estimate Engineering Properties of Soils

by
Mohammed A. Mulla

A dissertation submitted to the Graduate Faculty of
North Carolina State University
in partial fulfillment of the
requirements for the degree of
Doctor of Philosophy

Civil Engineering

Raleigh, North Carolina

2018

APPROVED BY:

_____	_____
Dr. Mohammed Gabr Co-Chair of Advisory Committee	Dr. Shamim M. Rahman Co-Chair of Advisory Committee
_____	_____
Dr. Akhtarhusein A. Tayebali	Dr. Murthy Guddati

DEDICATION

This dissertation is dedicated to my father and mother, and to my brothers and lovely sisters for their continuous love and support, both spiritually and financially. Without the financial support and encouragement of my younger brother Ahmad, achieving this goal would have been much harder. Furthermore, every phone call to my family was inspiring and motivated me to complete this Ph.D. degree. I know they will be very proud of this accomplishment for me.

This dissertation is also dedicated to my wife, who was very supportive and encouraged me to pursue my dreams. Also, to my sweetheart daughter Sarah and to my sons Laith and Maithem, whose love and support is both inspirational and motivating factors in my life.

I wrote the above dedication before the passing of my father. My father always had confidence in me, and always offered encouragement and support. I miss him every day, but I am happy to know he saw my journey through to its completion. He celebrated this accomplishment with me, and he was very proud of my achievement.

BIOGRAPHY

Mohammed Mulla moved from Kuwait to Montreal, Canada, to pursue a civil engineering degree. While waiting for an opening in Concordia University's civil engineering program, Mohammed enrolled for one semester at Concordia to improve his English. He then moved to the United States and enrolled in the civil engineering program at the University of North Carolina at Charlotte (UNCC). After graduating with a Bachelor's degree from UNCC, he worked for a small consulting firm to gain some experience. The following year he accepted a permanent position with North Carolina Department of Transportation in the soils and foundation design section. In 2009, Mohammed decided to pursue his goal to obtain a Master's degree in civil engineering from North Carolina State University (NCSU) while working full time. Mohammed was awarded his Master's degree in civil engineering in 2011. In 2012, with encouragement from his family, colleagues, and friends, he decided to pursue his Ph.D. in geotechnical engineering, under the guidance of Professor Mohammed Gabr and Professor Shamim Rahman.

ACKNOWLEDGEMENTS

I am truly grateful to many people for their advice, input, suggestions, encouragement, and support throughout this research study. I have been very lucky to have advisors such as Dr. Mohammed Gabr, Dr. Shamim Rahman, Dr. Akhtarhusein Tayebali, and Dr. Murthy Guddati for giving me valuable support, which gave me the opportunity to pursue my Ph.D. degree and allowed me to develop the portable MDPT device to assist and support the geotechnical and pavement community. It was only through their vision, guidance, encouragement, and mentorship that I can complete this dissertation. In addition to their extensive support in research and study, I deeply appreciate their friendship and continued mentorship.

I especially thank Dr. Gabr for supporting me when I accepted a leadership position at the North Carolina Department of Transportation (NCDOT). I still remember his advice to me: "Mohammed you will do great and you will select your best team to move forward, and do not worry about the few who are leaving". Dr. Gabr was correct—in my first year as a manager at NCDOT, my team and I saved more than $6,000,000 dollars by introducing and using foamed concrete (lightweight fill) in lieu of staged construction, temporary shoring, and a long construction waiting period. Also, I cannot thank Dr. Rahman enough for all of his continuous support.

I also express my sincere appreciation to the following people for their notable support and contributions:

- Dr. Roy Borden for his advice and continued support in my pursuit of a Ph.D. after his field visit inspecting the MDPT in action.
- Dr. Min Liu, for being part of my Ph.D. committee and for her valuable advice.

- Dr. Chris Chen from the NCDT Geotechnical Engineering Unit for his advice and suggestions in this research project.
- Mr. Scott Webb from the NCDT Geotechnical Engineering Unit for his assistance in field testing and for his many suggestions during the development of the MDPT.
- Mr. John Pilipchuk and Mr. Michael Wang from the NCDT Geotechnical Engineering Unit, for their continuous support.
- Mr. Mahdi Haeri, Mr. CK Su, and Ms. Suriyati Supaat from the NCDT Materials and Test Unit Geotechnical Lab for their unlimited support and vital assistance in the laboratory work and for the valuable experimental data applied in this research.
- All of my graduate school colleagues and friends who supported and encouraged me, including Dr. Mahdi Khalilzad, Dr. Mahdi Badoor, Dr. Amirhossein Norouzi, Dr. Zahra Ardabili, Dr. Jinfu Xiao, Dr. Zhangwei Ning, Mr. Ben Smith, and Mr. Arash Bozorgi. Thank you for your friendship and encouragement.
- A special thanks to my wife and children for their continued love and support, and for allowing me to spend many nights and weekends and nights away from them to complete this journey. I believe I have shown them that the only limit we have is ourselves, and that we can accomplish anything we want by setting goals and striving to achieve these goals one by one.
- I am particularly grateful to my father and mother for their dedication and support of my educational pursuits. They have always encouraged me to seek higher education, and even though my father never attended school, his support has been the driving factor in my pursuit of a Ph.D. I also greatly appreciate the support of my brothers and sisters, as their continued support has empowered me to go on this journey without any hesitation.

TABLE OF CONTENTS

LIST OF TABLES

LIST OF FIGURES

CHAPTER 1. INTRODUCTION

1.0 Introduction

In-situ penetration tests have been widely used in geotechnical engineering for site characterization for the analysis and design of foundations. The Standard Penetration Test (SPT) and the Cone Penetration Test (CPT) are the most widely used field testing procedures in the United States for foundation design and analysis. The CPT was invented in Holland in 1932 and introduced into U.S. practice more than 40 years ago (Schmertmann 1970). Early field operations used mechanical systems that collected two readings, cone resistance (q_t) and friction (f_s), at 7.87-in (200-mm) intervals. Data were recorded by hand, and the interpretation methods were based on limited knowledge and experience. Today, electric and electronic CPT systems are available in several sizes and cone tip configurations, and can provide three or more separate readings with depth, cone tip resistance (q_t), sleeve friction (f_s), and pore water pressure (u_2), usually taken at frequent vertical intervals between 0.4 in–0.8 in (10 mm–20 mm) (Lunne et al., 1997).

Robertson et al. (1986) proposed a CPT-SPT correlation where the ratio between normalized cone tip resistance (q_t/Pa) and N must be corrected to 60% energy ratio (N60). Kulhawy and Mayne (1990) extended the Robertson et al. (1983) correlation based on additional data that became available in the late 1980s, and developed an empirical equation for their updated SPT-CPT correlation. The SPT has an advantage due to the availability of a wide variety of soil parameters correlated to N-value data, and a soil sample is typically obtained with each test.

Dynamic cone penetrometers (DCPs) have been used in geotechnical applications for nearly 60 years. Different types and shapes of DCPs have been developed, such as the Scala

penetrometer, introduced in 1956, and the Sowers penetrometer, introduced in 1959. The DCP is used widely to evaluate pavement layers for pavement design such as base course material and subgrade soil. The DCP is performed by dropping a hammer from a certain fall height and measuring the penetration depth per blow for each tested depth. The DCP test is quick to set up, run, and evaluate on site, but it is designed to evaluate shallow soil layers at depths ranging from 4 ft–6 ft (1.2 m–1.8 m). In addition, the DCP has limitations with respect to its ability to evaluate the soil layers, and thus there is a great need to develop a simpler, more cost-effective procedure to determine in-situ parameters. Such a procedure will help geotechnical engineers conduct their analyses and designs using methods that are simpler and less equipment-intensive than SPT and CPT. This study reports the development of a portable Mini Dynamic Penetration Test (MDPT) to collect data on penetration resistance and skin resistance. The skin resistance is estimated using a torque wrench, as described and illustrated in Chapter 6.

The MDPT can be driven to a depth of 45± ft (13.7± m) below the ground surface with 5/8-in (160-mm) stainless steel rods extensions. The MDPT hammer configuration is designed to mimic the SPT tip and skin resistance behavior to produce 10% of the SPT total energy of 350 ft-lb (48.4 kg-m). The hammer consists of a 17.6 lb steel mass (7.98 kg) (hammer) falling 2 ft (609 mm) to develop 35 ft-lb (4.84 kg-m). Schematic sketches of the MDPT are provided in Chapters 1 and 7.

The MDPT can be operated manually or automatically using a gear-motor (shown in Chapter 7). The automatic MDPT consists of a 35-lb (15.88-kg) hammer falling 1 ft (300 mm) to develop 35 ft-lb (4.84 kg-m). Theoretically, the 140-lb (63.5-kg) SPT hammer dropped from 30 in (762 mm) should deliver 350 ft-lb (48.4 kg-m) of energy (140 lb x 30 in = 350 ft-lb) (63.5 kg x 0.762 = 48.4 kg-m) with each blow. Field testing indicated that the energy delivered to the rods

during an automatic SPT test can vary from 68%–94% of the theoretical maximum, with an average of 81%. SPT resistance values are normalized to 60% energy, because the correlations made before the advent of hammer-system calibration used safety hammers and the correlations made at that time are generally assumed to have been running at 60% efficiency. The normalization is made in design to compare resistance values to published correlations that were either assumed to be operating at or otherwise normalized to 60%. However, the measured field energy for this research is corrected to the standard 60% energy, and thus each blow will deliver (350 ft-lb x 0.6) = 210 ft-lb (48.4 x 0.6= 29 kg-m) to the sampler. Each blow count could be used as a unit measurement of delivered energy, in which one blow count equals 210 ft-lb (29 kg-m). The measured N value blows per ft (blows per 300 mm) is defined as the penetration resistance, which equals the sum of the number of blows required to drive the SPT sampler to a depth interval of 6–18 in (150–450 mm). The MDPT procedure will encompass the same effect of friction and other factors to reduce the delivered energy.

The main objective of this study is to correlate the MDPT n-value to the SPT N-value generated from an automatic hammer through the use of well-established empirical methods. Such a correlation is meant to take advantage of the vast database of empirical relationships as a function of N-value. Establishing the relationship between the MDPT-n data and the N-value can provide a cost-effective method for assessing key soil parameters in the field. The MDPT is currently used for projects with the North Carolina Department of Transportation (NCDOT) to confirm conditions during construction with previously conducted SPT data using automatic hammer, locate rock elevation, evaluate subgrade strength, and estimate soil properties.

1.1 Background

Most common in-situ tests are performed in conventional drilled borings, whereas specialized tests require a separate borehole or different insertion equipment. Field in-situ borehole tests can be grouped into three categories: correlation, deformation, and strength.

Correlation Tests

- Standard Penetration Test (SPT)
- Dynamic Penetration Test (DPT)

Deformation and Strength Tests

- Penetrometers, such as the Cone Penetrometer Test (CPT) and Piezocone
- Penetrometer Test (PQS)
- Pressuremeters (PMT) and Dilatometers
- Vane Shear and Borehole Shear Tests

For correlation tests, the obtained data may be correlated to several different design parameters such as relative density, angle of internal friction, and shear strength. The torque test is a direct measurement of the unit skin friction and can help in classifying the soil type.

To the author's knowledge, no portable, rapidly deployable instrument capable of reaching a depth of 45 ft (13.7 m) has been developed to drive deeper than the subgrade layers. Gabr et al. (2001) reported that widespread research has been performed to correlate the DCP to the California Rearing Ratio (CBR) and develop an empirical relationship. Abu-Farsakh et al. (2004) assessed the use of the DCP for quality control/assurance evaluation of pavement layers and embankments during construction. A summary of selected research studies that have correlated the DCP values to CBR, PLT, falling weight deflectometer (FWD) is provided in Chapter 2 Table 2.1.

The data points of the MDPT tests were compiled and organized for each geologic region. Comparisons between the MDPT blow counts (n) and the SPT blow counts (N) using an automatic hammer were made separately for the Coastal region and for the Piedmont region. It is assumed that the following factors affecting the SPT will be similar to those affecting the MDPT:

A. Variation in delivered energy (Robertson et al., 1983)
B. Equipment conditions
C. Both the SPT and MDPT are dynamic
D. Both the SPT and MDPT measure resistance based on vertical soil penetration
E. Both the SPT and MDPT have skin and tip resistance but not the same magnitude

Based on the correlation and calibration tables developed for MDPT and SPT tests, we can correct the SPT-N values based on the MDPT-n results adjacent to the SPT location. Development of site-specific correlations between SPT (N) values and the MDPT-n value can prevent many errors in design caused by using the wrong SPT (N) values. See Sabatini et al. (2002) and Phoon et al. (1995) for information on the variability associated with various engineering properties. Figure 4.3 in Chapter 4 page 56 shows the coefficient of determination R^2=0.92 and the correlation coefficient r=0.96 for the Piedmont region, R^2=0.93 and r=0.964 for the Coastal region, and the average for both regions of R^2 = 0.91 and r = 0.95. These indicate a clear relationship between the SPT- N values and the MDPT-n measurements.

Many researchers have performed correlations between SPT and soil properties, such as friction angle ϕ, unit weights γ, relative density Dr., and bearing capacity, among many others. Some published correlations are based on corrected N_{60} or $N1_{60}$ for overburden and hammer efficiency, and some are based on uncorrected (N) values. The designer must evaluate and study

the basis of the correlation and use either $N1_{60}$ or N as appropriate. In this study, Figures 4.3, 4.4, and 4.5, shown in Chapter 4, are used for the correlations between the MDPT-n, SPT (N), and the soil properties on the basis of the Standard Penetration Test SPT (N) values corrected ($N1_{60}$). Since the soil properties estimated from correlations tend to have greater variability than from measurements using laboratory performance data (Phoon et al., 1995), a minimum of 3–5 measurements from each geologic stratigraphy should be taken to estimate the soil properties.

1.2 Problem Statement

Evaluation of shallow foundations, proper compaction, bearing capacity, and soil properties are essential for foundation design and quality control during the construction of roadway projects. It is important to verify design parameters in the field for the spread footings to insure the soil has adequate strength to carry the required loads prior to construction. Monitoring subgrade and roadway embankments for adequate compaction also requires a large number of tests.

Small and simple projects tend to cost as much as complex projects, because the cost to use conventional methods such as SPT and (CPT) are usually based on the number and depth of holes, location of the project, and time to complete the project. The test equipment and procedures for geotechnical applications are not as advanced as in other engineering disciplines. The idea of developing a small, portable, and simple device with an inexpensive test procedure that can be performed by one person and correlated to conventional test methods is significant and will lead to considerable savings for geotechnical analyses and design.

The development of new in-situ testing and tools has declined over the past 30 years due to the following reasons:

- Excessive costs of research and development

- The quality of new tools began to suffer
- Lack of interest among young researchers and engineers
- Time limitations (it takes too long to develop and implement)
- The complexity of the new tools discourage engineers to demand their use
- Some of the new tools have no practical value
- Laboratory testing is used when possible to prevent the use of in-situ tools

The future will demand more research and development for new equipment and environmentally sound test procedures for characterizing, stabilizing, and monitoring the subsurface. Developing new equipment will require explanation of how new tools and technologies can be used to improve quality and address new applications in geotechnical fields. This paper presents the MDPT, a solution that offers tremendous value at a lower cost and in less time through a portable, inexpensive, device that can be operated by only one person manually or automatically. Advantages of the MDPT device include:

- Requires fewer boreholes for bridge foundation design as specified by NCDOT guidelines
- Provides ease of access in any terrain due to its portability
- Determines the depth of pile for the unknown foundation bridges
- Estimates unit skin friction by using a calibrated torque wrench
- Determines rock depth.
- Evaluates soil layer (blow counts) strength
- Estimates soil friction angle and undrained cohesion

The goal of this research is the development and testing of a portable mini dynamic penetration test (MDPT) and process to estimate soil strength and engineering properties. This work also focuses on the development and operation of a new mini, portable, dependable, and economical device capable of providing quick and practical characterization of soil properties in the field. To achieve this goal, the following specific objectives are devised:

1. Develop a portable rigid Mini Dynamic Penetration Test (MDPT) apparatus to estimate soil properties at different depths.
2. Perform a number of in-situ tests of the MDPT adjacent to the locations for which conventional in-situ tests such as SPT and CPT tests are available.
3. Evaluate the application of the MDPT apparatus in terms of repeatability.
4. Conduct analyses to provide empirical correlations between MDPT, SPT (automatic hammer), and CPT to estimate soil properties such as the friction angle ϕ.
5. Estimate unit skin friction by developing a relationship between the MDPT-t torque and unit skin friction.
6. Develop a correlation between dry density and MDPT n-blow counts and create a field (QA/QT) process for compaction.

1.3 Thesis Organization

The results of the development and the testing of the MDPT device are presented within eight chapters, as follows:

Chapter 1: Introduction, Background, Problem Statement and the Objective of This Study

Chapter 2: Literature Review

Chapter 3: Development of the MDPT Device

Chapter 4: Correlation of MDPT-n Blow Counts with SPT (N) Blow Counts and Estimating Engineering Soil Properties

Chapter 5: MDPT-t Torque Measurement and Correlation with Soil Strength Properties

Chapter 6: MDPT-t Torque and MDPT-n Blow Correlated to Cone Penetration Test (CPT)

Chapter 7: Mini Dynamic Penetration Test MDPT Verifying Soil Compaction and Bearing Pressure

Chapter 8: Conclusions, Contribution to State of the Art, and Recommendation for Future Works

CHAPTER 2. LITERATURE REVIEW

2.0 Historical Developments of the Dynamic Soil Testing Research Review

2.1 Dynamic Cone Penetrometer (DCP)

The Dynamic Cone Penetrometer (DCP) is used as an in-situ device for quickly estimating the structural properties of soil or pavement. The normal testing procedure is performed continuously from the ground level to the desire penetration depth. Originally developed by A. J. Scala in 1956 in Australia, the DCP consisted of a mass weight of 20 lb, a drop height of 20 in, and the cone angle was 30º with 0.5-in^2 surface area (0.8-in = 20.3 mm diameter). A cone angle of 60º is the current diameter, as published in the ASTM D 6951 method. Scala used the DCP with an extension to drive the cone 5.9 ft (1.8 m) below ground level to estimate soil strength, and he was the first one to develop a correlation between the CBR and the DCP for the pavement design. After that, many researchers developed and modified testing methods and equipment to investigate the foundation layers for pavement design.

Scala (1956) studied and developed the correlation between the DCP and the CBR for pavement design. Gawith and Perrin (1962) described the use of the same DCP in Australia, which was used to develop the DCP-CBR correlation curve. Sowers and Hedges (1966) built a lighter DCP device, with a weight of 15 lb (≈ 6.8-kg) and drop height of 20 in (508 mm). To minimize the driving resistance, the apex cone angle was 45º, as shown in Figure 2.1. This lighter DCP was used to verify the bearing pressure or soil condition at spread footing locations, and most of their DCP testing was performed in augured holes.

In 1973, a road department in South Africa used the DCP with a 30º cone tip to investigate soil layers for pavement design (Kleyn, 1975).

Siekmeier et al. (1999) evaluated the relationship between DCP results and the degree of compaction of fills materials, such as a mixture of clayey and silty sand, for the Minnesota Department of Transportation. Their procedure was to estimate the CBR from the DCPi values and then use published charts and formulas to estimate the resilient modulus from the estimated CBR to correlate the percent of compaction. However, the study showed no clear correlation or relationship between the moduli and the degree of compaction. In 2004, the ASTM D6951-03 introduced the standard test method in shallow pavement layers using the latest DCP design (ASTM, 2004).

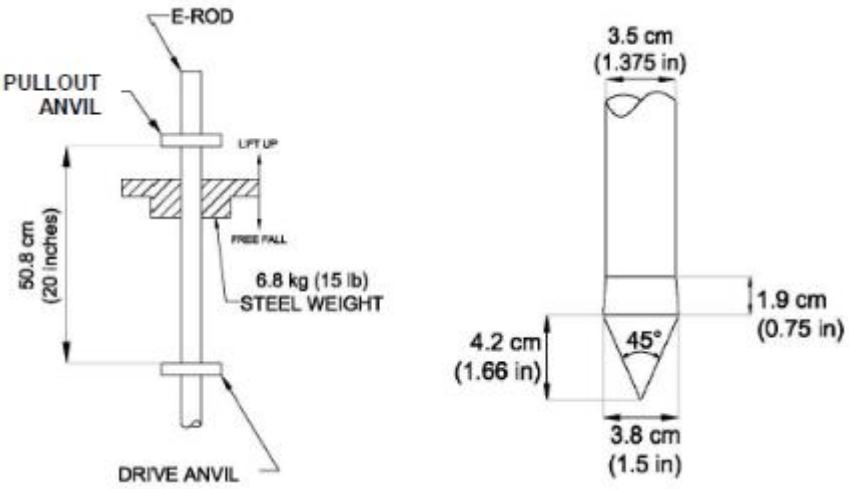

Figure 2.1 Sowers dynamic cone penetrometer (after Sowers and Hedges, 1966).

2.1.1 Developing Correlations Between DCP Readings and CBR Values

Several researchers have studied the relationship between the DCPi penetration index and the California Bearing Ratio (CBR). The in-situ CBRs determined with the DCP can be calibrated by using laboratory-soaked CBRs. The base, subbase, and the subgrade soil strength can be estimated from the cone penetration resistance, which can be converted into CBR, subgrade modulus k, resilient modulus E, and soil support value (SSV). Most researchers' equations for the CBR is expressed as a function of penetration rate (PR) (in mm/blow).

The following empirical correlations were developed by various researchers and agencies. The Australian Road Research Board (ARRB) (Smith and Pratt, 1983) studied the relationship between the CBR and the DCP penetration rate (PR) and produced the following empirical relationship:

$$\text{Log (CBR)} = 2.56 - 1.15 \text{ Log (PR)} \quad (2.1)$$

The North Carolina Department of Transportation (NCDOT) (Wu, 1987) established an empirical relationship between CBR and DCP based on the average of three DCP tests, and the field CBR within a distance of less than 1 ft (0.3 m) around the CBR test location:

$$\text{Log (CBR)} = 2.64 - 1.08 \text{ Log (PR)} \text{ or } \text{CBR} = 435/ \text{PR}^{1.08} \ (R^2=0.79) \quad (2.2)$$

Livneh developed the following relationship between CBR and the PR in 1987:

$$\text{Log (CBR)} = 2.20 - 0.7 [\text{Log (PR)}]^{1.5} \quad (2.3)$$

The U.S. Army Corps of Engineers (USACE) (Webster, Grau, and Williams, 1992) developed a relationship between the CBR and the PR of the DCP and expressed the following equation, which has been used by many state departments of transportation (DOTs) and federal highway agencies:

$$\text{Log (CBR)} = 2.465 - 1.12 \text{ Log (PR)} \text{ or } \quad \text{CBR} = 292/(\text{DCPI})^{1.12} \quad (2.4)$$

The difference between the USACE correlation and the NCDOT correlation was based on lab CBR values and field CBR values, respectively. Since it is known that the field CBR value is generally twice the value of lab CBR value, the results of these two independent studies match very well, as shown in Equations 2.2 and 2.4. Kleyn developed the following equation in 1992:

$$\text{Log (CBR)} = 2.62 - 1.27 \text{ Log (PR)} \quad (2.5)$$

Coonse presented the following correlation (Coonse, 1999):

$$\text{Log } (CBR_{field}) = 2.53 - 1.14 \text{ Log } (PR_{field}) \quad (2.6)$$

Equation 2.4 developed by USACE, was adapted by many researchers, practitioners, and agencies around the world, and it was selected as having the best correlations (Livneh 1995; Webster, Grau, and Williams, 1992; Siekmeier et al., 2000). Gabr et al. (2001) developed a correlation between the DCPi and plasticity index and saturation ratio based on laboratory tests of Piedmont residual soils from Davidson County, NC, with more than 60% fines. Gabr et al. used these correlations to predict the dry unit weight and water content of the soil.

Rahim and George (2002) correlated the resilient modulus (M_R) to DCPi and other soil properties. To determine the M_R, Shelby tube samples were collected and tested in accordance with AASHTO TP46 guidelines from 12 sites. They concluded that other soil properties are significant in predicting M_R value.

Abu-Farsakh et al. (2004) conducted both laboratory and in-situ testing to evaluate the use of DCP for quality control and quality assurance in pavement and embankment construction. The CBR, DCP, and the plate load tests (PLT) were performed in the laboratory on selected soils with a mixture of silty clay and clayey silt and compared to in-situ tests performed on subgrade pavement layers for several projects for the Louisiana DOT. Abu-Farsakh et al. concluded that the DCP was a dependable device for estimating the stiffness and the modulus of embankments, as well as for the base layers of pavement and subgrades. The results of their study indicated that the PR of 5.5 mm/blow is an acceptable value for the crushed limestone base.

Wu and Sargand (2007) evaluated the use of the DCP for evaluating the construction of pavement layers for the Ohio DOT. The penetration ratio (PR) was measured in mm/blow, and the data were collected based on ten projects tested over a two-year period. Data was collected

for both chemically treated and untreated subgrade. They concluded that the use of DCP during construction can significantly improve the quality control/quality assurance and the performance of the subgrade materials. They also determined the acceptable PR for both treated and untreated soil layers is 8 mm/blow (0.32 in/blow).

Puppala (2008) evaluated the correlation between DCPi rate values and the resilient modulus. He found out that many engineers, researchers, and agencies have used the DCP to estimate the moduli, and have used these values in many transportation projects for compaction subgrades and granular soil without addressing the site variability. However, he provided a valid warning message to the user of the DCP to be very careful when estimating and using moduli from different sites, because most of the correlations are site-specific and mostly empirical and their use for different soils requires careful evaluation and engineering judgment.

Gabr, Browning (2006) studied the effect of the cone tip apex angle on penetration resistance. The study included five different sizes of cone tip apex angles: 50º, 60º, 75º, 90º and 120º (see Figure 2.2). Based on the laboratory tests, the study concluded that increasing the cone tip apex angles increases the tip resistance

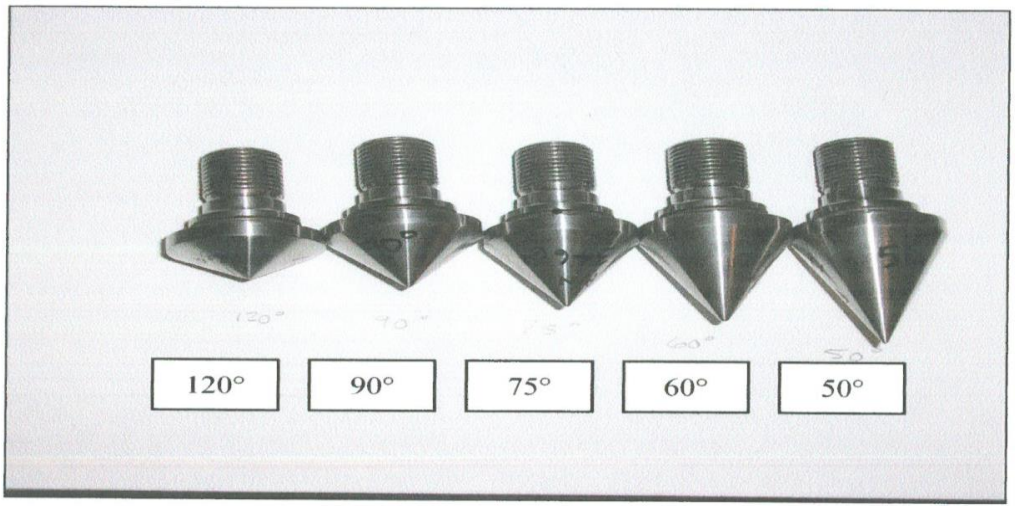

Figure 2.2 Cone tip apex angles (120º, 90º, 75º, 60º, 50º), Browning 2006.

Table 2.1 Correlations between CBR and PI (after Harison 1987 and Gabr et al. 2000).

Author	Correlation	Field or laboratory based study	Material tested
Kleyn (1975)	log (CBR) = 2.62 - 1.27· log(PI)	Laboratory	Unknown
Harison (1987)	log (CBR) = 2.56 - 1.16· log(PI)	Laboratory	Cohesive
Harison (1987)	log (CBR) = 3.03 - 1.51· log(PI)	Laboratory	Granular
Livneh et al. (1994)	log (CBR) = 2.46 - 1.12· log(PI)	Field and laboratory	Granular and cohesive
Ese et al. (1994)	log (CBR) = 2.44 - 1.07· log(PI)	Field and laboratory	ABC*
NCDOT (1998)	log (CBR) = 2.60 - 1.07· log(PI)	Field and laboratory	ABC* and cohesive
Coonse (1999)	log (CBR) = 2.53 - 1.14· log(PI)	Laboratory	Piedomont residual soil
Gabr (2000)	log (CBR) = 1.40 – 0.55· log(PI)	Field and laboratory	ABC*

*Aggregate base course

As can be seen from the above literature review, most of the testing was conducted with a DCP cone (Figure 2.2A) to correlate to CBR, resilient modulus (M_R), and soil parameters.

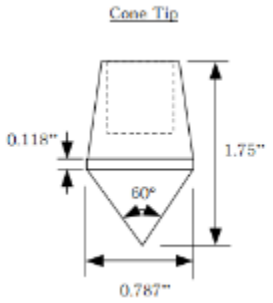

Figure 2.2A Typical DCP cone geometry.

The Dynamic Cone Penetrometer (DCP) (ASTM D6951) typically includes:

1. A steel rod ranging 1-2 m long
2. A standard size of hardened steel cone at the end
3. Drop hammers (4.6 kg for soft soils and 8 kg for stronger soils)

The soil strength and the compaction of the soil can be indirectly estimated by measuring the penetration of the cone against the number of drops of the weight. The DCP may also be used to obtain an approximate value of the California Bearing Ratio (CBR), which is an index of soil-bearing strength. The CBR and DCP have been used in practice for many decades, and many researchers have conducted tests and produced numerous data sets and empirical correlations between the penetration rate of a DCP rod, CBR, and soil strength.

The main advantage of the DCP is that it does not require any external reaction forces, relying only on the kinetic energy provided by a drop hammer. The concept of the DCP is to provide no friction mechanism during the test procedure. It is clear that during driving the only resistance is the surface area of the cone tip and no side friction. However, based on the size of the cone, depth of the testing layer, and the soil type, the DCP will have side friction (side resistance) due to soil collapse above the cone, as shown in Figure 2.3.

The MDPT penetration mechanisms are like CPT penetration mechanisms. Several authors have reported that the lateral displacement of the soil adjacent to the cone during the penetration phase of the CPT can be evaluated similarly to the bearing capacity of shallow foundation, as shown in Figure 2.5 (soil bulging above ground surface). Figure 2.4a and 2.4b shows the tip resistance Q will increase with depth until the critical depth is reached (Vesic, 1963), and then Q will stay constant or decreases, which is the behavior of deep (pile) foundations.

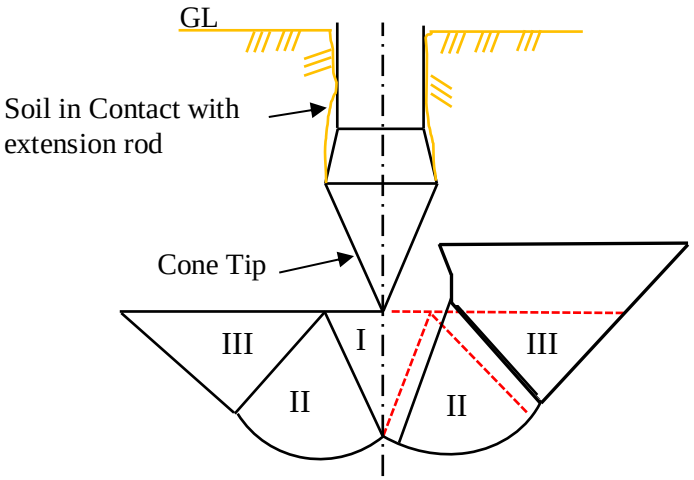

Figure 2.3 Theoretical boundaries of plastic failure.

Figure 2.3 shows that the effect of side friction of the shaft may become apparent and the shape of the shear zone may be altered and jeopardize the value of the blow count readings. The theoretical concept of the continuous penetrations caused by the hammer impact is explained in the classic study of bearing capacity failure modes. It can be categorized into three groups, as presented in Section 2.2.

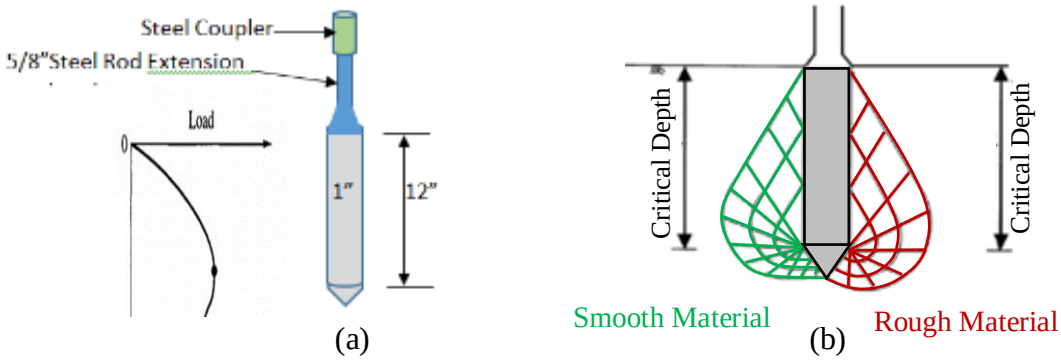

Figure 2.4 MDPT (a) and shape of critical depth (b).

2.1.2 Texas Cone Penetrometer TCP Test

The Texas Department of Transportation (TDOT) is currently using the Texas Cone Penetrometer (TCP), an in-situ test similar to the SPT and CPT. The TCP was developed by the TDOT's bridge foundation group in its Bridge Division, with the assistance of other groups within the TDOT, for estimating soil properties and determining the allowable soil- and rock-bearing capacity. Prior to 1940, there was no consistency in soil testing to determine soil- and rock-bearing capacity in the foundation design. The TDOT Geotechnical Manual (2000) mentioned that the first use of the TCP was in 1949, and the first publication of the test procedure and charts was in the Foundation Exploration and Design Manual in 1956. Since then, many modifications to the correlations have been made to improve TCP results.

The advantage of using the TCP test is the evaluation of both soil and rock, and the TCP N blow count values correlate to SPT, friction angle shear strength parameters. The TCP consists of (1) a hammer, 170 ± 2 lb. with 24 ± 0.5-in drop; (2) a drill stem rig with sufficient torque to accomplish testing to the desired depth; (3) an anvil threaded to fit the drill stem and slotted to accept the hammer; and (4) a TCP cone (conical driving point) with a diameter of 3 in and a 2.50 in-long point. However, the TCP requires the use of a heavy drill rig and drilling operation, which can be very costly for small projects or for planning purposes.

2.2 Three Groups of the Bearing Capacity Failure Modes

2.2.1 General Shear Failure

General shear failure is created by a total rupture of the soil underneath the applied load. As shown in Figure 2.5, there is a continuous shear failure of the soil (solid lines) from the tip of the cone (red line) to the ground surface. General shear failure causes ground surface rupture and pushes up the soil on both sides of the applied load.

A general shear failure occurs for dense soils and soils in the hard state.

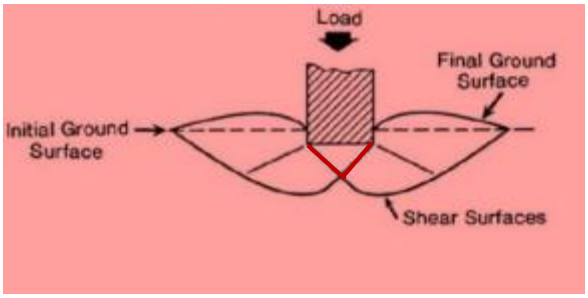

Figure 2.5 General shear failure (after Vesic, 1963).

2.2.2 Local Shear Failure

Local shear failure, as shown in Figure 2.6, ruptures the soil only immediately below the cone (red line). Soil expands on both sides of the load, but the bulging is not as significant as in general shear. Local shear failure is considered to be the transitional phase between general shear and punching shear.

Local shear failure occurs in medium-dense soils or firm-state soil.

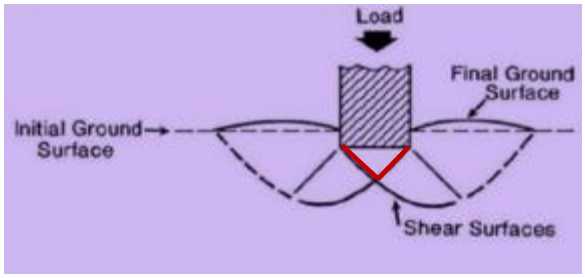

Figure 2.6 Local shear failure (after Vesic, 1963).

2.2.3 Punching Shear Failure

For punching shear, the soil outside the loaded area remains relatively uninvolved and there is minimal movement of soil on both sides of the load. The process for the cone deformation involves compression of the soil directly below the load, as well as the vertical shearing of soil around the cone perimeter. As shown in Figure 2.7, punching shear failure does

not develop a clear shape of shear surfaces similar to the general shear failure, as shown in Figure 2.5.

Punching shear failure occurs in loose or soft-state soils.

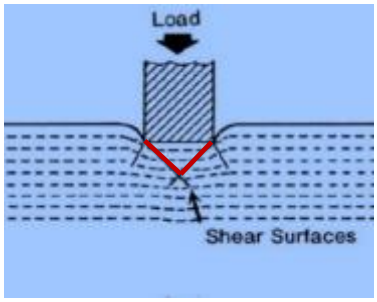

Figure 2.7 Punching shear failure (after Vesic, 1963).

Table 2.2 presents the type of bearing capacity failure summary for both cohesionless and cohesive soils clay soils that can be developed based on soil properties.

Table 2.2 Type of Bearing Capacity Failure Summary Vs. Soil Properties (After Vesic 1963).

	Cohesionless Soil (e.g., sands)			Cohesive soil (e.g., clays)	
Type of Bearing Capacity Failure	Density condition	Relative density (Dr)	$(N_1)_{60}$	Consistency	Undrained shear strength (Su)
General Shear Failure (Figure 2.5)	Dense to very dense	65–100%	>20	Very stiff to hard	> 2000 p*fs* > 100 kPa
Local Shear Failure (Figure 2.6)	Medium	35 – 65 %	5 - 20	Medium to stiff	500 – 2000 psf 25 – 100 kPa
Punching Shear Failure (Figure 2.7)	Loose to very loose	0 – 35 %	< 5	Soft to very soft	< 500 psf < 25 kPa

2.3 Current NCDOT DCP Methods Description

2.3.1 Description of Equipment

Refer to ASTM D 6951 Section Five for equipment specifications. The 17.6-lb hammer is used in this test method. Dynamic Cone Penetrometer is abbreviated as DCP. A schematic of apparatus is shown in Figure 2.8.

2.3.2 Procedure

Refer to ASTM D 6951 Section Six for the operation of DCP. The PR is marked on a survey stake for each blow during the test. Each test is advanced to a minimum of 32 in.

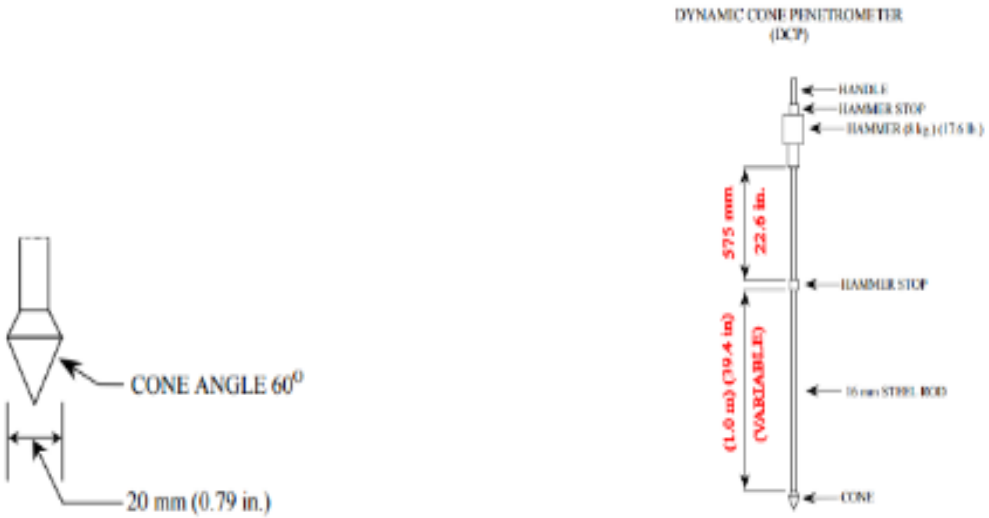

Figure 2.8 Schematic of apparatus, NCDOT–Geotechnical Engineering Unit DCP.

2.4 Summary and Recommendation

From the review of the literature, and as described in this chapter, many researchers and the developers have focused their work on the DCP, CBR, CPT, and the SPT correlations. Furthermore, most of their studies focused on the evaluation of the correlations between the DCP and CBR to characterize the soil properties for pavement layers and fill embankments. No study or research was performed similar to the development of the MDPT, as presented in this study. Therefore, the preliminary results of the proposed study, the development of MDPT, and the literature review have demonstrated the need for developing the MDPT.

CHAPTER 3. DEVELOPMENT OF MDPT

3.0 Design and Select a Shape, Size of the MDPT Device

3.1 History

The development and design of the MDPT was inspired by the improvement of the 0.5-in (13-mm) steel rod used by the North Carolina Department of Transportation (NCDOT). In the early 1970s, the NCDOT did not perform a subsurface investigation (SI) for every bridge. SI was limited to only large and important bridges and performed using the Standard Penetration Test (SPT). The investigation of small and low-impact bridges was limited to rod sounding performed by the NCDOT's Hydraulic Engineering Unit. The rod sounding consisted of a 5-ft (1.5-m) steel rod with a diameter of 0.5 in (13 mm), which was driven by a 16-lb (7.3-kg) hammer, as shown in Figures 3.1 and 3.2. The rod was driven to refusal with the use of a steel coupler to connect the steel rods together. The test is performed by driving the 0.5-in (13-mm) steel rod into the ground with a 16-lb (7.3-kg) hammer falling freely through a constant distance of 24 in (609 mm). The penetration depth is recorded every 12 in (305 mm). The signs of refusal, an indication of reaching rock or cemented soil layer, were very clear. The following are indications of driving refusal:

1. When the hammer bounces back and produces multi drops
2. When steel rod does not penetrate with the hammer impacts

If the bridge was considered to be important, a full subsurface investigation was conducted to assist with the foundation design. The foundation section was in the NCDOT's Structure Design Unit, with one engineer assigned to the foundation design.

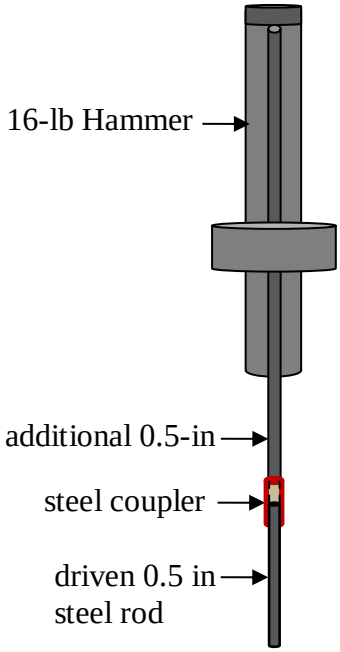

Figure 3.1 Sketch of 0.5-in steel rod and 16-lb hammer.

Figure 3.2 In-situ testing using 0.5-in steel rod device to estimate rock elevation.

3.1.1 Type of Foundations Used in the Early 1970s at NCDOT

Footing on piles was the common foundation type in Piedmont soil. The main reason for using footing on piles was the subsurface investigation using the SPT. In the Piedmont region, when the SPT test shows low blow counts (low N values) for the piedmont soil, the foundation design will be footing on piles. The Piedmont soil usually consists of residual soil with sufficient strength to use spread footing for a bridge foundation. However, when the SPT test shows lower blow counts (lower soil strength), the bridge foundation will be footing on piles to prevent bridge settlement and provide an adequate factor of safety. However, the NCDOT foundation engineering team thought that spread footing instead of footing on pile could be used to provide sufficient foundation support for some bridges in the Piedmont region, if it could be justified.

The NCDOT foundation engineering team believed the SPT is used because of its simplicity, familiarity, and low cost. It provides useful information in very specific types of soil conditions, and basic soil testing procedures give reasonably consistent results in fine-grained sands, but it is not as consistent in coarse materials or clays. To justify the use of spread footing for bridge foundations in areas where the SPT gives unreasonable results and produces low blow counts, NCDOT developed and designed a full-scale Plate Load Test (PLT) program. The PLT test frame was designed and performed by the NCDOT Geotechnical Unit and the Bridge Maintenance Unit.

North Carolina comprises of three major geographic regions: Coastal Plains, Piedmont, and Mountains. The justification program for using spread footing was focused on the Piedmont area, which is the middle region of the state, located between the Coastal Plain and the Mountain regions. Piedmont is a French word meaning “foot of the mountain”; therefore, the Piedmont region lies between the foot of the mountains and the Coastal Plain regions. Its materials

typically consist of interbedded sands, silts, and clays. Clays can be low to highly plastic, and in some cases, may be over consolidated. The above-soil formations are ideal for in-situ testing due to the lack of very stiff/hard soils and rock.

3.2 NCDOT Plate Load Test (PLT) Development to Verify 0.5-in Steel Rod

The NCDOT Plate Load Test was designed and performed by NCDOT soils and foundation engineers in the early 1980s. The test frame was built by the NCDOT Bridge Maintenance Unit. The PLT was used for soil types A-5 and A-4, which are frequently encountered in Piedmont, especially in Winston Salem and in Raleigh, North Carolina. The test was designed to determine the ultimate bearing capacity of the different types of soils and the likely settlement under a given load. During the test, static loads were applied onto the plate to determine whether the ground had sufficient bearing capacity to support structures. The PLT provided valuable data to justify the use of spread footing instead of footing on piles for bridge foundations. The PLT program also made the development of the 0.5-in (12.7-mm) steel rod a necessary field tool to verify the results of the PLT and the required bearing pressure in the field.

The PLT consisted of steel truss, 50-ton jacks, load cell, dial gauges, and steel anchors to the ground. The plate load test correlated the SPT (N) and the 0.5-in (12.7-mm) steel rod blow counts to the dry density and relative density. The steel rod was also correlated to the bearing capacity and to other tests to correlate the dry density. The steel rod is still in use by NCDOT to verify bearing capacity for spread footing and retaining wall foundations. The limitations of the 0.5-in (12.7-mm) rod was the inspiration for building a portable device that can be used continuously at different depths to estimate soil strengths and bearing capacity, as well as soil properties and soil density.

3.3 MDPT Development

The current practice for soil testing according to FHWA, AASHTO, and almost all state DOTs is the SPT and CPT for small or large projects. Therefore, it was necessary to develop a portable and mini device that mimics both the SPT and CPT mechanism. The portable device is designed to generate 10% of the SPT total energy of 350 ft-lb. The SPT has a drop weight of 140 lb (63.5 kg) and drop height of 30 in or 2.5 ft (762 mm), which generates energy or force of 140 lb*2.5 ft = 350 ft-lb (48.4 kg-m).

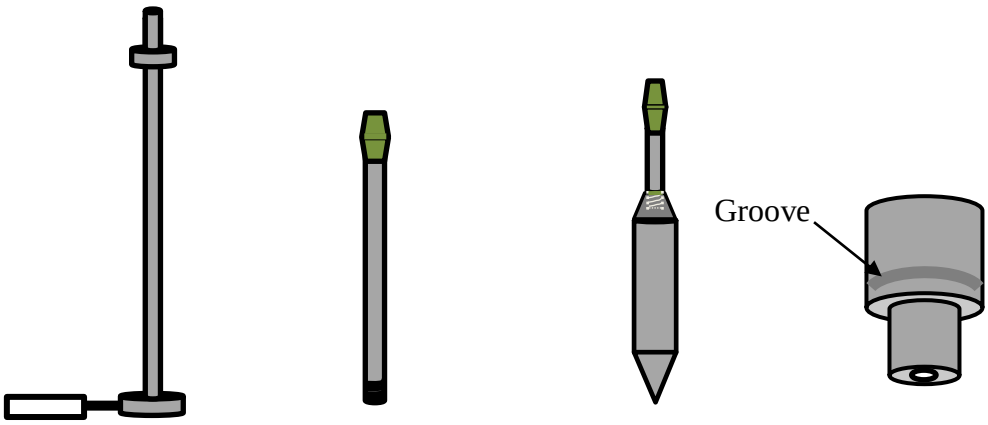

Figure 3.3 Sketch of the MDPT parts.

(a) Top part with anvils provide 24-in drop height
(b) Extension steel rod with coupler 2.5 ft
(c) Cylindrical shape with cone head at 60º
(d) Drop weight of 17.5 lb (7.9 kg) with groove

The MDPT as a dynamic test was designed to mimic the SPT tip and skin resistance behavior to produce 10% of the SPT total energy of 350 ft-lb (48.4 kg-m). The hammer weight is 17.6 lb (7.98 kg), falling freely from a height of 2 ft (609 mm) to generate energy of 35 ft-lb (4.84 kg-m). Figures 3.3 and 3.4 shows the MDPT schematic sketch and actual image. The MDPT can be operated manually or automatically using a gear-motor, as shown in Figure 3.5.

The MDPT procedure encompasses the same effect of friction and other factors to reduce the delivered energy.

Figure 3.4 Actual image of MDPT.

3.4 Testing Procedure

The equipment required for the MDPT includes the drive-weight assembly, a cylindrical shape with a steel cone head, as shown in Figure 3.4, along with steel rod extensions. The MDPT procedure is performed by continuously driving from the ground surface until a termination depth is reached. The cone has a 60º apex angle. The drive-weight assembly consists of a 17.5-lb (7.9 kg) hammer and a 5/8-in (15.9 mm) diameter stainless rod with two anvils (see Figures 3.3, 3.4, 3.5, and 4.1). The process of driving the cylindrical steel cone head (CSCH) with the 17.5-lb (7.94 kg) hammer is to lift the hammer 2 ft (609 mm) and let it drop freely, causing the anvil to drive the CSCH into the soil. The total blow counts are recorded in 1-ft (0.3m) intervals to the desired depth. The test is usually performed adjacent to SPT boring or CPT soundings for local calibration.

3.4.1 MDPT Energy Measurement

The MDPT was field-tested to measure the hammer energy efficiency and compare the data with SPT energy efficiency. The measurements were made using Pile Dynamics, Inc.

Model PAX with strain and accelerometer (see Figure 3.5). The test was performed by Applied Foundation Testing, Inc. (AFT). The energy transmitted to the steel rod from the hammer during the impact, as determined by the F-V method (EFV) and the theoretical potential energy (ETR) values, was approximately between 27–33 ft-lb (3.7–6 kg-m) and 77%–94%. The standard deviation for all data increments for EFV and ETR was 1.5 ft-lb (0.21 kg-m) and 4.2%, respectively. The energy measurement tests confirmed that the MDPT energy and efficiency are within the same range of the SPT energy and efficiency; therefore, no correction is needed between the MDPT values and SPT N values.

3.5 In-situ and Lab Testing Scheme of MDPT

In-situ penetration tests have been widely used in geotechnical and foundation engineering for site investigation in support of analysis and design. The standard penetration test (SPT) and the cone penetration test (CPT) are two typical in-situ tests. The MDPT is similar to the SPT penetration test, as it is performed by dropping a 17.5-lb hammer from a 2-ft fall height and measuring the penetration depth per blow or measuring the blow counts per ft for each tested depth (see Chapter 4).

Pile Driving Analyzer (PDA)^{TM}.

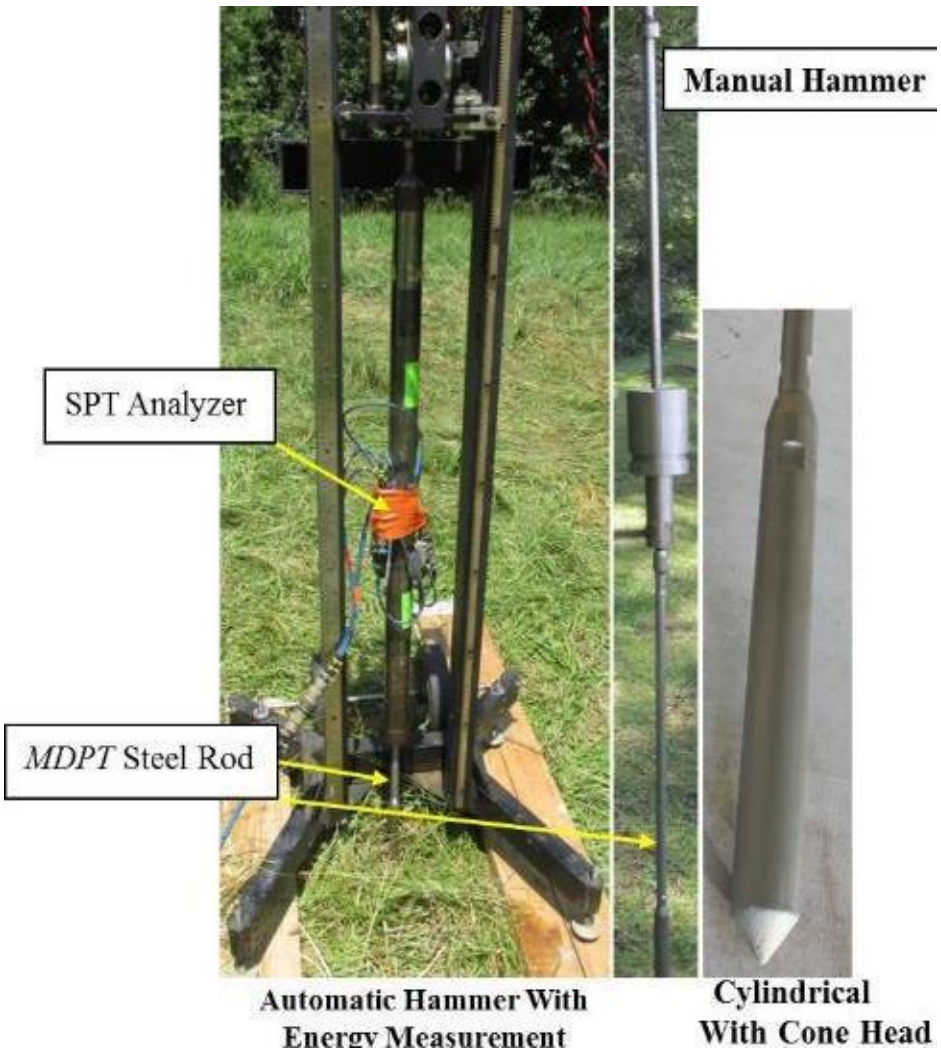

Figure 3.5 Image of MDPT: Automatic and manual hammers; cylindrical shape with cone head; illustration of SPT analyzer processing equipment and PDA during MDPT hammer energy test.

Figure 3.6 Field testing of MDPT in different sites.

Based on the literature, many of the in-situ testing tools used to determine the physical and engineering properties of soils have been developed during the last two decades. This chapter, however, focuses only on those MDPT field tests that are newly developed and used for NCDOT projects. Extreme care and sound engineering judgment should be taken during in-situ testing so that the test results truly characterize the in-situ soil strength values for each project. Local calibration is always the preferred practice for any new device.

3.6 In-situ Testing Scheme

The testing program was divided into two geological regions to represent the most sites in North Carolina. As shown in Figure 4.2, eight counties from the Piedmont region and six counties from the Coastal Region were tested with SPT and MDPT and some CPT to correlate between the three tests. Figure 4.2 on page 54 and Table 4.2 on page 55 shows the MDPT used in different projects and various locations to develop the correlations.

3.7 Laboratory Testing Program

Many factors can influence the accuracy and the repeatability of the in-situ test results, including soil type, soil strength, sampling technique, sample preparation, quality control, and operator. Horizontal and vertical variability can occur naturally in the field, and based on our experience at NCDOT field testing, variability will occur even under the best of conditions and identical adjacent test results should not be expected. When identical results are not achieved from repeated testing, concerns about soil test reliability and repeatability is often expressed. The major objective in controlling the impact in soil variation is to minimize the effect and to understand and study the factors identified above, which can cause large variation.

In this study, it was difficult to evaluate repeatability in the field due to soil variability. To study the repeatability of the MDPT, two 2.5 in x 2.5 in x 1.5 in (762 mm x 762 mm x 457 mm) wooden boxes were constructed, and soil types A-4 and A-7-5 were delivered in 100-lb bags from the Winston Salem area by the NCDOT Geotechnical Unit (see Figures 3.7 and 3.8). The wooden boxes and the soil served to eliminate the soil horizontal and vertical variability and provide a controlled testing program for the compaction and repeatability. The laboratory wooden boxes in this study served three purposes:

1. Control the soil type and strength
2. Control the boundary condition to produce identical test results
3. Study the compaction at different compaction levels

The soil sample from Winston Salem was placed in Box 1 and Box 2. Each box had a different type of soil (A-4 and A-7-5) and was compacted by three methods:

1. Placing the soil without compaction (very loose), as shown in Figure 3.8 (A)
2. Compact the soil by walking, as shown in Figure 3.8 (B)

3. Compact the soil by tamping weight, as shown in Figure 3.8 (C)

Figure 3.7 Wood boxes 1 and 2.

Figure 3.8 (A) Place the soil without compaction. (B) Compact the soil with walking compaction. (C) Compact the soil with tamping weight. (D) MDPT tests for In-situ soil at the M&T facility of NCDOT.

4. MDPT test in-situ soil as shown in Figure 3.8 (D).

3.8 Site Descriptions

The data obtained from 14 counties in North Carolina are presented in Chapter 4 (see Figure 4.2, page 54) The data are for sites representing two geological regions of the state: the Coastal Plain and the Piedmont, as shown in Table 4.2, page 55. Each project site was carefully selected and evaluated based on the level of safety to perform the MDPT tests, subsurface investigation, locations, rock deeper than 10 ft (3.05 m), site accessibility, and reasonable SPT (N) values.

The Coastal Plain geology consists mostly of marine sedimentary rock, which is usually overlain by sand and clay. The materials are primarily sand and clay from oceans and rivers that have been laid down over many thousands of years.

The Piedmont region is the middle region of the state, located between the Coastal Plain and the Mountain regions. Piedmont is a French word meaning "foot of the mountain"; therefore, the Piedmont region lies between the foot of the mountains and the Coastal Plain regions. The materials typically consist of interbedded sands, silts, and clays. Clays can be low to highly plastic, and in some cases, may be over-consolidated. The above-soil formations are ideal for in-situ testing due to the lack of very stiff/hard soils and rock.

The Coastal region has depths ranging from 13 ft (3.962 m) to 30 ft (9.144 m), with an average depth of 20 ft (6.096m). The total data points for the coastal region were 237. Each data point has MDPT blow counts n-values at a specific depth that will be compared with the uncorrected SPT N-values at the same specific depth. Both SPT and MDPT were performed adjacent to each other. Similarly, Piedmont MDPT data points were compared to the SPT. The total numbers of the Piedmont data points were 131. The lower number of data points and the shallow depths are due to the presence of shallow weathered rock or hard rock. The depth for the

Piedmont points ranged from 11 ft (3.353 m) to 20 ft (6.096 m). The MDPT tests were performed at times after the SPT was performed, and most of the SPT borings were easy to locate on the site; however, at some locations it was difficult to locate the exact SPT boring locations due to grass covering the vicinity of the boring. Each MDPT test was performed within 1–3 ft (30.5 cm–91.5 cm) of the exact location of the SPT borings. The maximum depth of the MDPT at the Piedmont region was 46 ft (14 m).

3.8.1 Site Locations

The NCDOT project sites were specifically selected to be newly sampled and tested by SPT and CPT in both the Piedmont and Coastal regions, if possible. The locations of the test sites are presented in Figure 4.2, page 54; the details, including the number of tests at each site, is presented in Table 4.2, page 55. The pink circle in Figures 4.2 and 5.12 indicates completed SPT, CPT, and MDPT tested sites. Some sites have both SPT and CPT tests completed. The project sites from 14 counties were tested by SPT, some by CPT, and some by pressuremeter by NCDOT. To have adequate test values for the correlation, MDPT was performed at multiple locations at each project site.

3.9 Test Patterns and Depths

The MDPT tests were performed within 2 ft (610 mm) or less of the SPT test to limit spatial variability. The literature review showed that spatial variability is approximately ±40% when the comparing the results from adjacent soundings (6-ft–12-ft distance (1.83 m–3.66 m)). The MDPT tests depths varied based on the rock elevation and the SPT and CPT depths.

In Chapter 4, Figure 4.2 shows a map of North Carolina and the counties tested with SPT, CPT, and MDPT. Figure 4.2 was used to select the specific projects sites to complete the MDPT study and the correlations between the SPT (N) values and MDPT-n blow counts per ft.

3.10 Typical NCDOT Process for Subsurface Investigation of Bridges, Roadways and Retaining Walls

Piedmont: Due to the variation of rock elevation, the subsurface investigation has two borings for each bent for the bridge. The depth of each boring is estimated based on the foundation type and the engineer conducting the investigation. Borings for retaining walls are typically required every 50 ft (15.24 m), with a minimum of one boring at each end of the wall. Boring depths are as shown in Table 3.1 based on wall height (H).

Table 3.1 NCDOT Boring Depth for Several Types of Retaining Walls.

Type of Wall	Boring Depth
Fill walls (e.g., gravity, MSE, concrete, etc.)	2H
Cantilever walls (e.g., sheet pile, pile panel, soldier pile, etc.)	2H
Non-cantilever (e.g., soil nail, anchored, etc.)	H

For the roadway, the spacing of borings or soundings is typically at intervals of 200 ft (60.96 m) linearly. The spacing may be adjusted to be less than or greater than 200 ft (60.96 m) depending on site conditions or project design. SPT borings are usually advanced to a minimum depth to ensure that the subsurface investigation is adequate for evaluating embankment stability. A standard depth of 1.5 times the height (1.5xH) of the proposed embankment typically used for planning purposes, with a minimum boring depth of 10 ft (3.048 m).

3.11 Repeatability of MDPT

Repeatability analysis for the MDPT is very important for interpreting the data. One of the identified sources of uncertainty in soil testing is the soil variability, both vertically and horizontally. To prevent soil variability impact and to study the repeatability of the MDPT, a test scheme was carried out to determine the repeatability of MDPT tests. Ninety-five MDPT penetrations tests were performed in proximity to each other to a depth of 1.5 ft in the laboratory

(see Tables 3.2 and 3.3 and see Figure 3.10 for each test point orientation). The field tests consisted of 20 different tests at various locations and depths (see Table 3.4).

Testing was carried out under field conditions, and the results are those expected under such conditions and under ideal "laboratory-type" conditions. The results indicated that the coefficient of variation of the laboratory testing of the MDPT was between 4% and 5%. However, the results of the field tests of the MDPT was 14%, as shown in Figure 3.9, for the material at the test locations. The results confirmed the soil variability, the need for MDPT development, and the need for more testing for each project at different locations to obtain adequate soil properties for accurate, efficient, and safe design. As previously described, local calibration is always the preferred method for the MDPT to obtain adequate data.

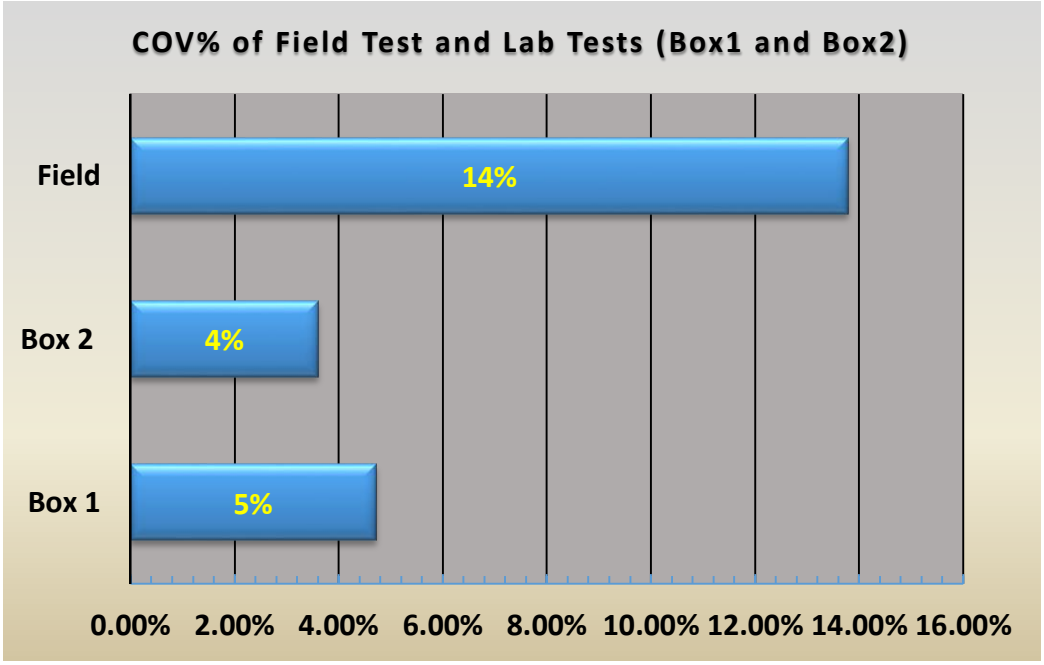

Figure 3.9 Coefficient of variation (COV) graph from laboratory (Box 1 and Box 2) and field-testing of MDPT.

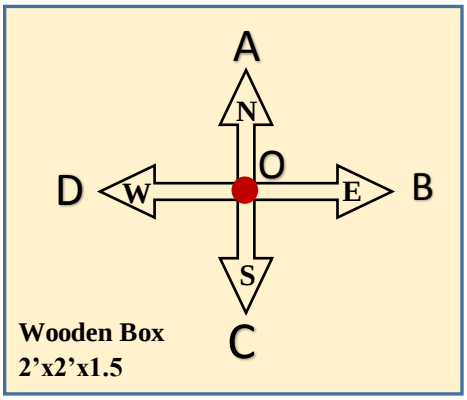

Figure 3.10 Sketch of the test orientation for each test location of the wooden box.

Table 3.2 Data Analysis from Laboratory (Box 1) for MDPT Tests for Different Depths and Locations.

	Locations	Box1 no comp.	Box1 no comp.	Box1 no comp.	Box1 walking	Box1 walking	Box1 walking	Box1 Tamp 1'	Box1 Tamp 1'	Box1 Tamp 1.5'	Box1 Tamp 1.5'	Box1 Tamp 1.5'	
		6"	1'	1.5	6"	1'	1.5	6"	1'	6"	1'	1.5	
Box 1	O	0	0	1	3	5	5	8	8	6	10	9	
	A	0	0	1	3	5	5	8	8	6	10	10	
	B	0	0	1	3	4	4	8	8	5	10	10	
	C	0	0	1	3	5	5	8	8	6	9	10	
	D	0	0	1	3	5	5	8	7	6	9	10	
	STD (σ)	0	0	0	0	0.45	0.45	0	0.45	0.45	0.55	0.45	
	Mean (M)	0	0	1	3	4.8	4.8	8	7.8	5.8	9.6	9.8	
	COV=σ/M	#DIV/0!	#DIV/0!	0	0	0.09	0.09	0	0.06	0.08	0.06	0.05	Average
	COV%	#DIV/0!	#DIV/0!	0.0%	0.0%	9.3%	9.3%	0.0%	5.7%	7.7%	5.7%	4.6%	4.7%

Table 3.3 Data Analysis from Laboratory (Box 2) for MDPT Tests for Different Depths and Locations.

	Locations	Box2 no comp.	Box2 no comp.	Box2 no comp.	Box2 Tamp 1'	Box2 Tamp 1'	Box2 Tamp 1.5'	Box2 Tamp 1.5'	Box2 Tamp 1.5'	
		6"	1'	1.5	6"	1'	6"	1'	1.5'	
Box 2	O	0	0	0	2	4	6	10	9	
	A	0	0	0	2	4	6	10	9	
	B	0	0	0	2	4	5	11	9	
	C	0	0	0	2	4	5	11	9	
	D	0	0	0	2	4	6	9	9	
	STD (σ)	0	0	0	0	0.00	0.55	0.84	0.00	
	Mean (M)	0	0	0	2	4	5.6	10.2	9	
	COV=σ/M	0	0	0	0	0.00	0.10	0.08	0.00	Average
	COV%	#DIV/0!	#DIV/0!	#DIV/0!	0.0%	0.0%	9.8%	8.2%	0.0%	3.6%

Table 3.4 Data Analysis of the Field Tests for MDPT Tests for Different Depths and Locations.

	3' below the ground											
	Locations	1	2	3	4	5	6	7	8	9	10	
Field	Hole 1											
	Hole 2											
	Hole 3	15	20	19	28	29	25	31	31	28	28	
	Hole 4	12	27	21	32	35	34	33	29	35	40	
	STD (σ)	2.12	4.95	1.41	2.83	4.24	6.36	1.41	1.41	4.95	8.49	
	Mean (M)	13.50	23.50	20.00	30.00	32.00	29.50	32.00	30.00	31.50	34.00	
	COV=σ/M	0.16	0.21	0.071	0.09	0.13	0.22	0.04	0.05	0.16	0.25	AVERAGE
	COV%	15.7%	21.1%	7.1%	9.4%	13.3%	21.6%	4.4%	4.7%	15.7%	25.0%	13.8%

3.12 Summary and Conclusions

The preliminary testing of the MDPT showed promising test results, and a full testing program was planned and performed to understand the mechanism of the rigidity of the device as an investigation tool. The MDPT device was tested in different environments and the final configuration was selected. As a portable and economical in-situ tool, the MDPT will provide planning and design engineers with the necessary data to improve their work.

The reliability of the MDPT values is significantly influenced by its repeatability. In this study, the repeatability of the MDPT device was evaluated using the coefficient of variation based on 115 in-situ and laboratory tests in proximity to each other. The results of the analysis show that the MDPT has very good repeatability. The coefficient of variation analysis showed the range is between 4%–14%, as shown in Figure 3.9 and in Tables 3.2, 3.3, and 3.4.

CHAPTER 4. DEVELOPMENT OF A PORTABLE MINI DYNAMIC PENETRATION TEST (MDPT) AND PROCEDURE TO ESTIMATE SOIL STRENGTH AND ENGINEERING PROPERTIES

M. A. Mulla[1], M. A. Gabr[2] and M. S. Rahman[3]

[1]Graduate Student
Department of Civil, Construction and Environmental Engineering
North Carolina State University (NCSU)
Raleigh, NC 27695-7908
E-mail: mamulla@ncsu.edu

[2]Professor, Ph.D., P.E.
Department of Civil, Construction and Environmental Engineering
North Carolina State University
Raleigh, NC 27695-7908
E-mail: gabr@eos.ncsu.edu
Phone: 919-515-7904
Fax: 919-515-7908

[3]Professor, Ph.D.
Department of Civil, Construction and Environmental Engineering
North Carolina State University
Raleigh, NC 27695-7908
E-mail: rahman@eos.ncsu.edu
Phone: 919-515-7633
Fax: 919-515-7908

Development of a Portable Mini Dynamic Penetration Test (MDPT) and Procedure to Estimate Soil Strength and Engineering Properties

4.0 Abstract

Understanding soil strength and other engineering properties are essential to foundation design and necessary for adequately assessing the load-carrying capacity of soil during the design and construction process. Currently, no portable, manual or automatic, easy-to-use field device exists that can measure field resistance to depths of 45 ft (13.7 m). This paper presents the development of a new portable Mini Dynamic Penetration Test (MDPT) and examines the correlation between the penetration resistance (n-value) and the N-value from the standard penetration test (SPT). The basic motivation is to develop a new portable, versatile, and cost-effective alternative device and method for estimating the strength and engineering properties of soils. The MDPT was tested in 14 counties from the Coastal region (CR) and the Piedmont region (PR) of the state of North Carolina (NC).

Correlations were conducted without taking into account soil types and groundwater elevation. Analyses of the data show a clear linear relationship between the measurements from the SPT (N) value and MDPT-n value. In-situ test results from MDPT demonstrate that the soil properties can be estimated from portable dynamic penetration test data without the use of heavy and costly drill rigs or trucks. The MDPT can be used to evaluate subgrade and soil layer strength, as well as estimate soil properties using correlations with other in-situ testing methods.

4.1 Introduction

In-situ penetration tests have been widely used in geotechnical engineering for site characterization in support of analysis and design. The Standard Penetration Test (SPT) and the Cone Penetration Test (CPT) are the most widely used field testing procedures for geotechnical engineering in the United States. The CPT was invented in Holland in 1932 and introduced into

U.S. practice more than 40 years ago (Schmertmann, 1970). Early field operations used mechanical systems that collected two readings: cone resistance (q_t) and friction (*fs*) at 7.87 in (200 mm) intervals. Data were recorded by hand and the interpretation methods were based on limited knowledge and experience. Today, electric and electronic CPT systems are available in several sizes and configurations of the cone tip, and provide three or more separate readings with depth: total cone tip resistance (q_t), sleeve friction (*fs*), and pore water pressure (u_2), usually taken at frequent vertical intervals between 0.4 in–0.8 in (10–20 mm) (Lunne et al. 1997).

Robertson et al. (1986) proposed a CPT-SPT correlation in which the ratio between the normalized cone tip resistance (q_t/Pa) and N must be corrected to a 60% energy ratio (N60). Kulhawy and Mayne (1990) extended the Robertson et al. (1983) correlation based on additional data that became available in the late 1980s, and developed an empirical equation for their updated SPT-CPT correlation. The advantages of the SPT include availability, a wide variety of developed soil parameters based on SPT N-value data, and a soil sample is typically obtained with each test.

Dynamic cone penetrometers (DCP) have been used in geotechnical applications for nearly 60 years. Different types and shapes of DCP have been developed with the Scala penetrometer, introduced in 1956, and the Sowers penetrometer, introduced in 1959. The DCP was widely used to evaluate pavement layers, such as base course material and subgrade soil, for pavement design. The DCP is performed by dropping a hammer from a certain fall height and measuring the penetration depth per blow for each tested depth. The DCP test is quick to set up, run, and evaluate on site, but it is designed to evaluate shallow soil layers at depths ranging 4 ft–6 ft (1.2 m–1.8 m). In addition, the DCP has limitations with respect to its ability to evaluate the soil layers, and thus there is a great need to develop a simpler, more cost-effective procedure to

determine in-situ parameters. Such a procedure will help geotechnical engineers conduct their analyses and designs using methods that are simpler and less equipment-intensive than SPT and CPT. In this study, the development of a portable MDPT is reported for collecting data on penetration resistance and skin resistance behavior. The skin resistance is estimated using a torque wrench, as shown in Figure 4.6.

The MDPT can be driven to a depth of 45± ft (13.7± m) below the ground surface with 5/8-in (160-mm) stainless steel rod extensions. The MDPT hammer configuration was designed to mimic the SPT tip and skin resistance behavior to produce 10% of the SPT total energy of 350 ft-lb (48.4 kg-m). It consists of a 17.6-lb (7.98-kg) steel mass, or hammer, falling 2 ft (609 mm) to develop 35 ft-lb (4.84 kg-m). A schematic sketch of the MDPT is provided in Chapter 3, Figures 3.3, 3.4 and 3.5.

The MDPT can be operated manually or automatically using a gear-motor (shown in Figure 3.5). The automatic MDPT consists of a 35-lb (15.88-kg) hammer falling 1 ft (300 mm) to develop 35 ft-lb (4.84 kg-m). Theoretically, the 140-lb (63.5-kg) SPT hammer dropped from 30 in (762 mm) should deliver 350 ft-lb (48.4 kg-m) of energy (140 lb. x 30 in = 350 ft-lb) (63.5 kg x 0.762 = 48.4 kg-m) with each blow. Field testing indicated that the energy delivered to the rods during an SPT test can vary from 68%–94% of the theoretical maximum, with an average of 81%. SPT resistance values are normalized to 60% energy, because the correlations made before the advent of hammer-system calibration used safety hammers and it was generally assumed that the correlations were running at 60% efficiency.

Normalization is made in design to compare resistance values to published correlations that were either assumed to be operating at or otherwise normalized to 60%. However, the measured field energy for this research was corrected to the standard 60% energy, and thus each

blow will deliver (350 ft-lb x 0.6) = 210 ft-lb (48.4 x 0.6= 29 kg-m) to the sampler. Each blow count could be used as a unit measurement of delivered energy in which one blow count equals 210 ft-lb (29 kg-m). The measured N value blows per ft (blows per 300 mm) is defined as the penetration resistance, which equals the sum of the number of blows required to drive the SPT sampler a depth interval of 6 in–18 in (150–450 mm). The MDPT procedure will encompass the same effect of friction and other factors to reduce the delivered energy.

The main objective of this study is to correlate the MDPT n-value to the SPT N-value using well-established empirical methods. Such a correlation is meant to take advantage of the vast database of empirical relationships as a function of the N-value. Establishing the relationship between the MDPT data and the N-value can provide a cost-effective method for assessing key soil parameters in the field. The MDPT is currently used by the NCDOT to verify and confirm project conditions during construction, estimate rock elevation, evaluate subgrade strength, and estimate soil properties.

4.2 Background

To the author's knowledge, no portable and rapidly deployable instrument capable of reaching a depth of 45 ft (13.7 m) has been developed to drive deeper than the subgrade layers. Gabr et al. (2001) reported that widespread research was performed to correlate the DCP to the California Rearing Ratio (CBR) and develop an empirical relationship. Abu-Farsakh et al. (2004) assessed the use of DCP for quality control/assurance evaluation of pavement layers and embankments during construction. A summary of selected research studies that have correlated the DCP values to CBR, PLT, falling weight deflectometer (FWD), is provided in Chapter 2 Table 2.1.

The data points of the MDPT tests were compiled and organized for each geologic region. Comparisons between the MDPT blow counts (n) and the SPT blow counts (N) using an automatic hammer were made separately for the Coastal region and for the Piedmont region. It is assumed that the factors affecting the SPT will be similar to those affecting the MDPT. The following factors are noted:

A. Variation in delivered energy (Robertson et al., 1983)
B. Equipment conditions
C. Both are dynamic
D. Both measure resistance based on vertical soil penetration
E. Both have skin and tip resistance albeit not the same magnitude

Based on the correlation and calibration tables developed for the MDPT and SPT tests using an automatic hammer, we can correct the SPT(N) values based on the MDPT results adjacent to the SPT location. Development of site-specific correlations between the SPT(N) values and the MDPT-n value can prevent many design errors caused by using the wrong SPT(N) values. See Sabatini et al. (2002) and Phoon et al. (1995) for information on the variability associated with various engineering properties. The data shown in Figure 4.3 shows the coefficient of determination R^2=0.92 and the correlation coefficient r=0.96 for the Piedmont region, R^2=0.93 and r=0.964 for the Coastal region, and the average for both regions of R^2 = 0.91 and r = 0.95 and mean square error (MSE) = 4.7. These indicate a strong correlation between the resistance from SPT(N) s and the MDPT-n measurements.

Many researchers have performed correlations between SPT and soil properties such as friction angle ϕ, unit weights γ, relative density Dr, bearing capacity, among many others. Some published correlations are based on corrected N_{60} or $N1_{60}$ for overburden and hammer efficiency,

and some are based on uncorrected (N) values. The designer must evaluate and study the basis of the correlation and use either $N1_{60}$ or N as appropriate. In this study, Figure 4.4 and Figure 4.5 are used for the correlations between the SPT and the soil properties on the basis of the Standard Penetration Test (N) values corrected ($N1_{60}$). Since soil properties estimated from correlations tend to have greater variability than measurements using laboratory performance data (Phoon et al., 1995), a minimum of 3–5 measurements from each geologic stratigraphy should be taken to estimate the soil properties.

4.3 Testing Process

Equipment required for the MDPT includes the drive-weight assembly, a cylindrical shape with a steel cone head, as shown in Figure 4.1, and steel rod extensions. Typically, the MDPT test is continuously driven from the ground surface until a termination depth is reached. The cone has a 60º apex angle. The drive-weight assembly consists of hammer and a 5/8-in (160-mm) diameter stainless rod with two anvils (see Figure 4.1, and Figure 3.5 on page 29). The process of driving the cylindrical steel rod (CSR) with the 17.6 lb (7.94 kg) hammer is to lift the hammer 2 ft (0.6 m) and let it drop, forcing the anvil to drive the CSR into the soil. The total blow counts are recorded at 1-ft (0.3-m) intervals to the desired depth.

4.3.1 Field Testing

Data obtained from 14 counties in North Carolina are presented. The data are from the sites representing the Coastal Plain and the Piedmont regions. The locations of the test sites are presented in Figure 4.2; the details, including the number of tests at each site, are presented in Table 4.2.

The Coastal Plain geology consists mostly of marine sedimentary rock which is usually overlain by sand and clay. The materials are primarily sand and clay from oceans and rivers that have been laid down over many thousands of years.

The Piedmont is the middle region of the state, located between the Coastal Plain and the Mountain regions. Piedmont is a French word meaning "foot of the mountain"; therefore, the Piedmont region lies between the foot of the mountains and the Coastal Plain regions. The materials typically consist of interbedded sands, silts, and clays. Clays can be low to highly plastic and may be over-consolidated in some cases. The above-soil formations are ideal for in-situ testing due to the lack of very stiff/hard soils and rock.

Data for the Coastal regions have depths ranging from 13 ft (3.9 m) to 30 ft (9 m) with an average depth of 20 ft (6.09 m). The total data points for the Coastal region were 237. Each data point has MDPT blow count n-values at a specific depth, which will be compared with the uncorrected SPT N-values at the same specific depth. Both SPT and MDPT were performed adjacent to each other. Similarly, Piedmont MDPT data points were compared to the SPT. The total numbers of the Piedmont data points were 131. The lower number of data points and the shallow depths are due to the presence of shallow weathered rock or hard rock. The depth for the Piedmont points ranged from 11 ft–20 ft (3.353 m–6.096 m). The MDPT tests were performed at times after the SPT was performed. While most of the SPT borings were easy to locate on the site, at some locations it was difficult to locate the exact SPT boring locations due to grass covering the vicinity of the boring. Each MDPT test was performed within 1 ft–3 ft (30.5 cm–91.5 cm) of the exact location of the SPT borings. The maximum depth of the MDPT at the Piedmont region was 46 ft (14 m).

4.4 Mini Dynamic Penetration Test (MDPT) Energy Measurement

The MDPT was field-tested to measure the hammer energy efficiency and compare the data to the SPT energy efficiency. The measurements were made using Pile Dynamics, Inc. / Model PAX with strain and accelerometer (see Figure 3.5 on page 29). The test was performed by Applied Foundation Testing, Inc. (AFT). The energy transmitted to the steel rod from the hammer during the impact, determined by the F-V method (EFV) and the theoretical potential energy (ETR) values were 77%–94%. (approximately between 27–33 ft-lb (3.7–4.6 kg-m)). The standard deviation for all data increments for EFV and ETR was 1.5 ft-lb (0.21 kg-m) and 4.2%, respectively. The energy measurement tests confirmed that the MDPT energy and efficiency are within the same range of the automatic hammer SPT energy and efficiency. The hammer efficiencies averaged 80% for both MDPT and automatic SPT; therefore, no correction is needed between the MDPT n_{80} values and SPT N_{80} values. See Table 4.4 for the MDPT PDA test results.

4.5 Correlations to Estimate Engineering Soil Properties of Soil

The friction angle of granular soil estimated from the corrected N-value from the SPT-$N1_{60}$ parameter shall be determined based on the correlation shown in Table 4.3 and Figure 4.4. The correlation by Peck, Hanson, and Thornburn (1974) falls within the ranges specified in Table 4.3. While experience in each region and type of soil should apply when selecting specific values within the ranges, generally the finer materials (i.e., with significant silt-sized materials) and materials in which the particles are rounded will fall in the lower range. However, coarser materials with less than 5% fines and materials in which the particles are sub-angular to angular will fall in the higher range (reported in AASHTO 2014). It is good practice to be careful when using any correlations of SPT and soil properties, especially correlations with higher values.

4.6 Using MDPT to Estimate the Corrected SPT – ($N1_{60}$)

Step 1: After collecting the in-situ MDPT n_{80} for projects in the Coastal or Piedmont area, examine the data and eliminate any data points far from the trend. Observe boring log descriptions for gravel or rock present at the site from previous site investigations within the vicinity of the project, then follow Steps 2-5.

Step 2: Use the appropriate graph and formula shown in Figure 4.3 (A), (B), or (C), depending on the region, to estimate the uncorrected SPT-N_{80} value.

Step 3: Correct the SPT N_{80}-value for overburden and hammer efficiency $N1_{60}$ values where the relationship between SPT N-value and the MDPT-n value are as follows:

Piedmont region: $N_{80} = 0.27n$ (as shown in Figure 4.3 C) (4.1)

Coastal region: $N_{80} = 0.23n$ (as shown in Figure 4.3 B) (4.2)

Average for both regions $N_{80} = 0.25n$ (as shown in Figure 4.3 A) (4.3)

SPT N values shall be corrected for hammer efficiency, if applicable to the design method or correlation being used, using the following relationship:

$$N_{60} = (ER/60\%)\, N_{80} \quad (4.4)$$

where n is n_{80}, N_{80} is the uncorrected SPT value (blows/ft), N_{60} is the SPT blow count corrected for hammer efficiency (blows/ft), and ER is the hammer efficiency expressed as percent of theoretical free-fall energy delivered by the hammer system actually used.

The following value for ER may be assumed if hammer-specific data are not available:

ER = 80% for automatic trip hammer (NCDOT requires automatic hammer only).

N-values shall be corrected for overburden pressure N1. The overburden correction equation is:

$$N1 = C_N N \quad (4.5)$$

$$C_N = [0.77 \log10 (40/ \sigma'_v)], C_N < 2.0 \quad (4.6)$$

where C_N is the correction factor for overburden, N_{60} is the N-value corrected for hammer efficiency, and σ'_v is the vertical effective stress at the location of the SPT N-value (ksf).

N values corrected for both overburden pressure and the hammer efficiency shall be designated as $N1_{60}$.

$$N1_{60} = C_N N_{60} \quad (4.7)$$

Cited from the American Association of State Highway and Transportation Officials (AASHTO). LRFD Bridge Design Specification, Seventh Edition, 2014 Article 10.

Step 4: Use the corrected ($N1_{60}$) to estimate the friction angle ϕ using Figure 4.4.

Step 5: Use the corrected ($N1_{60}$) to estimate the moist unit weight γ for granular soil unit weight using Figure 4.5.

4.7 Estimate Friction Angle from MDPT- n Values for the Uncorrected SPT N-Values Using NCDOT Method

Estimate the friction ϕ directly from the MDPT-n values, where n = MDPT blows/ft:

(a) For Coastal region $\phi = 0.3(90 + 0.23n)$ (4.8)

(b) For Piedmont region $\phi = 0.3(90 + 0.27n)$ (4.9)

(c) For average value $\phi = 0.3(90 + 0.25n)$ (4.10)

The friction angle ϕ estimated from MDPT-n values will be equivalent to the friction angle ϕ estimated using uncorrected SPT N values. Round the friction angle ϕ to the nearest 1º. The n value for the MDPT-n is the

The maximum range of ϕ angles for any $N1_{60}$ is 5º, as shown in Table 4.3. The adjustment factors for particle size and roundness should be limited to only 1º or 2º. The following bulleted list provides guidance in determining which curve to use for a given $N1_{60}$ and soil type or classification:

- Use the high for GW
- Use the average for GM and SP
- Use the low for SC
- Use the low for ML
- Use the average for SW
- Use the average for GC
- Use the high for GP

Unified Soil Classification system letters:
G = Gravel
P = Poorly graded (uniform particle size)
S = Sand
W = Well graded
M = Silt
H = High plasticity
C = Clay
L = Low plasticity
O = Organic

Values may also be increased with increasing grain size and/or particle angularity and decreased with decreasing grain size and/or increasing roundness. Roundness and angularities are terms used to describe the shape of the corners on a particle. Choose the unit weight for the soil type based on the following guidelines:

- Use the high values for well-graded sands and gravels
- Use the average values for poorly-graded sands and gravels
- Use the low values for elastic silt, and clayey or silty sands and gravel
- Deduct up to 20% for dry soils

4.8 Discussion of Results

The MDPT-n values from the field measurements were recorded at the same elevation as those from the SPT (N-values) for both the Piedmont and the Coastal Plain regions. Statistical analysis methods were used to determine the strength of the relationship between the SPT (N) and the MDPT-n values. The theoretical basis of the data interpretation was developed and

verified in the field. The liner correlation was found to be the best fit for all graphs. The coefficients of determination R^2 in this study are very close to each other, and thus average correlations can be used for projects in both regions. This correlation was achieved regardless of soil type or the groundwater table. Data from the MDPT can be used for many tasks, such as:

- Estimating the rock or refusal elevation without mobilizing a drill rig and three crew members at a cost of $3,500/day; in comparison, MDPT costs less than $500/day.
- Estimating the minimum pile embedment for unknown foundation bridges.
- Estimating the unit skin friction to assist the design engineer in pile foundation design.
- Evaluating the California Bearing Ratio (CBR) (blow counts versus depth for pavement design).
- Estimating bearing capacity, density, and relative density Dr.
- Reducing the number of bore holes required for bridge foundation design, as specified by NCDOT guidelines. Only few boreholes are needed to calibrate the MDPT, which can then be used to complete the investigation.
- Evaluate the strength of the soil layers (blow counts) without mobilizing specialized equipment, thereby reducing costs and expediting work.

It should also be noted that the MDPT is safer to use than the SPT because of its smaller size.

4.9 Summary and Conclusions

This paper presents the correlation of MDPT blow counts (n-value) to the SPT blow counts (N-value) for expediently assessing the strength of a wide range of soils to a depth of 40 ft. The study focused on the Coastal Plain and the Piedmont regions of North Carolina. Data from the MDPT and the SPT were compiled, organized, and analyzed. Both the correlation coefficient (R) and the coefficient of determination (R^2) indicated a strong positive linear

relationship between the SPT (N) values and the MDPT-n values for both regions. MDPT expediently gives a continuous evaluation of the soil layers, while SPT yields soil strength evaluations every 5 ft (1.6 m), thus increasing the risk of missing valuable information. In general, the MDPT was found to be a reliable method for assessing soil strength. The use of MDPT yields soil properties without heavy drill rigs and costly equipment. The MDPT data reduction approach could be improved with additional field testing and correlations to CPT and triaxial test data.

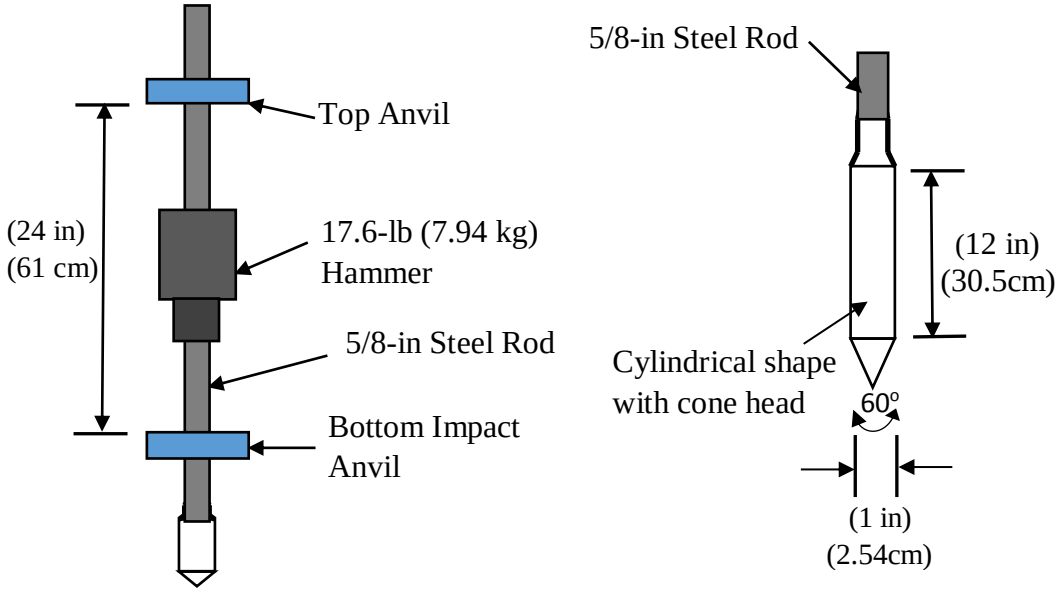

Figure 4.1 MDPT schematic sketch (not to scale).

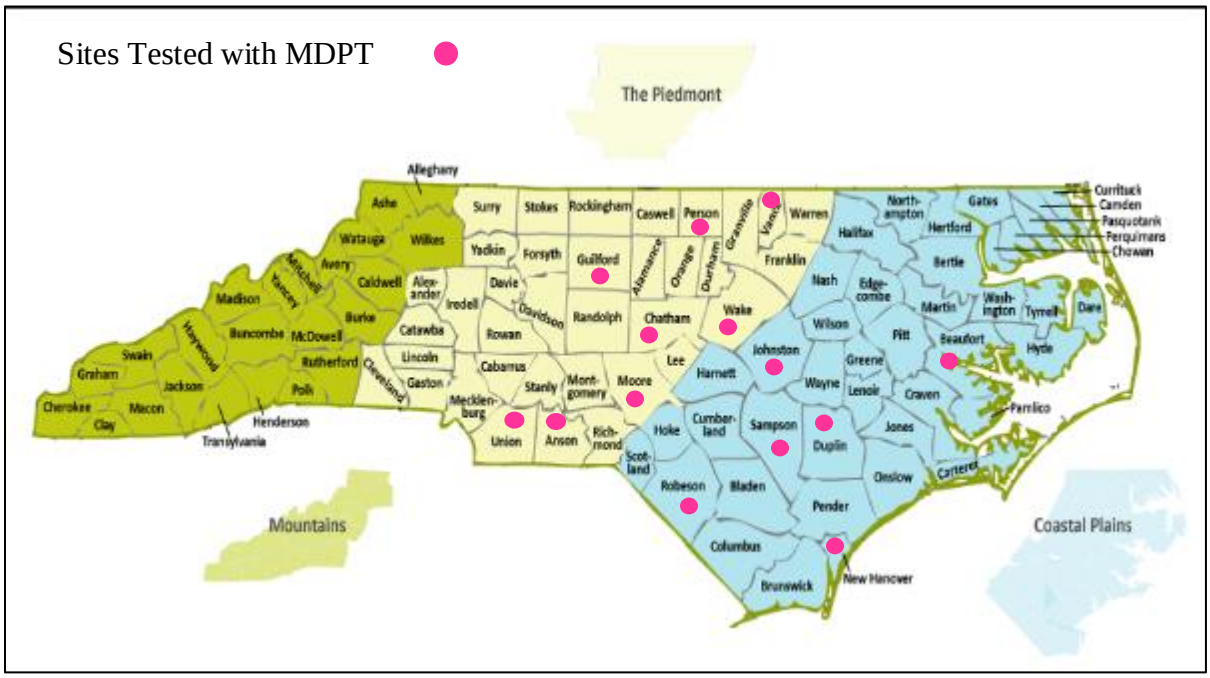

Figure 4.2 North Carolina map showing the counties tested with SPT and MDPT.

Table 4.1 Summary of Research Study Areas for DCP.

Researchers	Study Area
Sowers and Hedges (1966)	Present DCP device 15 lb (6.8 kg) falling 20 in (508 mm).
Sampson (1984)	DCP used to estimate bearing capacity.
Harison (1987)	Presented a linear relationship between DCP and CBR.
Ayers et al. (1989)	Study DCPi and shear strength correlations for sand.
Ayers (1990)	Effect of overburden pressure on DCP.
Bratt et al. (1995)	Correlation between DCPi and dry density.
Hassan (1996)	Correlation between DCPi and resilient modulus.
Parker et al. (1998)	Built automated DCP.
Gabr et al. (2001)	Correlation between DCPi and liquidity index.
Abu-Farsakh et al. (2005)	Studied relationship between DCP, Plate Load Test (PLT), FWD and CBR. Presented correlation between unsoaked CBR values and elastic modulus.
Puppala (2008)	Studied the correlation between of the resilient modulus and the DCPi. He cautioned that the correlation is site-specific and to use good engineering judgment in different areas.

Table 4.2 Project Studies Summary.

Case NO.	County	Project	# of MDPT tests	Region
1	Wake	Maint. Yard	3	Piedmont
2	Wake	M&T Test Area	2 (Density), DCP	Piedmont
3	Wake	B-5113	1 EB1-A	Piedmont
4	New Hanover	R-2633BB	2	Coastal
5	Johnston	B-4936 (Br. 41)	2	Coastal
6	Moore	SF-620100	2	Piedmont
7	Moore	SF-620008	2	Piedmont
8	Duplin	SF-300140	2	Coastal
9	Duplin	SF-300384	2	Coastal
10	Sampson	SF-810167	2	Coastal
11	Sampson	SF-810224	2	Coastal
12	Person	SF-720142	2	Piedmont
13	Chatham	SF-180061	1 mini + 1 DCP	Piedmont
14	Wake	MT & Test	SPT, DCP, ½”Rod	Piedmont
15	Robeson	I-4927	Mini + DCP	Coastal
16	Guilford	U-2412B	2, CPT, SPT	Piedmont
17	Vance	I-0914BA	1, SPT	Piedmont
18	Guilford	U-2412B	2, CPT, SPT	Piedmont
19	Guilford	U-2412B	4, CPT, SPT	Piedmont
20	Guilford	U-2525C	4, CPT, SPT	Piedmont
21	Beaufort	Airport	4, CPT	Coastal
22	Anson	SR 1252 (FDR)	4, Density	Piedmont
23	Union	R-3329 & R-2559	6, Density	Piedmont

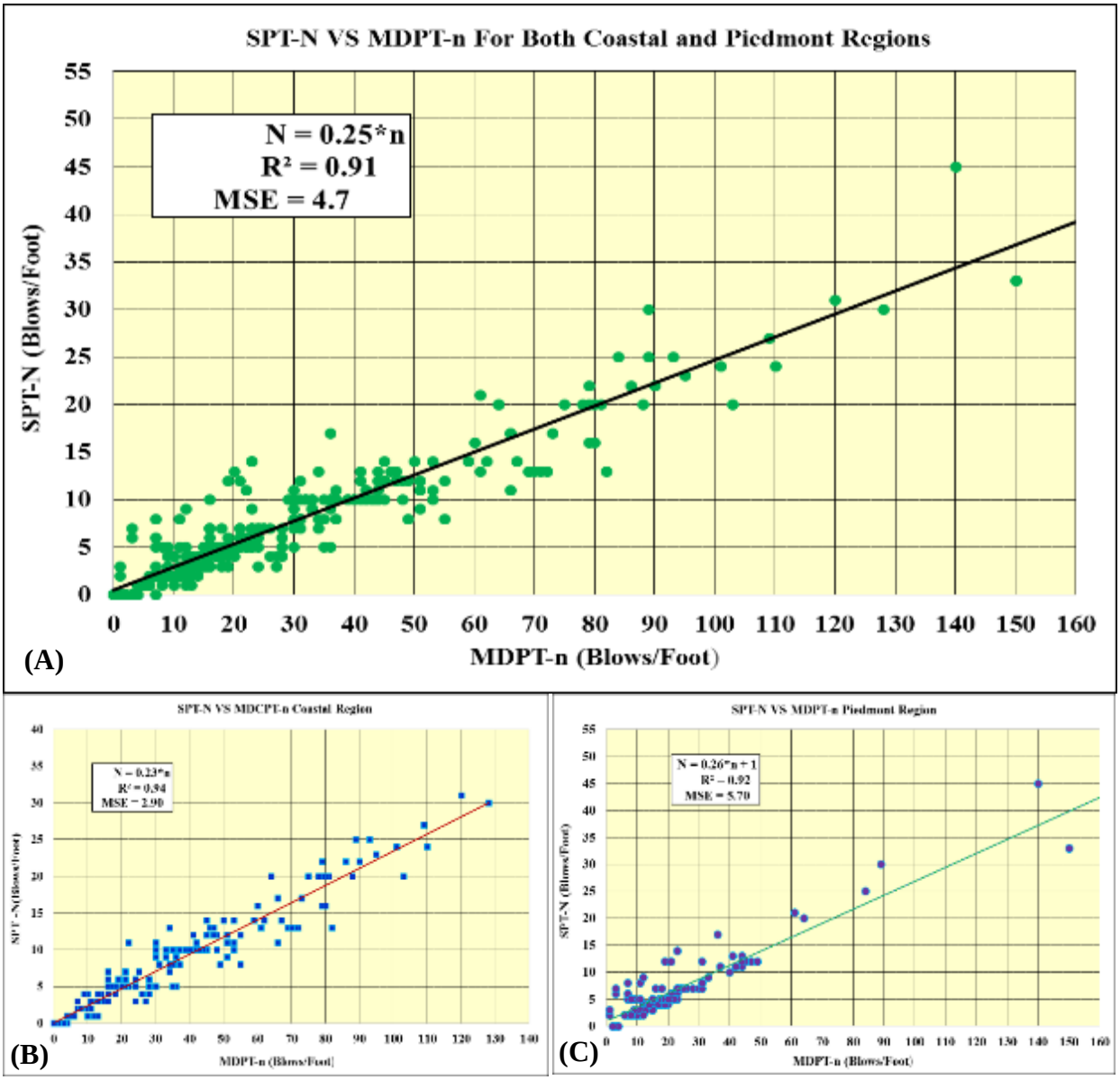

Figure 4.3 (A) Correlation between SPT and MDPT for both Coastal and Piedmont regions. (B) Correlation between SPT and MDPT for Coastal region. (C) Correlation between SPT and MDPT for Piedmont region.

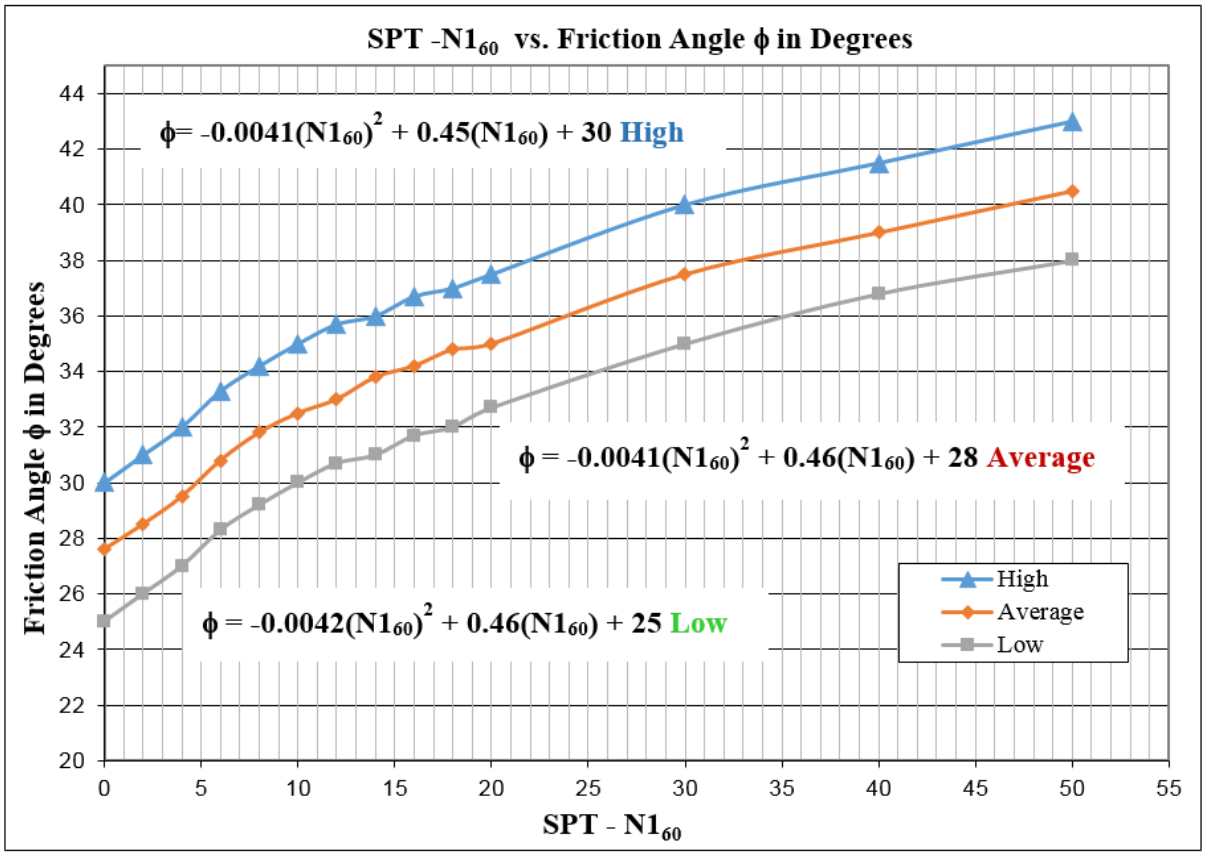

Figure 4.4 Correlation of SPT $N1_{60}$ with friction angle ϕ (after Bowles, 1977) for granular soil friction angle.

Table 4.3 Correlation of SPT $N1_{60}$ Values to Drained Friction Angle of Granular Soils (Modified After Bowles, 1977, As Reported in AASHTO 2014).

N160 from SPT (blows/ft)	ϕ (degrees)
<4	25-30º
4	27-32º
10	30-35º
30	35-40º
50	38-43º

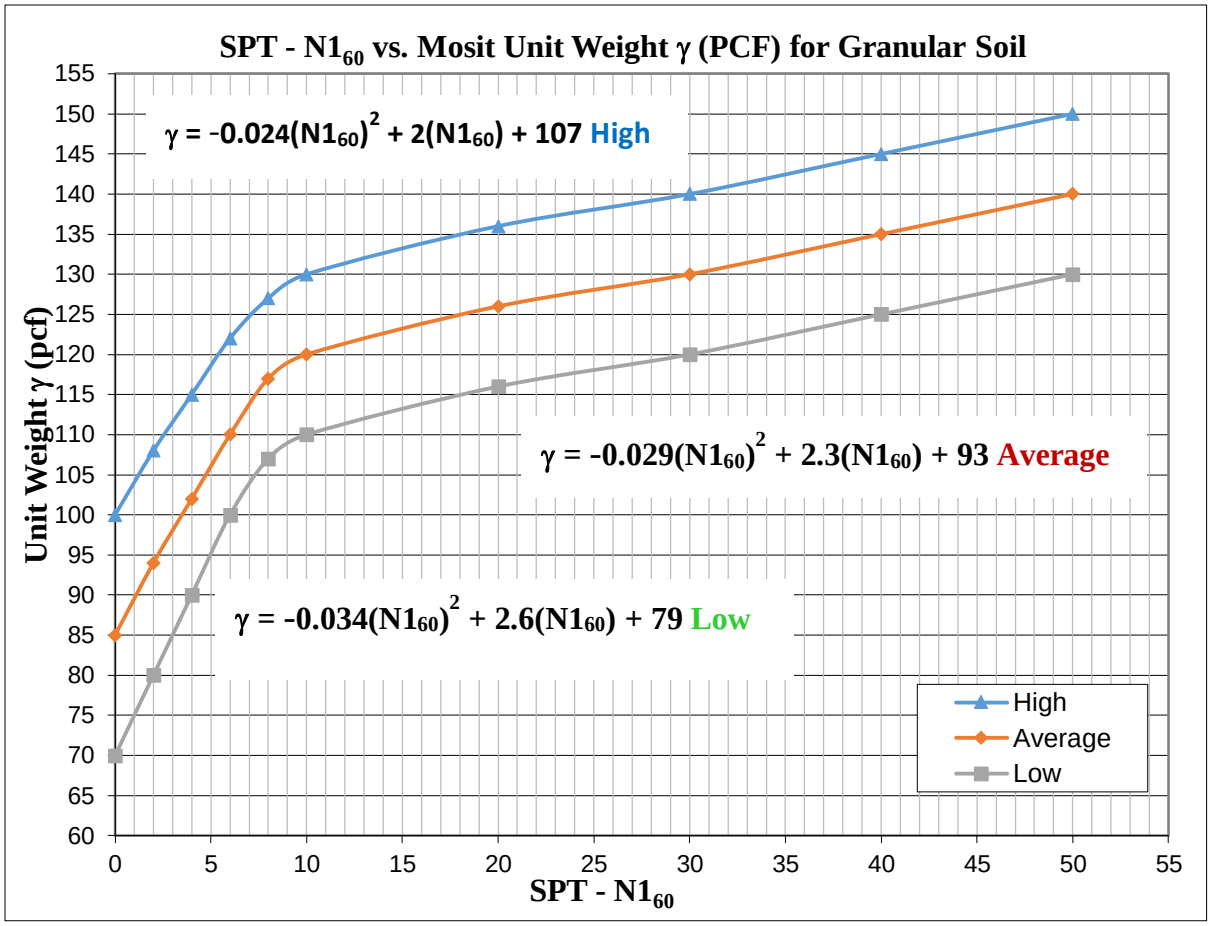

Figure 4.5 Correlation of SPT $N1_{60}$ with moist unit weight γ (after Bowles, 1977) for unit weight of granular soil.

Figure 4.6 Torque wrench to estimate unit skin friction.

Table 4.4 MDPT Delivered and Averaged Energy Using PDA.

Delivered Energy Kip-feet	Blows/min	Percentage of Delivered Energy	Delivered Energy lb-feet
0.0272	27.9	77.76	27.2
0.0269	28.1	76.96	26.9
0.0268	28.1	76.48	26.8
0.0271	28.1	77.55	27.1
0.0269	28.3	76.86	26.9
0.027	28.3	77.16	27
0.027	28.1	77.12	27
0.0268	28.2	76.45	26.8
0.0266	28.1	76.01	26.6
0.0269	27.8	76.88	26.9
0.027	27.9	77.2	27
0.0268	28.4	76.7	26.8
0.0275	28.3	78.67	27.5
0.0274	28.1	78.37	27.4
0.0282	27.8	80.53	28.2
0.0283	27.8	80.83	28.3
0.0286	28	81.85	28.6
0.0294	27.9	84.06	29.4
0.0292	27.8	83.43	29.2
0.0293	28	83.82	29.3
0.0295	28	84.39	29.5
0.03	27.9	85.77	30
0.0302	27.6	86.34	30.2
0.0305	27.8	87.27	30.5
0.0305	27.9	87.22	30.5
0.031	27.6	88.46	31
0.0317	27.5	90.45	31.7
0.0315	27.7	89.92	31.5
0.0319	27.8	91.03	31.9
0.0323	27.6	92.4	32.3
0.0326	27.5	93.21	32.6
0.0328	27.6	93.7	32.8
0.0331	27.7	94.71	33.1
0.0324	27.6	92.65	32.4
0.0326	27.2	93.23	32.6
0.0325	27.5	92.79	32.5
	Blows/min.	**% Energy**	**Energy**
Average	**27.9**	**83.8**	**29**
STDDEV	**0.274**	**6.5**	**2.3**
C. Variation	**0.98**	**8%**	**8%**

CHAPTER 5. MDPT-T TORQUE MEASUREMENT AND CORRELATION WITH SOIL STRENGTH PROPERTIES

5.0 Abstract

In-situ estimation of soil properties such as unit skin friction (*fs*) for pile foundation design is essential in sands and clay where undisturbed sampling is difficult to obtain. Many in-situ tests and design analysis methods and techniques have been developed to estimate unit skin friction, but they require heavy and costly equipment and often provide unsatisfactory results. The developed portable Mini Dynamic Penetration test with torque (MDPT-t) device was tested in the Coastal and Piedmont regions of North Carolina as an economical alternative for estimating the unit skin friction, the friction angle ϕ, and the cohesion in different soil layers. Many researchers have suggested that the estimated unit skin friction (*fs*) values from static pile load tests compared best with the directly measured (*fs*) from the in-situ tests.

The results from the MDPT-t in-situ tests are encouraging, as the correlations and measurements provided reasonable values of unit skin friction (*fs*) for different geologic regions. Extensive statistical analyses were performed to correlate the MDPT blow counts and the torsional torque values MDPT-t to estimate the soil properties for each layer.

5.1 Introduction

The use of in-situ tests for estimating the design parameters for deep foundations is important in situations where undisturbed sampling is difficult to obtain due to the limitations of sampling equipment, the different soils encountered, and the strength of material. This chapter presents the development of the MDPT-t device as an alternative tool for economical and convenient in-situ testing. The new test results can be correlated to conventional soil testing methods and can estimate the unit skin friction and other soil properties. Testing with this new device is quicker and more economical than with available tools.

This chapter focuses on the use of the MDPT-t for estimating soil parameters and unit skin friction in order to estimate the shaft skin friction of driven piles. Static analysis is typically used to determine the ultimate axial pile capacity. Axial bearing capacity includes the determination of the end bearing and shaft resistance of the pile. The shaft resistance is the side friction along the entire embedded length of the pile and is determined by multiplying the total pile surface area by unit skin friction (*fs*). This chapter also addresses the direct and indirect correlations between the in-situ MDPT-t torque (lb-ft) with the laboratory cohesion and the friction angle from the triaxial tests for the specific residual soils in the Greensboro U-2412B project.

The split spoon of the Standard Penetration Test with Torque (SPT-T) can be used to directly measure the unit skin friction (*fs*) between the spoon and the surrounding soil. The spoon is rotated to measure the maximum number of torques causing the rotation using a torque wrench or a torque measurement device mounted to the SPT. Engineers can use the torque measurement to calculate the unit skin friction at different elevations. Many researchers have correlated the unit skin friction (*fs*) from the SPT-T with the SPT N_{60}. However, the Mini Dynamic Penetration Test (MDPT) supplemented with the torque measurement (MDPT-t) also can be used to obtain a direct measurement of soil unit skin friction (*fs*) after rotating the cylindrical cone with a calibrated torque wrench more quickly and economically than with heavy and expensive equipment. The number of blow counts per ft of penetration (n) obtained from the MDPT during this test can also be empirically correlated to the N-value obtained from the Standard Penetration Test (SPT) or Cone Penetration Test (CPT).

Engineering soil properties such as soil strength, frictional resistance, friction angle, cohesion, and adhesion can also be correlated to SPT. The MDPT-t consists of a graduated

stainless-steel rod with a cone head 12 in- (305 mm-) long with on one end and an anvil attached to the other. A hammer weighing 17.5 lb (7.9kg) dropped from a height of 24 in (609 mm) is used to drive the device into the ground. The MDPT-t sketch and its components are shown in Chapter 6, Figures 6.1 and 6.2.

Testing involves driving the 12-in (305-mm) steel rod with the cone head into the soil layer to be tested and recording the number of blows for every 6 in (152 mm) of penetration. After driving the steel rod to a desired depth, a torque adapter is connected to the top of the steel rod extension, and a torque wrench is used to rotate the steel rod and record the maximum torque value (lb-ft). The driving and torque test is repeated to the desired depth. To measure the torque, the MDPT-t steel rod extension is rotated using an adapter and a calibrated torque wrench. The soil unit skin friction can be estimated from the torque measurements and steel rod dimensions, which is then used in pile design. Based on limited experience, the MDPT-t is found to be useful for both sand and clay to a depth of about 40-45 ft (13.7 m) depending on the soil stiffness.

5.2 MDPT Test Development

5.2.1 Problem

Geotechnical design depends on strength, stiffness, and other soil parameters. The use of conservatively estimated values of these parameters for design can increase construction costs, but realistic parameters obtained from appropriate in-situ testing can reduce these costs. The MDPT testing device may also provide a planning technique that will improve the subsurface investigation of a project before mobilizing expensive equipment. Studies have shown that estimating the direct unit skin friction in the field during the investigation stage will improve the calculation of the required pile length tremendously, while poor estimation of the unit skin friction will cause many constructions claims and errors in orders of pile length.

The MDPT-t device was developed with the following motivations:

- Portability for ease of access in many difficult terrains
- Estimation of the unit skin friction by using a calibrated torque wrench
- Easy evaluation of soil properties at different soil layers and depths

5.3 MDPT Development

The current practice for soil testing, according to FHWA, AASHTO, and almost all state DOTs, is the SPT and CPT for small or large projects; therefore, it was necessary to develop a portable and mini device to mimic both the SPT and CPT mechanism for a variety of correlations. The MDPT device was built to be small and portable, and designed to generate 10% of the SPT total energy of 350 ft-lb (48.4 kg-m). The SPT has a drop weight of 140 lb (63.5kg) and drop height of 30 in or 2.5 ft (762 mm), which generates an energy of 140 lb*2.5 ft = 350 ft-lb (48.4 kg-m).

The MDPT can be driven to 45± ft (13.7± m) below the ground surface with 5/8-in (16-mm) stainless steel rods extensions. The MDPT hammer configuration was designed to mimic the SPT tip and skin resistance behavior to produce 10% of the SPT total energy of 350 ft-lb. (48.4 kg-m). It consists of a 17.5-lb (7.9-kg) steel hammer that drops 2 ft (609 mm) to create 35 ft-lb (4.84 kg-m) energy.

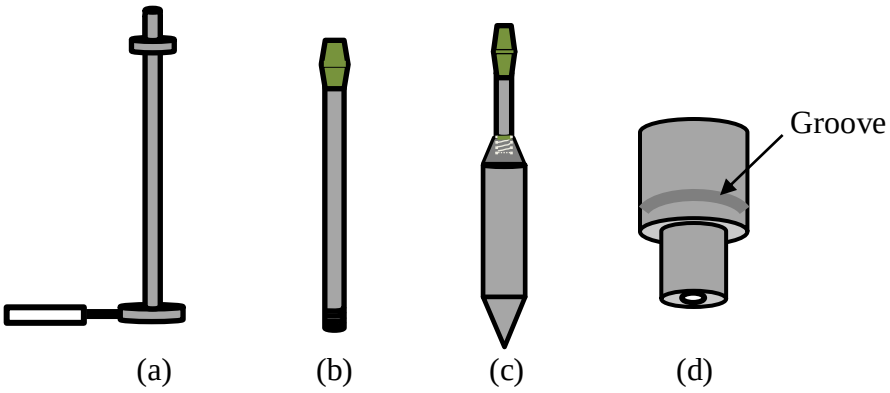

Figure 5.1 Sketch of the MDPT parts.

a) Top part with anvils provide 24-in (609 mm) drop height

b) Extension steel rod with coupler

c) Cylindrical shape with 60º cone head

d) Drop weight of 17.5 lb (7.9 kg) with groove.

Figure 5.2 Image of actual MDPT and torque wrench.

Figure 5.2 shows a schematic sketch of the MDPT. The MDPT can be operated manually or automatically using a gear-motor. Field testing indicated that the energy delivered to the rods during an SPT test can vary from 68%–94% of the theoretical maximum with an average of 81%. SPT resistance values are normalized to 60% energy, because the correlations made before the advent of hammer-system calibration had used safety hammers, and the correlations were

generally assumed to have been running at 60% efficiency to estimate N_{60}. The MDPT can be rotated with a torque wrench to estimate soil properties (MDPT-t), as described in Section 5.1.

5.4 Background and Literature Reviw

Geotechnical design engineers often prefer to use simple and quick charts and empirical methods to estimate soil properties to evaluate pile capacity. Most of the developed static analysis methods for estimating the axial capacity of the pile foundations have shown inconsistencies and poor results. The axial capacity of the pile consists of the skin friction and the tip bearing. Many researchers have investigated the use of the SPT-T to generate maximum torque by rotating the split spoon after driving to measure the maximum torque to evaluate the unit skin friction for each layer.

The SPT-T is an in-situ test to improve the SPT test procedure. Ranzine (1988) did some modifications to the SPT procedure and was the first to measure the torque to classify soil type. Torque was created by rotating the top of the drill rod and split spoon with a calibrated torque wrench after driving to fail the bonds between the split spoon and surrounding soil. The torque generated from rotating the split spoon with the torque wrench after driving was used to estimate the unit skin friction.

An ASTM standard for the SPT-T has yet to be developed. The current testing procedure for the SPT-T is based on the procedure developed by Bullock and Schmertmann (2003), Winter et al. (2005). Many other researchers have performed and studied the SPT-T (Decourt, 1992, 1994, 1998; Peixoto and Carvalho, 1999, studied and reported that the unit skin friction for concrete piles in unsaturated soil has good correlation with SPT-T unit skin friction; Lutenegger and Kelley, 1999; Kelley and Lutenegger 2005).

Most common in-situ tests such as the SPT-T are performed by using heavy drill rigs and calibrated torque wrenches in conventional drilled borings. The SPT-T test may involve a separate borehole to obtain soil data for correlation to a number of different design parameters, such as the angle of internal friction, shear strength, and unit skin friction. The torque test is a direct measurement of the unit skin friction and can assist in classifying the soil type.

5.4.1 Correlations Between SPT (N) Values and Soil Parameters

The earliest correlations between the SPT (N) value and the effective internal friction angle ϕ' to estimate the ϕ' were established by Meyerhof (1956) in form of tables (see Table 5.1). Almost two decades later, Peck, Hanson and Thornburn (1974) introduced a more conservative estimation of ϕ'as shown in Figure 5.3 and Table 5.1 (Peck et al.1974). Specifically, Table 5.1 shows the empirical correlations between the SPT N-value and the effective friction angle ϕ' of sand based on the relative density from very loose to very dense soil. The effective friction angle ϕ' increases in proportion to the SPT N-values.

Table 5.2 illustrates the relationship between the cone tip resistance (q_t) measured by the cone penetration test (CPT) and the effective friction angle ϕ' of sands for different relative density ranging from very loose to very dense. The trend is proportional: as the cone resistance increases, the effective friction angle increases.

Table 5.1 Relationship Between the SPT N-Value and Effective Friction Angle ϕ' of Sand.

SPT N-Value	0 to 4	4 to 10	10 to 30	30 to 50	>50
Compactness	Very loose	Loose	Medium	Dense	Very Dense
Relative Density Dr. (%)	0 to 15	15 to 35	35 to 65	65 to 85	85 to 100
Angle of Internal Friction (ϕ' After Peck et al. (1974)	< 28 °	28 ° to 30 °	30 ° to 36 °	36 ° to 40 °	>41 °
Angle of Internal Friction (ϕ') °After Meyerhof (1956)	< 30 °	30 ° to 35 °	35 ° to 40 °	40 ° to 45 °	>45 °

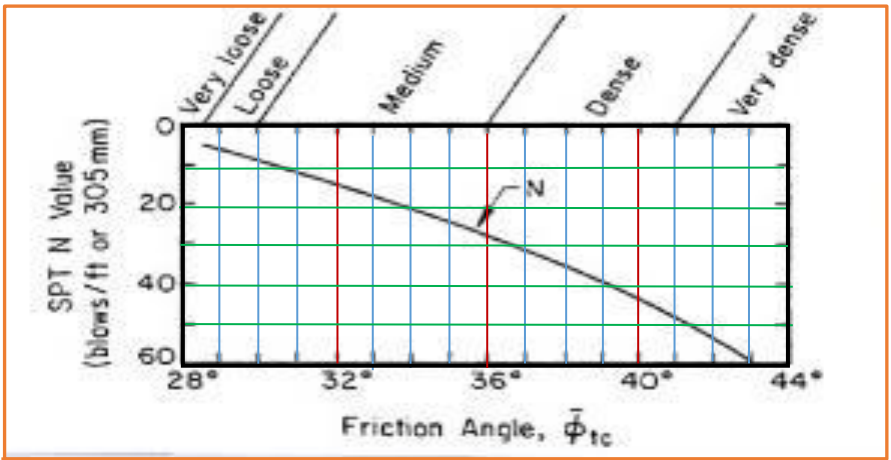

Figure 5.3 SPT N value vs. friction angle ϕ'. After Peck 1974

Table 5.2 Relationship Between Cone Tip Resistance q_t and Effective Friction Angle ϕ' of Sand (After Kulhawy and Mayne, 1990) Based On Relative Density.

Normalized Cone Tip Resistance (q_t /pa)	<20	20 to 40	40 to 120	120 to 200	>200
Compactness	Very loose	Loose	Medium	Dense	Very Dense
Relative Density Dr. (%)	0 to 15	15 to 35	35 to 65	65 to 85	85 to 100
Approximate effective friction angle (ϕ') ° After Meyerhof (1956)	< 30 °	30 ° to 35 °	35 ° to 40 °	40 ° to 45 °	>45 °

Undrained Young's Modulus:

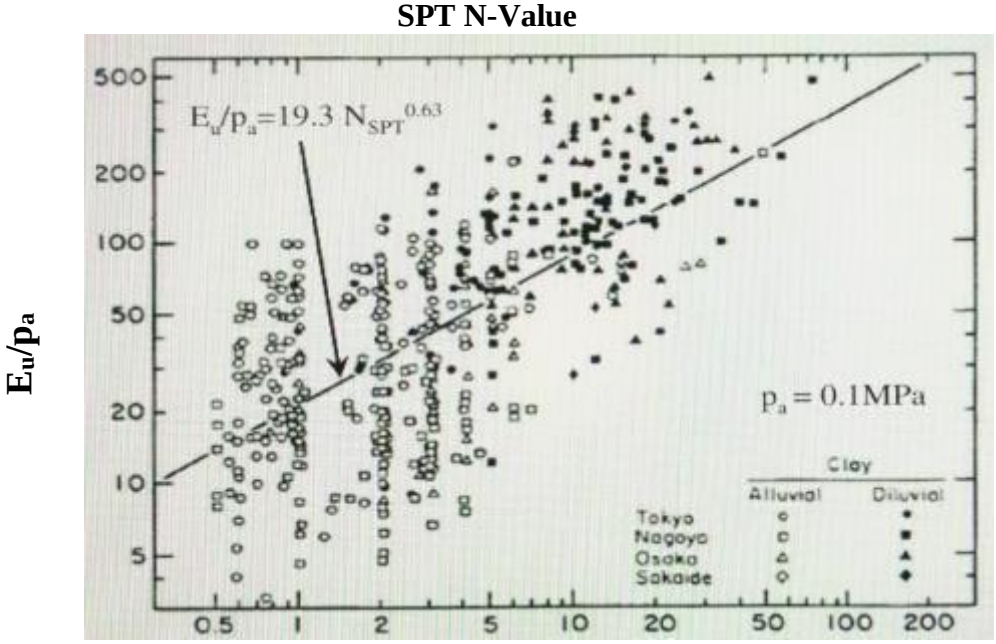

Figure 5.4 Regression between the SPT N-value and undrained Young's modulus of clay (after Ohya et al., 1982; Kulhawy and Mayne 1990; Phoon and Kulhawy 1999b).

Mair and Wood (1987), Briaud (1992), Wang and O'Rourke (2007) reported that the undrained young modulus can be measured directly using in-situ pressuremeter tests; however, this test is very expensive and time-consuming.

Kulhawy and Mayne (1990), Clayton (1995), and Mayne et al. (2002) used empirical correlations to estimate the Young's modulus for small projects using the typical SPT tests. Figure 5.4 shows the correlation between the measured Eu using pressuremeter tests and the N-values.

$$E_u/pa = 19.3\ N_{\mathbf{spt}}^{0.63} \qquad (5.1)$$

where Eu is the estimated Young's modulus, pa is the atmospheric pressure (pa= 100 kPa), and N is the SPT blow counts per ft.

5.4.2 Unit Side Friction (Skin) from SPT

Vesic's (1970) empirical approach to estimate the unit skin friction using the relative density Dr. is as follows:

$$fs \text{ (tsf)} = 1.5 * 0.08(10)^{1.5Dr^4} \text{ for driven piles} \qquad (5.2)$$

Meyerhof (1956, 1976) was one of the first engineers to study and report the conservative empirical relationship between the SPT N-value and the unit skin friction (*fs*) for both driven and bored piles in granular soils. Meyerhof (1976) presented the following correlations:

$$fs = N_{avg}/50 \quad \text{(for driven piles)} \qquad (5.3)$$

$$fs = N_{avg}/100 \quad \text{(for bored piles)} \qquad (5.4)$$

where *fs* is the unit side or skin friction (tsf) and N_{avg} is the average SPT N-value over the length of the pile.

The above correlation was based on full-scale loading tests to calculate the values of *fs* and the average values of N_{avg}. Equations 5.3 and 5.4 can be rewritten in SI units as:

$$fs = 1.91N_{avg} \quad \text{(for driven piles)} \qquad (5.5)$$

$$fs = 0.96N_{avg} \quad \text{(for bored piles)} \qquad (5.6)$$

where *fs* is the unit side resistance (kPa).

One of the concerns about the above correlations is that the average SPT N-values used by Meyerhof (1956, 1976) were typically obtained from older drill rigs which used manual hammers and produced lower energy levels upon impact compared with new automatic hammers which produce higher energy levels.

Poulos (1989) summarized many reported correlations between pile side resistance and SPT-N values and provided the following general equation:

$$fs = \beta + \alpha N \qquad (5.7)$$

Alan J. Lutenegger (2009) summarized the work completed by other authors and researchers about the correlations between SPT- N values and unit side skin friction for both driven and bored piles for different soil types, as shown in Table 5.3. The variation of the reported values of β shown in Table 5.3 are quite large and will be difficult to use without any clarification and correction. However, general observations can be concluded from Table 5.3:

1. Table 5.3 has 37 different correlations for β and α.
2. The value of β is equal to zero (0.0) for 27 of the 37 correlations and the remaining range is from 10 to 35.

Using zero for β will simplify Equation 5.7 with minimal impact on the correlation to Equation 5.8.

$$fs = \alpha N \qquad (5.8)$$

The high variation of α, as shown in Table 5.3, is due to the variabilities of both the pile data and the SPT data.

The recommendation was to use the correlations in Table 5.3 with caution; therefore, developing different methods and improving the SPT procedure is necessary for improving estimation of the soil properties and the bearing capacity of pile foundations. The MDPT-t will improve the SPT and provide unique and valuable information to designers at any time during the planning, investigation, design, and construction stages. The device is small, portable, and can be operated by one person. The MDPT offers many ways of testing and estimating the soil strength and properties.

Table 5.3 Reported Correlations Between SPT N-Value and Pile Side Resistance (Lutenegger, 2009).

Pile Type	Soil	β	α	Reference
driven displacement	granular	0	2.0	Meyerhof (1976)
	miscellaneous soils (f_s < 170 kPa)	10	3.3	Decourt (1982)
	cohesive	0	10	Shioi & Fukui (1982)
	cohesive cohesionless	0 0	3 1.8	Bazaraa & Kurkur(1986)
	sandy clayey	29 34	2.0 4.0	Kanai & Yubuuchi (1989)
	misc	0	1.9	Robert (1997)
Bored	granular	0	1.0	Meyerhof (1976)
	granular	55	5.8	Fujita et al. (1977)
	cohesionless	0	3.3	Wright & Reese (1979)
	cohesive (f_s < 170 kPa)	10	3.3	Decourt (1982)
	cohesive	0	5.0	Shioi & Fukui (1982)
	cohesive cohesionless	0 0	1.8 0.6	Bazaraa & Kurkur (1986)
	residual soil & weathered rock	0	2.0	Broms et al. (1988)
	clay sand	0 0	1.3 0.3	Koike et al. (1988)
	sandy soil cohesive	35 24	3.9 4.9	Kanai & Yubuuchi (1989)
	residual soil	0	4.5	Winter et al. (1989)
	gravel sand silt clay	0 0 0 0	6.0 4.0 2.5 1.0	Hirayama (1990)
	residual soils	0	2.0	chang & Broms (1991)
	clayey soil sandy soil	0 0	10.0 3.0	Matsui (1993)
	misc.	17.3 18.2	1.18 0.65	Vrymoed (1994)
	misc.	0	1.9	Robert (1997)
	sand	0	5.05	Kuwabara & Tanaka (1998)
	weathered rock	0	4	Wada (2003)
Cast-in-Place	cohesionless cohesive	0 0	5.0 10.0	Shoi & Fukui (1982)
	cohesionless (f_s < 200 kPa) cohesive	30 0	2.0 5.0	Yamashita et al.(1987)

Note: $fs = \beta + \alpha N$ (fs in units of kPa)

5.5 Theoretical Development

An important aspect of the SPT-T testing mechanism is the shear resistance between the split spoon and the soil at their interface. Kishida and Uesugi (1987) and Subba Rao et al. (2002) studied and evaluated the shear strength between steel and soils in Japan. Tsubakihara et al. (1993) developed relationships of the coefficient of friction and roughness in clay and sand-clay soils. Other researchers such as Maksoud (2006) and Soni and Salokhe (2006) published the relationship between soil and steel. Maksoud (2006) developed the relationship between soil adhesion, soil-steel friction angle, and soil shear strength.

For the MDPT-t test, the torque force gradually increases when using a torque wrench to rotate the cylindrical cone until it overcomes the resistance from the soil to identify the maximum torque force at the desired depth. The analysis used the free-body diagram shown in Figure 5.5, which illustrates the process for applying the maximum torque to the system to cause failure as the system rotates by exceeding τ_{SIDE} and τ_{TIP}.

The direction of the applied maximum torque rotates the cylindrical cone in the opposite direction of the shearing stresses on the interfaces. The shearing stresses form along a cylindrical cone, as shown in Figure 5.7. The shear surfaces are at the interface between the soil and the side of the cylindrical cone ($A1_{SIDE}$) and cone head ($A2_{TIP}$), as shown in Figures 5.6 and 5.7. The cylindrical side shear provides most of the resistance (the surface area of the cone head is very small); therefore, Equation 5.11 ignores any contribution to the torque measurement from the cone head surface area at the base (tip) of the cone (ignore $A2_{TIP}$).

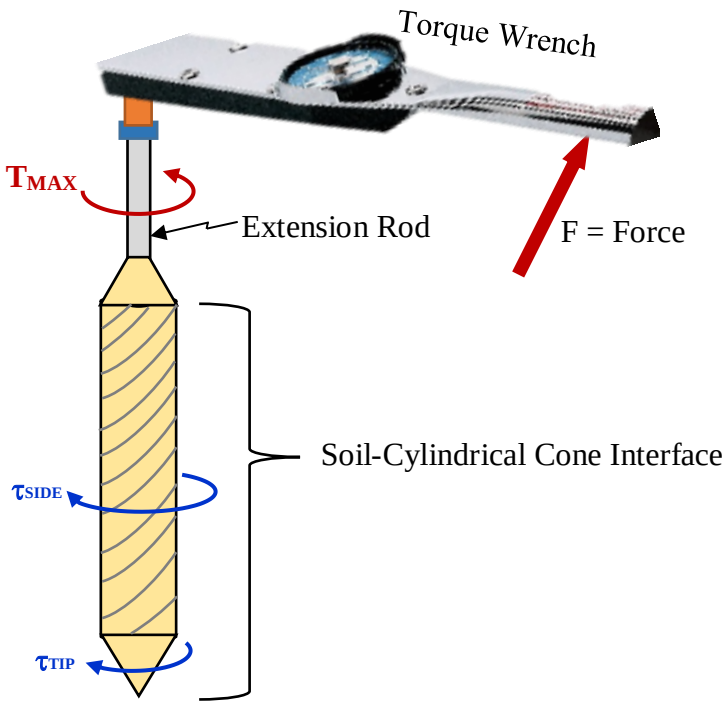

Figure 5.5 Free-body diagram of the MDPT-t torque test.

The typical definition of torque is defined as a moment or moment force. The moment is calculated simply by multiplying the force by the arm. From Figure 5.5:

$$T_{MAX} = F \times r \qquad (5.9)$$

where T_{MAX} is the maximum measured torque (at the top of the adapter rod), F is the force, r is the arm (is the 0.5d) half the diameter of the cone, and d is the diameter of the cone = 2.5 cm (1 in).

From Equation 5.9, the force from the measured torque can be calculated by dividing the measured torque by the moment arm, as shown in Equation 5.10.

$$F = T_{MAX} / r \qquad (5.10)$$

The unit side friction (*fs* $=\tau_{SIDE}$) acting on the cone surface area may be obtained by dividing the force (F) by the cone surface area (A1):

$$fs = \frac{F}{0.5d * A1} \quad (5.11)$$

where A1 is the cylindrical cone surface area.

$$A1_{SIDE} = (2*\pi*0.5d*L) = (\pi*d*L) \quad (5.12)$$

where L is the length of penetrated cone = 1 ft, h is 1 in, and d is 1 in.

$$fs = \frac{2T}{\pi d^2 L} \quad (5.13)$$

The relationship between T_{MAX} and τ_{SIDE} is expressed in Equation 5.14.

$$T_{MAX} = \boldsymbol{\tau_{SIDE}} (A1_{SIDE}) \quad (5.14)$$

Equation 5.14 can be written as

$$T_{MAX} = \boldsymbol{\tau_{SIDE}} (2 *\pi* r* L)* r \quad (5.15)$$

or

$$T_{MAX} = \boldsymbol{\tau_{SIDE}} (0.5*\pi*d*L)*d$$

Figure 5.6 shows the dimensions and parameters, where L is the length of the cylindrical shape, r is the radius, and h is the height of the cone shape at the base.

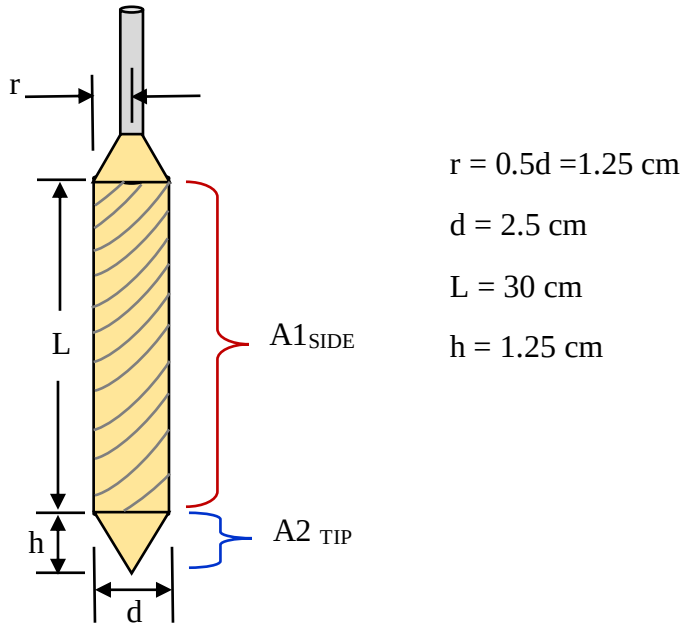

Figure 5.6 Dimensions and parameters of the MDPT-t torque test.

5.5.1 Analysis Using Soil Mechanics

The MDPT-t tests were performed to estimate the direct values of unit skin friction by using a torque wrench to rotate the steel cylindrical cone shape after driving to measure the corresponding maximum torque. In this sense, the MDPT-t acts as a mini pipe pile.

5.5.2 Typical Load Capacity of Single Piles

There are two forms of soil resistance provided by the pile to the applied axial loads: shaft resistance and base resistance. Driven piles will mobilize the ultimate skin and tip resistance at each soil layer. The ultimate bearing capacity can be written as:

$$Qu = Qs + Qb \qquad (5.16)$$

where Qu is the ultimate pile capacity, Qs is the ultimate shaft resistance, and Qb is the ultimate base resistance.

Many researchers have studied and developed expressions for skin friction based on effective stress methods for driven piles in soft clay due to pore pressure dissipation. Chandler

(1968) suggested using a design method based on the effective stress method, which assumes the interface soil is failing in shear.

$$\tau_{skin} = C_u \, COS \, \phi' \qquad (5.17)$$

The value of the C_u is the undrained shear strength during the pile installtion before pore water pressure dissipation. The value of the C_u will depend on the degree of the adjacent soil remoulding during or after pile installation and the amount of strength gain from pore water pressure dissipation. Therefore, the value of the undrained shear strength in Equation 5.17 could be greater or less than the actual value of the undisturbed soil.

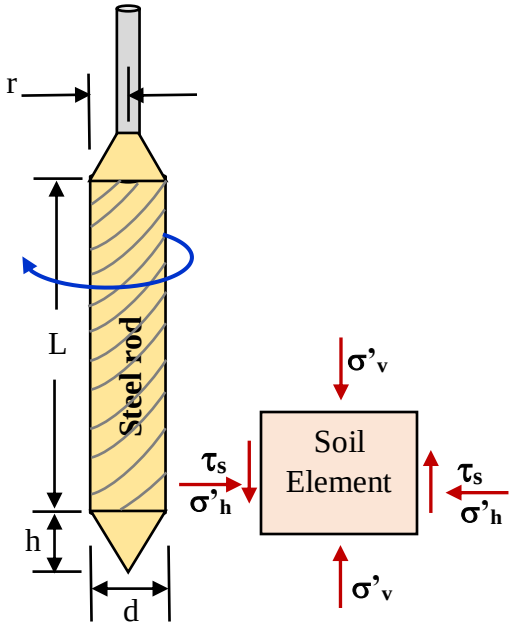

Figure 5.7 Stress on a soil element adjacent to the steel rod after driving and torqueing.

The focus of this research is to estimate the unit skin friction to determine the shaft resistance of the pile or the MDPT-t. Therefore, Qs is the shear strength of the soil multiplied by the surface area of shaft (MDPT-t) in contact with the soil.

For clay layers: $Qs = C_a * d * L$ (5.18)

For sand layers: $Qs = fs * d * L$ (5.19)

where C_a is the adhesion, *fs* is the unit skin friction, d is the diameter of the pile, and L is the length of pile in contact with the soil.

The soil mechanics theory indicates that the ultimate shaft friction for driven piles is related to the horizontal effective stress (σ'_h) acting on the shaft and the effective angle of friction between the pile and the soil (δ). Thus,

$$\tau_{SIDE} = Ca + \sigma'_h \tan(\delta) \quad (5.20)$$

where τ_{SIDE} is the unit shaft friction at any point.

A further simplifying assumption is made that σ'_h is proportional to the vertical effective overburden pressure σ'_v. Thus,

$$\sigma'_h = K\sigma'_v \quad (5.21)$$

$$\tau_{SIDE} = K\sigma'_v \tan(\delta) \text{ in sand} \quad (5.22)$$

where K is the earth pressure coefficient (see Figure 5.8).

The τ_{SIDE} is found using Equation 5.23, where C_a is the adhesion between the cylindrical shape and the soil (steel and soil), σ'_v is the effective vertical stress, and δ is the soil-steel interface friction angle.

$$\tau_{SIDE} = C_a + K\sigma'_v \tan(\delta) \text{ in clay} \quad (5.23)$$

$$\sigma'_v = \gamma * z \quad (5.24)$$

Adhesion between the soil and the steel rod can be estimated by using Figure 5.9 with a known cohesion value.

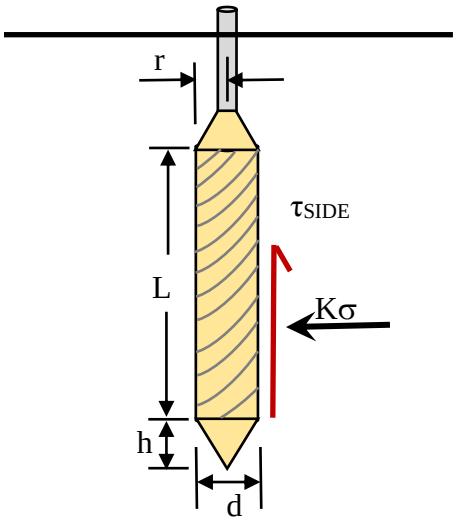

Figure 5.8 Dimensions, parameters and side resistance of the MDPT-t torque test.

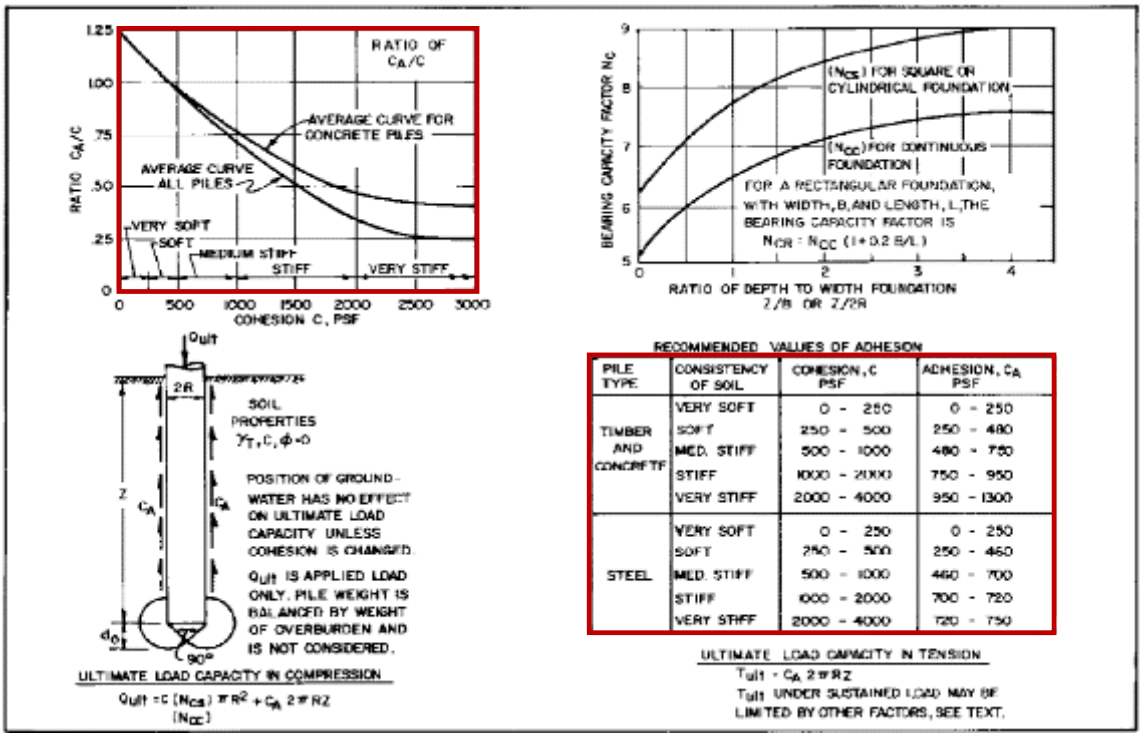

PILE TYPE	CONSISTENCY OF SOIL	COHESION, C PSF	ADHESION, C_A PSF
TIMBER AND CONCRETE	VERY SOFT	0 - 250	0 - 250
	SOFT	250 - 500	250 - 480
	MED. STIFF	500 - 1000	480 - 750
	STIFF	1000 - 2000	750 - 950
	VERY STIFF	2000 - 4000	950 - 1300
STEEL	VERY SOFT	0 - 250	0 - 250
	SOFT	250 - 500	250 - 460
	MED. STIFF	500 - 1000	460 - 700
	STIFF	1000 - 2000	700 - 720
	VERY STIFF	2000 - 4000	720 - 750

Figure 5.9 Ultimate load capacity of a single pile or pier in cohesive soils and adhesion values. (Figure 2 of the Navy Design Manual 7.2, page 196, 1986.)

5.6 Torque Test Procedure (MDPT-t)

MDPT-t can be used to determine the skin friction between steel and soil using a similar relation as the vane shear test equation. Figure 5.10 shows the MDPT schematic sketch. Equation

5.13 can be used to estimate the unit skin friction using the measured torque from the MDPT-t device.

$$fs = \frac{2\,T}{\pi d^2 L} \qquad (5.13)$$

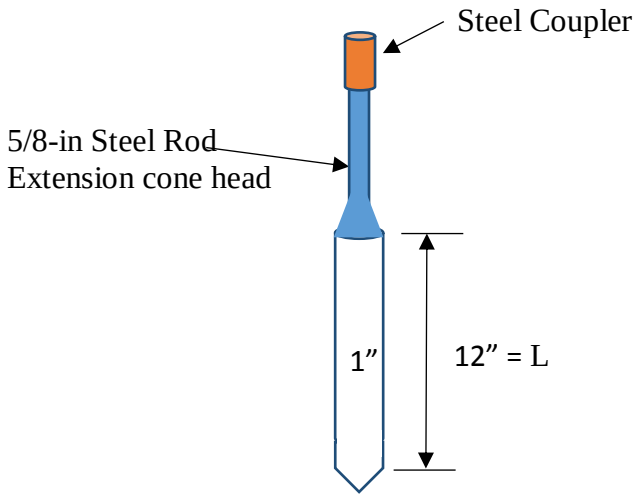

Figure 5.10 MDPT Schematic sketch.

where *fs* is the unit skin friction, T is the maximum measured torque (ft-lb), L is the length of the 1 in-thick steel rod with cone head (L=12 in), and D is the outer diameter of the steel rod (d = 1 in).

Equation 5.13 ignores any soil friction from the steel couplers for the steel rod extension due to the size of the couplers. The torque may be affected by the elastic deformation of the steel rods due to the length, as well as the many threaded connections at the coupler locations.

5.6.1 MDPT-t Torque Rotation Procedure

Rausche et al. (1996) reported that torque rotation of 180º is adequate to reach the maximum value of adhesion, which typically occurs between 5º–10º. The filed test of the MDPT-t was performed according to the following steps:

1. Drive the MDPT cone to the desired depth.
2. Place adapter to the top of MDPT rod to attach a torque wrench to the adapter, and then turn the rods at a slow but continuous rate.
3. Measure torque by taking readings at intervals of 10–20 s. Once the maximum torque is achieved and locked, rotate the wrench 360º twice. Adequate results can be achieved at a rotation speed ranging 5–8 rpm. Figure 5.11 illustrates the schematic sequence of the torque test.

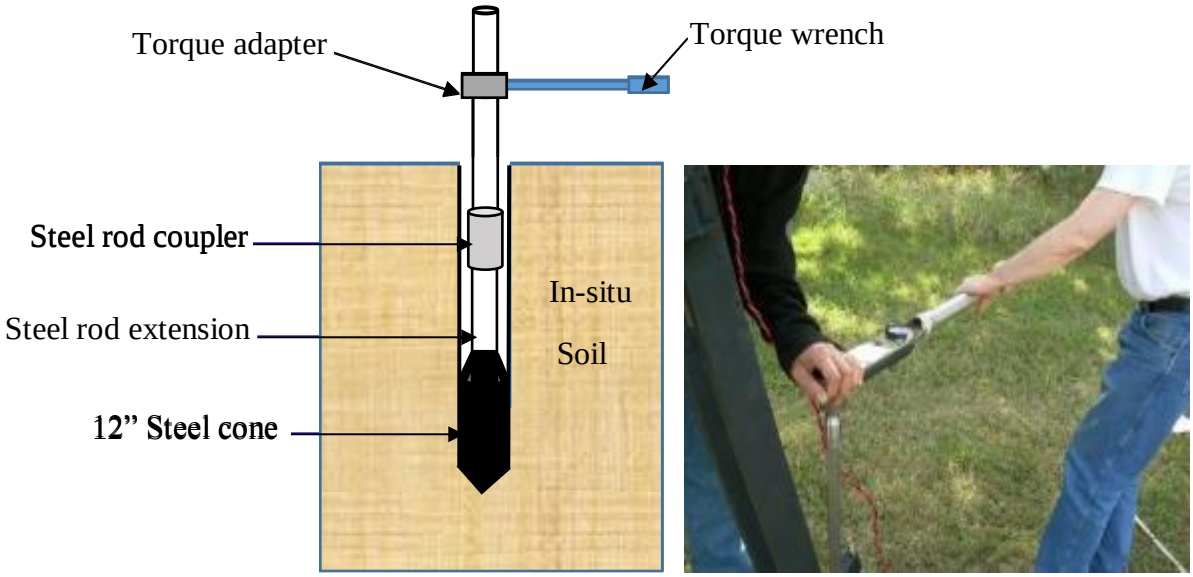

Figure 5.11 Schematic of torque test and image of torque wrench during testing.

5.7 In-situ Testing Program

5.7.1 Test Areas and Soil Description

The test areas were divided into three sections, as described below. The data for the first two sections obtained from 14 counties in North Carolina are presented here. The data are for the sites that represent two geological regions of the state: the Coastal Plain and the Piedmont. The locations of the torque test sites are presented in Figure 5.12 marked in pink circles.

Section One: The Coastal Plain geology consists mostly of marine sedimentary rock, which is usually overlain by sand and clay. The materials are primarily sand and clay from oceans and rivers that have been laid down over many thousands of years. The depths of Coastal regions range from 13 ft (3.96 m)–30 ft (9 m), with an average depth of 20 ft (6 m).

Section Two: The Piedmont is the middle region of North Carolina, located between the Coastal Plain and the Mountain regions. Piedmont is a French word meaning "foot of the mountain"; therefore, the Piedmont region lies between the foot of the mountains and the Coastal Plain regions. The materials typically consist of interbedded sands, silts, and clays. Clays can be low to highly plastic, and in some cases, may be over-consolidated. The above-soil formations are ideal for in-situ testing due to the lack of very stiff/hard soils and rock.

Figure 5.12 Location of Section Three test site in two different regions within North Carolina (pink circles).

Section Three: The data was obtained from NCDOT project U-2412B, located in the Piedmont region, at Alamance Road, Greensboro, Guilford County, in North Carolina. This site was selected because of another study, "The Design of Temporary Slopes Excavations in Residual Soils" conducted by North Carolina State University for NCDOT by Dr. Roy Borden and Dr. Mohammed Gabr. NCDOT retrieved 94 Shelby tubes (ST) from ten different borings from station 403+45 to station 405+70 (3 ft–94 ft right of center line). The tubes were extracted from depths ranging from 2–52 ft. (0.6 m–15.5 m). The Material and Test Unit of the NCDOT laboratory performed the CIU triaxial test and consolidation test on 20 Shelby tubes. Table 5.6

shows the CIU triaxial tests locations, depths, ST number, and soil classification for each test; the soil is described below.

5.7.1.1 Physiography and Geology

The project was located in the gently rolling terrain of the Piedmont Physiographic Province. Geologically, the project was located within the Carolina Slate Belt. Soils within the Slate Belt are derived from the underlying metamorphosed granite, diorite, and gabbro intrusions. Rocks in the Carolina Slate Belt are generally foliated and trend in a northeasterly direction.

5.7.1.2 Soil Properties

The soil at this site is considered a residual soil, with mostly red silty clay at shallower depths and tan sandy silt at deeper depths. The soils according to the AASHTO classification at this site are divided into three main groups, A-4, A-5, and A-7-5, and to USCS classifications to ML and MH, as shown in Table 5.6.

Alluvial soils occur where streams cross the project corridor. These soils consist primarily of sandy clay that is brown to gray, soft to medium stiff, and moist to wet, (A-5) and of silty clay that is tan-brown, soft, and moist to saturated (A-7-5).

Residual soils are derived from the weathering of underlying metamorphosed granite, diorite, and gabbro intrusions. These soils consist of sandy and silty clay that is gray, orange, red to red-brown and tan-brown to yellow-brown, moist to wet, and medium stiff to very stiff, (A-5, A-7-5), and sandy silt that is tan-brown, gray and white, moist to wet, and soft to very stiff (A-4/A-5). The soils also consist of smaller amounts of silty sand that is tan, brown, white and yellow-tan, dry to moist, and medium dense to very dense (A-2-4). The surficial residual silty

clays exhibit moderate to high plastic indices. Residual soils grade into weathered rock, which retains the characteristics of the metamorphosed intrusions.

5.7.2 Grain Size Distribution for the Guilford County Soils

The predominate soils at the Guilford County project are mainly red silty clay and tan sandy silt. The soil at shallower depths experienced a higher degree of weathering, which results in a higher percentage of finer particles. The soil at deeper depths was less exposed to weathering and thus has lower fines content.

In soil mechanics, the soil type can be determined by the size of the grains. Grain size distribution (GSD) information can be used to estimate rough soil engineering properties such as permeability and strength. Sands may be either poorly graded (uniformly graded) or well graded depending on the value of the coefficient of curvature and the coefficient of uniformity.
The coefficient of gradation (curvature) (Cc) may be estimated as:

$$C_c = \frac{D_{30}{}^2}{D_{10} \times D_{60}} \tag{5.25}$$

The coefficient of curvature ($1 < C_c < 3$) will range between 1–3 for well-graded sand. The coefficient of uniformity (C_u) is given by:

$$C_u = \frac{D_{60}}{D_{10}} \tag{5.26}$$

Soils with $C_u \geq 6$ are considered to be well-graded or uniform,

where D60 is the particle size at 60% finer, D30 is the particle size at 30% finer, and D10 is the particle size at 10% finer.

For a sand to be classified as well graded, the following criteria must be met:

$$C_u \geq 6 \text{ and } 1 < C_c < 3$$

If both of these criteria are not met, the sand is classified as poorly graded (SP). If both of these criteria are met, the sand is classified as well-graded (SW).

Table 5.4 shows the soil gradations used in this project. The grain size distribution was analyzed according to ASTM (D422-2000) specifications. The soil was classified as uniformly graded sand; the grain size distribution is shown in Figures 5.13, 5.14, and 5.15.

Table 5.4 Gradation and Information for the Three Types of Residual Soil.

Soil Type	D_{10}	D_{30}	D_{60}	$C_u > 6$	C_c	$1 < C_c < 3$
A-4	0.006	0.06	0.09	15	7	No = SP
A-5	0.005	0.02	0.06	12	1	Yes = SW
A-7-5	0.003	0.04	0.065	22	8	No = SP

Many researchers, including Randolph et al. (1994), have indicated that the magnitude of the interface friction angle (δ) between the soil and the steel cone is affected by the grain size distribution of the soil. The typical value of the δ is ranges between 0.6 to 0.7 multiply by the peak effective friction angle of sand ϕ ($\delta = 0.6 - 0.7 * \phi$). The shear test is routinely used to estimate δ for a variety of sand and steel surfaces. Some key factors have a major influence on the pile-soil interface friction angle, including the type and particle size distribution of the sand and the surface roughness.

The value of the interface friction angle (δ) decreases with increasing mean particle size (d_{50}). The interface friction angle (δ) typically ranges between 28°–29° for sand, as suggested by Jardine et al. (2005).

The pore water pressure will be affected by the grain size distribution (GSD). Poorly graded soil will have less pore water pressure build up during the driving of the MDPT (pile) due

to the presence of void spaces in this type of soil. Table 5.4 shows soil A-4 and A-7-5 as a poorly graded soil, and soil A-5 as a well-graded soil. In addition, the grain size of the soil will have impact on the compaction of roadway embankment fill and retaining wall backfill material. A well-graded soil typically will compact better than a poorly graded soil; therefore, most of these projects will have specific soil gradation requirements that must be met before placement.

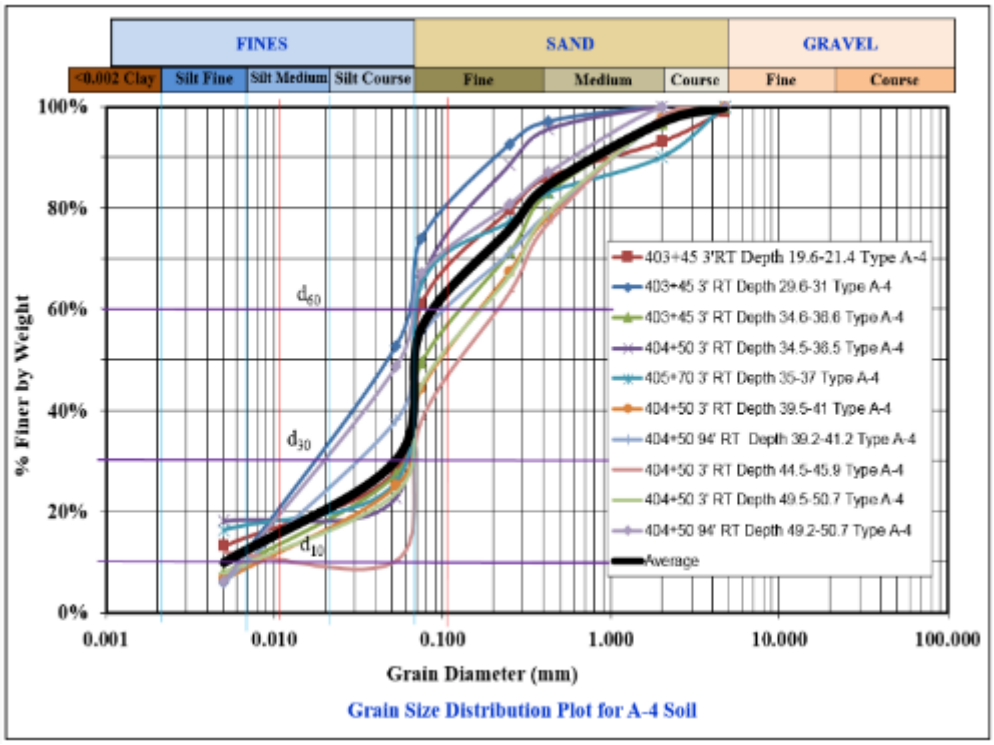

Figure 5.13 Grain size distribution of A-4 soil.

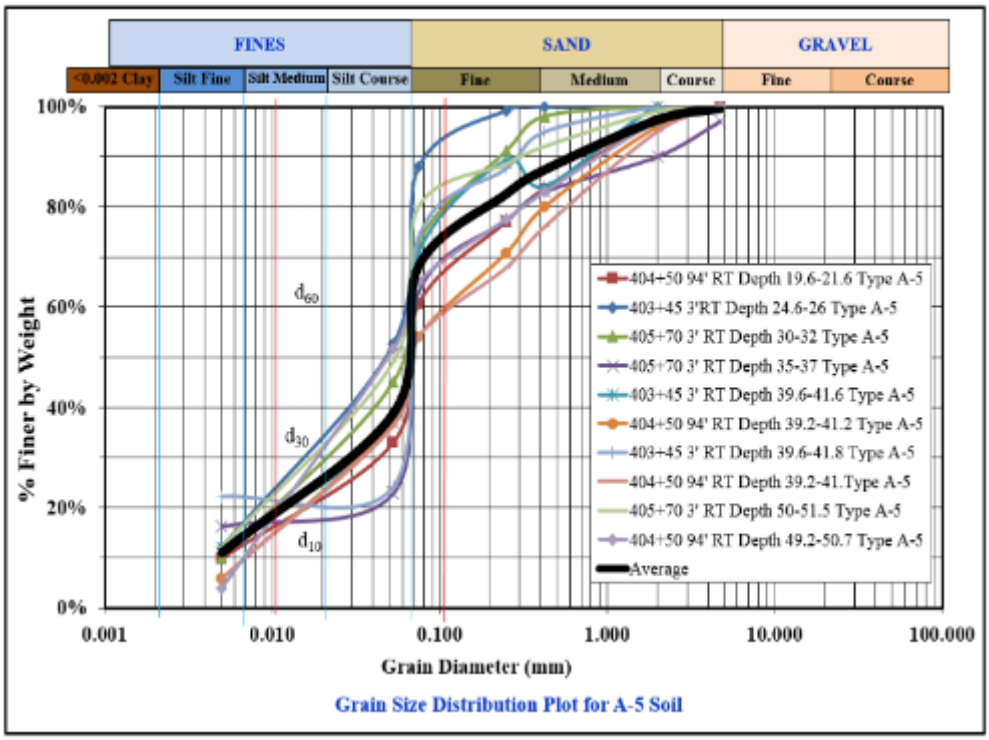

Figure 5.14 Grain size distribution of A-5 soil.

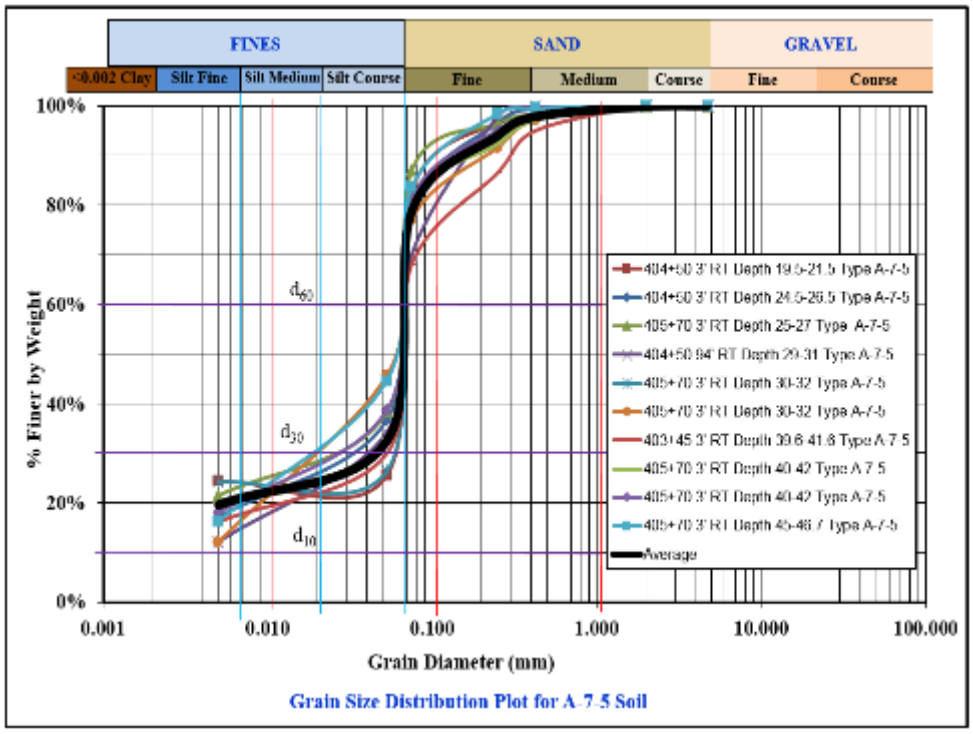

Figure 5.15 Grain size distribution of A-7-5 soil.

5.8 Torque Data Reduction

The author was the only person to perform the torque test throughout the test program in order to limit the variability of the maximum torque applied on each test. The force was applied using a 2-ft (0.91-m) torque wrench from the centerline of the MDPT extension steel rod (center line of hole). The torque wrench was rotated carefully to apply consistent force at a steady rate. The torque was completed by rotating 360º in order to prevent a false reading. After completing each test, the field data was compiled and transferred to a Microsoft Excel spreadsheet.

5.9 Triaxial Shear Testing and Soil Classification

The site of the U-2412B project in Guilford County was used for the shallow slope research. The research was performed by North Carolina State University (NCSU) for NCDOT. The NCDOT Geotechnical Engineering Unit and NCSU prepared and collected more than 100 Shelby tubes at different stations for different depths. The NCDOT Material and Test Unit has performed many triaxial and soil quality tests at different depths. The detailed laboratory tests and soil properties for each Shelby tube are listed in Tables 5.5 and 5.6 summarizes the soil type and soil classification performed by the NCDOT Material and Test Unit laboratory.

Table 5.5 Summary of the Soil Classification for the Greensboro Site.

Stations	Depth (ft)	Sample NO.	AASHTO Classification	USCS Classifications
403+45	29.6 - 31	ST-22	A-4(7)	ML
403+45	34.6 - 36.6	ST-23	A-4(0)	
404+50	34.5 - 36.5	ST-13	A-4(5)	
404+50	39.5 - 41	ST-14	A-4(0)	
404+50	39.2 - 41.2	ST-33	A-4(2)	
403+45	24.6 - 26	ST-21	A-5(4)	ML
403+45	39.6 - 41.6	ST-24	A-5(6)	
404+50	19.6 - 21.6	ST-29	A-5(2)	
404+50	19.5 - 21.5	ST-11	A-7-5(20)	MH
404+50	24.5 26.5	ST-12	A-7-5(13)	
405+70	25 - 27	ST-2	A-7-5(21)	
405+70	30 - 32	ST-3	A-7-5(17)	
405+70	30 - 32	ST-3	A-7-5(14)	
405+70	40 - 42	ST-5	A-7-6(13)	

Station	Depth (ft)	Sample No.	AASHTO Classification	USCS Classifications
403+45	29.6 - 31	ST-22	A-4(7)	ML
404+50	39.2 - 41.2	ST-33	A-4(2)	
403+45	24.6 - 26	ST-21	A-5(4)	ML
403+45	39.6 - 41.6	ST-24	A-5(6)	
404+50	19.5 - 21.5	ST-11	A-7-5(20)	MH
404+50	29 - 31	ST-31	A-7-5(12)	
405+70	25 - 27	ST-2	A-7-5(21)	
405+70	30 - 32	ST-3	A-7-5(17)	
405+70	30 - 32	ST-3	A-7-5(14)	
405+70	40 - 42	ST-5	A-7-6(13)	

5.10 Results and Discussion

The MDPT can produce a direct measurement of the unit skin friction from the torque test, as shown in Figure 5.5. The objective of the research described in this chapter was to measure and evaluate the in-situ torque or unit skin friction and correlate it to the MDPT blow counts and to the triaxial tests for the Greensboro project. As previously described, the in-situ torque test and the unit skin friction test was conducted by connecting the torque wrench to the MDPT extension rod with an adapter, and then slowly rotating the torque wrench to measure the torque. The rotation must be performed with controlled techniques to produce adequate results.

The test program was divided into three steps. The first step was to conduct a preliminary torque test to determine if there is any relationship between the MDPT blow counts and the torque measured. The initial test results were promising and reasonable for a simple relationship between the MDPT-t and the MDPT blow counts, as shown in Figure 5.16 and Figure 5.17. The torque ft-lb can be converted to unit skin friction, as shown in Figure 5.17.

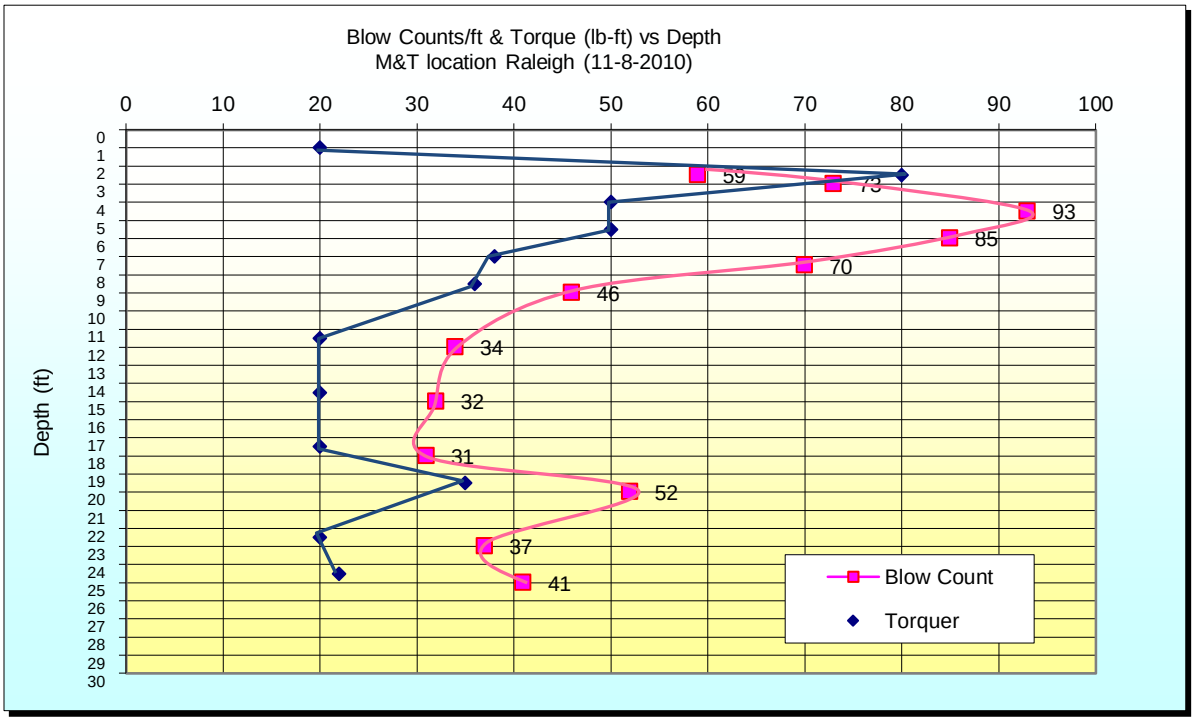

Figure 5.16 MDPT blow counts and measured torque at different depths.

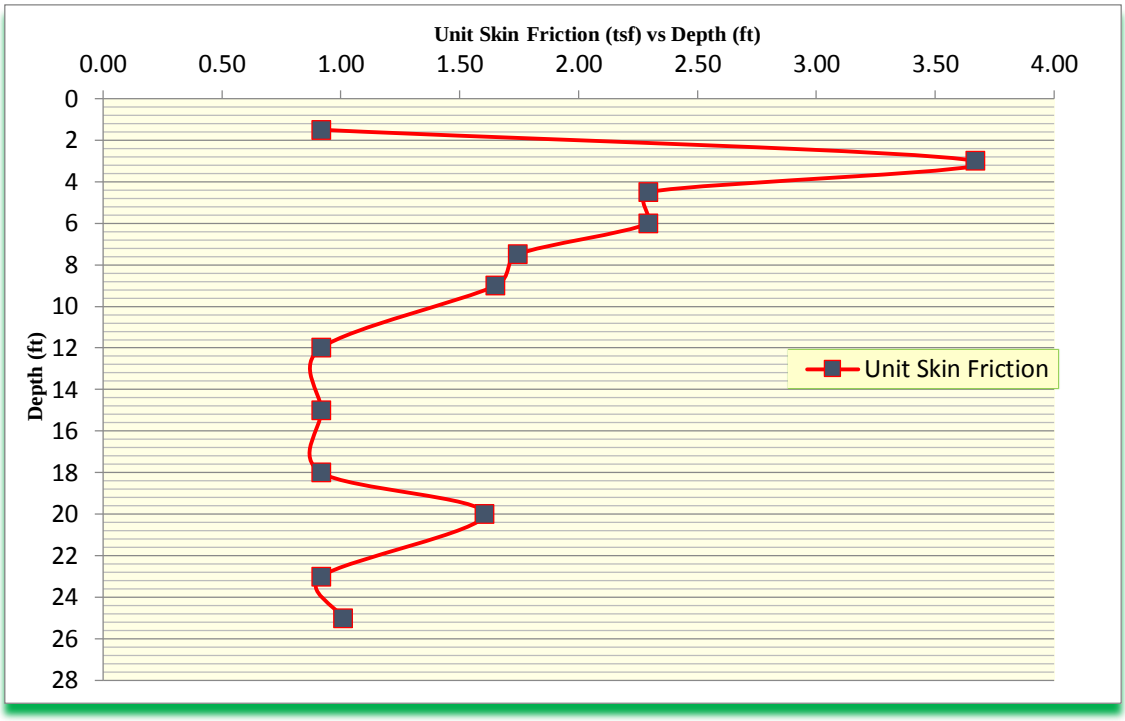

Figure 5.17 Unit skin friction (tsf) from torque at different depths.

The second step was to develop a test program to measure and evaluate the torque in the Coastal and the Piedmont regions in North Carolina. The objective was to correlate the MDPT-n blow counts per ft to the measured torque from the MDP-T tests.

Figures 5.19 A and B show plots of the test results from more than 14 counties in the Piedmont and Coastal regions. Each point on the graph represents different locations and different depths. The data was compiled for statistical analysis. Figures 5.19 A and B show simple linear correlations between the measured torque from MDPT-t and the blow counts from the MDPT for the Coastal and Piedmont regions. The R^2 was 0.92 and 0.93 for the Piedmont and the Coastal regions, respectively. The difference for R^2 was based on the soil characteristics of each region, and thus the correlation is soil-specific or region-specific. The CPT test provided a similar conclusion between the ratio of the local sleeve friction and soil type, as shown in Figure 5.18. The lower the ratio of the sleeve friction to tip resistance represents sand and gravel. The

Coastal geology is mainly sand and the Piedmont geology is mainly residual soil consisting of silt and clay.

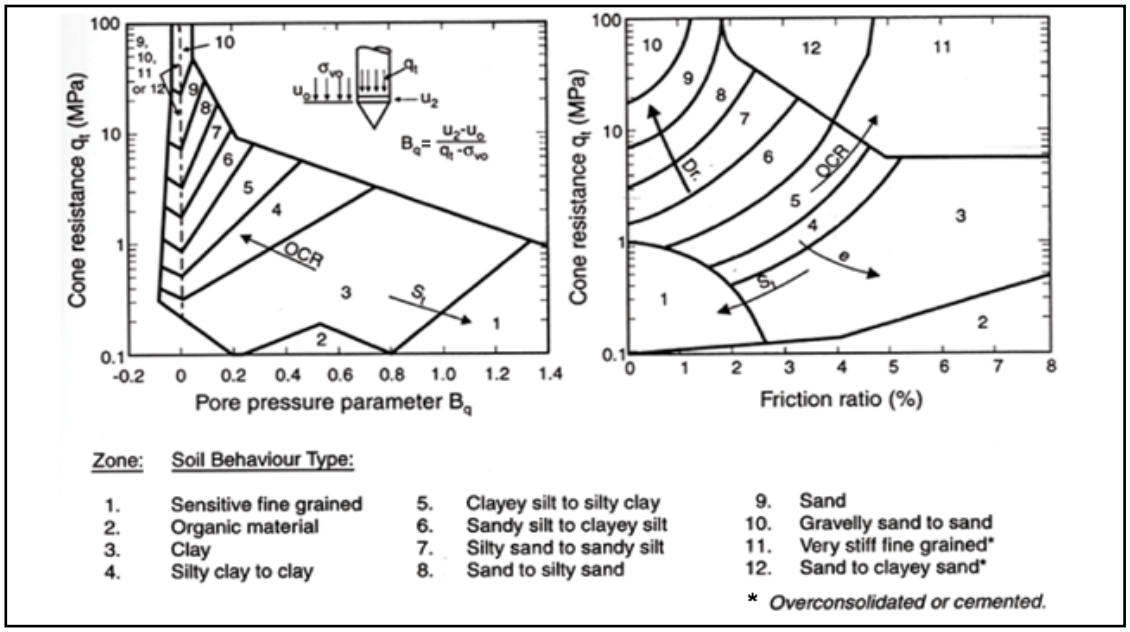

Figure 5.18 Proposed soil classification chart from piezocone data by Robertson et al., 1986.

The third step was to correlate the measured torque lb-ft or unit skin friction from the torque using the MDPT-t apparatus with the effective cohesion (C'), adhesion (Ca), and soil friction angle (ϕ'). This step focused on using the triaxial tests from the NCDOT Greensboro U-2412B project in Guilford County that were conducted for other research projects. The NCDOT Material and Test Unit performed the triaxial and soil quality tests for many Shelby tubes at different stations and depths. Table 5.6 shows a summary of the laboratory test results and the in-situ measured torque using the MDPT for the Greensboro project. The data was carefully compiled and organized based on soil types. Table 5.6 shows the soil types encountered in the MDPT test locations: A-4, A-5, and A-7-5.

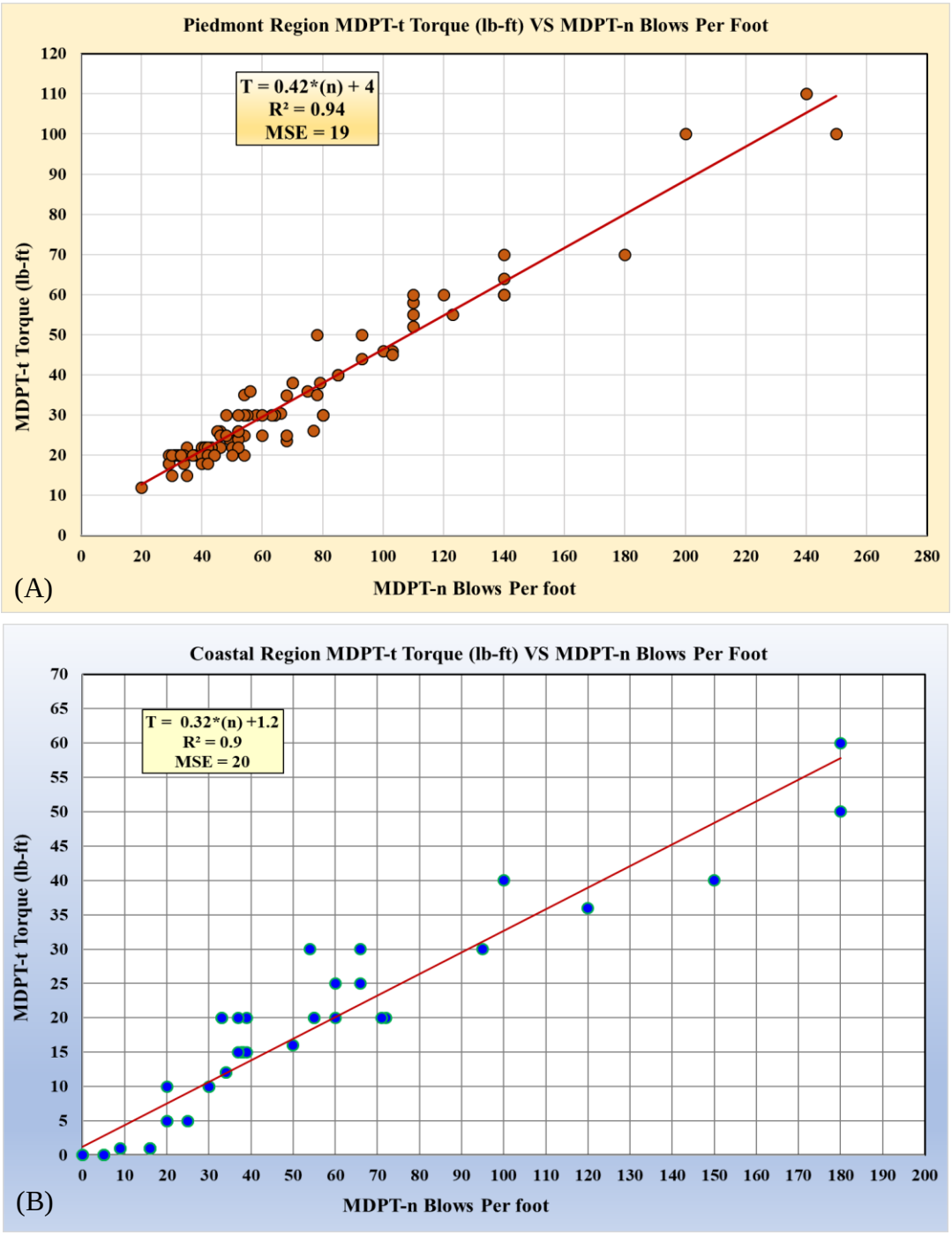

Figure 5.19 (A) Piedmont region torque (ft-lb) vs. MDPT (n) blows per ft. (B) Coastal region torque (ft-lb) vs. MDPT (n) blows per ft.

Table 5.6 Summary of the Laboratory Test Results and the In-Situ Measurements for the U-2412B Projects in Greensboro, Guilford County.

Station	Depth (ft)	Sample NO	Classification	In-Situ Measurements						Laboratory Test Results							
				CPT Tip (tsf)	CPT Skin (tsf)	SPT Blows/ft (N)	MDPT Blows/ft (n)	MDPT-T Torque (lb-ft)	Unit Skin (psf)	Moisture (%)	ϕ(eff) Degrees	C' (psf)	LL (%)	PI	Dry Density (pcf)	Water Content (%)	Saturated Density (pcf)
403+45	29.6 - 31	ST-22	A-4(7)	61	2.1	20	80	30	2746	26.12	33	513	40	9	105	23.9	130.1
403+45	34.6 - 36.6	ST-23	A-4(0)	65.2	3.6	15	103	45	4119	21.79	31	1200	31	5	104.6	20.2	125.7
404+50	34.5 - 36.5	ST-13	A-4(5)	41	2.5	14	68	25	2288	27.69	30	116	40	8	102.1	24.7	127.3
404+50	39.5 - 41	ST-14	A-4(0)	46	3	20	80	30	2746	21.43	33	164	37	5	105.6	21.4	128.2
404+50	39.2 - 41.2	ST-33	A-4(2)	27	1.33	12	52	22	2014	28.33	30	333	40	4	93.1	25.1	116.5
405+70	45 - 46.7	ST-6	A-4(10)	NA	NA	33	140	45	4119	27.51	31		40	10	98.6	23	121.3
403+45	24.6 - 26	ST-21	A-5(4)	48	2.4	19	80	30	2746	23.22	28	432	42	NP	107.9	20.1	129.6
403+45	39.6 - 41.6	ST-24	A-5(6)	37.2	1.07	12	50	20	1831	25.1	28	288	41	8	105.7	28.7	136.0
404+50	19.6 - 21.6	ST-29	A-5(2)	30	1.7	11	48	25	2288	29.79	33	72	43	3	91.6	21.5	111.3
405+70	35 - 37	ST-4	A-5(3)	59	3	18	140	60	5492	43.47	37		49	12	77.1	24.4	95.9
404+50	19.5 - 21.5	ST-11	A-7-5(20)	20	1.1	5	20	12	1098	58.38	22	144	67	17	66	47	97.0
404+50	24.5 26.5	ST-12	A-7-5(13)	18	1	8	35	15	1373	44.56	28		52	13	77.3	36.8	105.7
404+50	29 - 31	ST-31	A-7-5(12)	30	1.75	12	60	25	2288	42.24	20	612	54	15	79.4	41.4	112.3
405+70	25 - 27	ST-2	A-7-5(21)	25	1.3	6	40	18	1648	60.39	24	266	66	17	66	55	102.3
405+70	30 - 32	ST-3	A-7-5(17)	20	0.9	9	44	20	1831	54.39	30	432	60	16	69.6	49.2	103.8
405+70	30 - 32	ST-3	A-7-5(14)	20	0.9	9	42	18	1648	49.4	30	432	56	14	72.7	46.6	106.6
405+70	40 - 42	ST-5	A-7-6(13)	36	0	30	123	60	5492	31.76	33	576	45	17	89.2	26.9	113.2

As shown in Table 5.6, a variety of laboratory and in-situ tests was performed at the Greensboro site for the other research project. Unfortunately, the number of triaxial tests we could use was limited to 17 due to the NCDOT's construction schedules and our limited access to the site. Also, many of the Shelby tests were at conducted in shallow depths and thus could not be used. A specific data analysis was performed for the Greensboro site to validate the initial correlations between the MDPT-n blow counts and the MDPT-t measured torque, as shown in Figure 5.20 A, B, C, and D. The relationship between the measured torque and the corresponding MDPT blow counts at the same depths and within a few feet from the actual locations was plotted for the three soil types (A-4, A-5, and A-7-5), as presented in Table 5.6.

Regression analysis was carried out to calculate the least squares fit for the given data points, and the R^2 values were calculated to determine the accuracy of the correlations. For soil A-4, the correlation between the MDPT-t and the MDPT-n blow counts is presented in Figure 5.20 (A). The same procedure was performed for soil types A-5 and A-7-5, and the results are presented in Figure 5.20 (B) and (C). The results of the linear regression analysis, shown in Figure 5.20, were similar in value with the linear regression analysis for the Piedmont region. Even though the number of data points were limited, the finding validates that the relationship between the measured torque and the MDPT-n blow counts exists and can be estimated using the newly developed MDPT device.

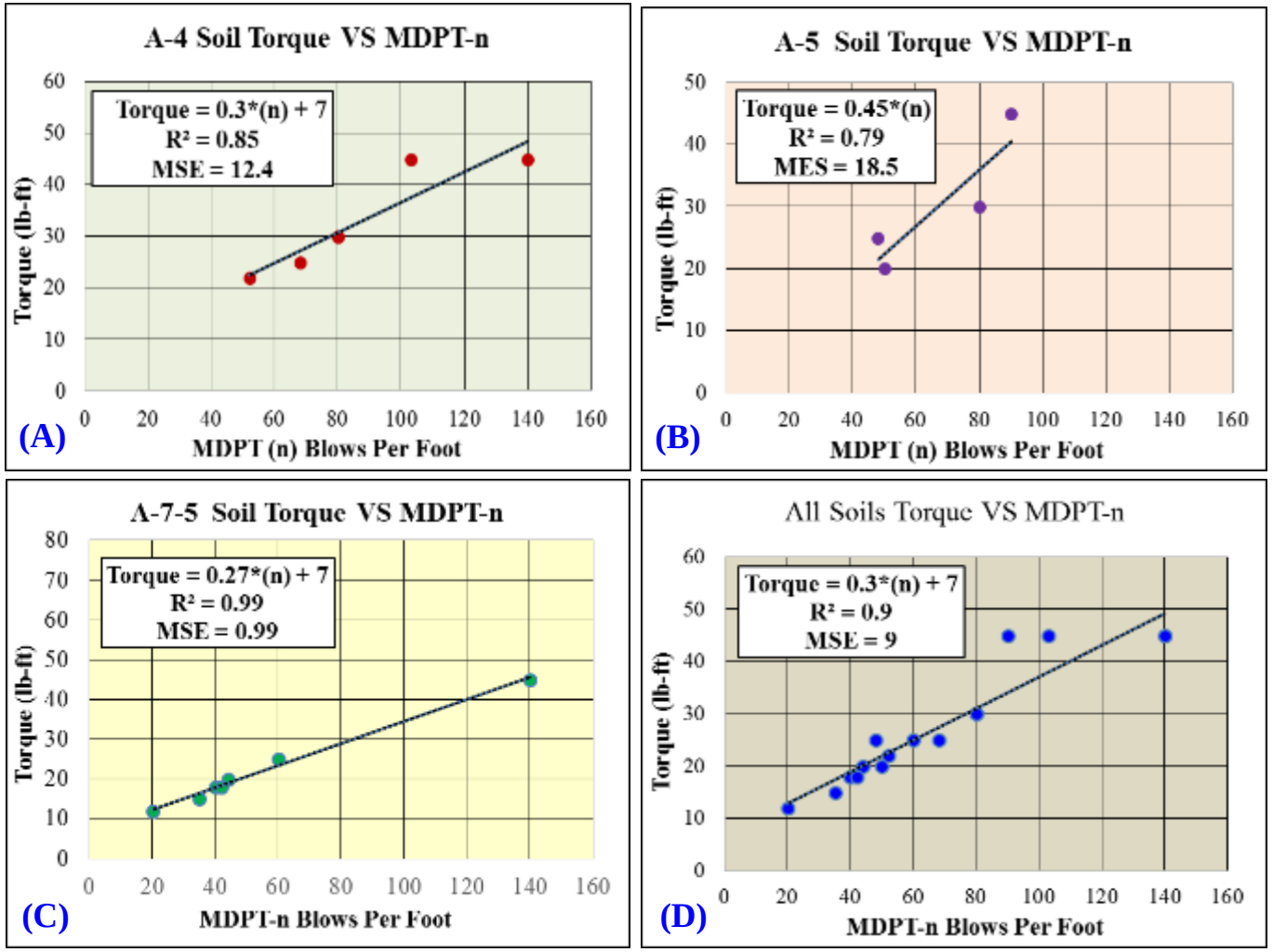

Figure 5.20 Correlations of measured torque vs. MDPT (n) blow count per ft for **(A)** Soil type A-4, **(B)** Soil type A-5, **(C)** Soil type A-7-5, and **(D)** for three types of soils.

The data for the three types of soils are plotted in Figure 5.20 D. Linear regression analysis was carried out using the following formula, which had a corresponding regression coefficient R^2 =0.90:

$$\text{Torque} = 0.3 * \text{MDPT-n} + 7 \quad (5.27)$$

5.10.1 Correlation Between the MDPT-t Measured Torque with the Effective Friction Angle ϕ' from Triaxial Tests

This section evaluates the relationship between the in-situ MDPT-t (lb-ft) directly with the measured friction angle (ϕ) in degrees from the laboratory triaxial tests. Figure 5.21 shows the relationship and the linear trend line between the friction angle (ϕ) from the triaxial tests and the in-situ torque (lb-ft) using MDPT-t.

Selected data from Table 5.6 was used to correlate the effective friction angle (ϕ') and the measured torque using the MDPT-t in the three predominant soils. There is a definite trend between the measured torque and the ϕ'. As shown in Figure 5.21, the higher the torque is the effective friction angle ϕ'. Regression analysis was carried out on the data to develop the correlation between ϕ' determined from the triaxial tests and the in-situ measured torque. From the linear regression analysis, the Pearson r (correlation coefficient) was 0.61 and the significance (F), or p-value, was 0.0099. Comparing the R^2 = 0.367 and the r =0.61, it can be concluded there is a significant positive relationship between the friction angle (ϕ') and the MDPT-t values; however, due to the limited triaxial tests, it will be difficult to generalize this relationship.

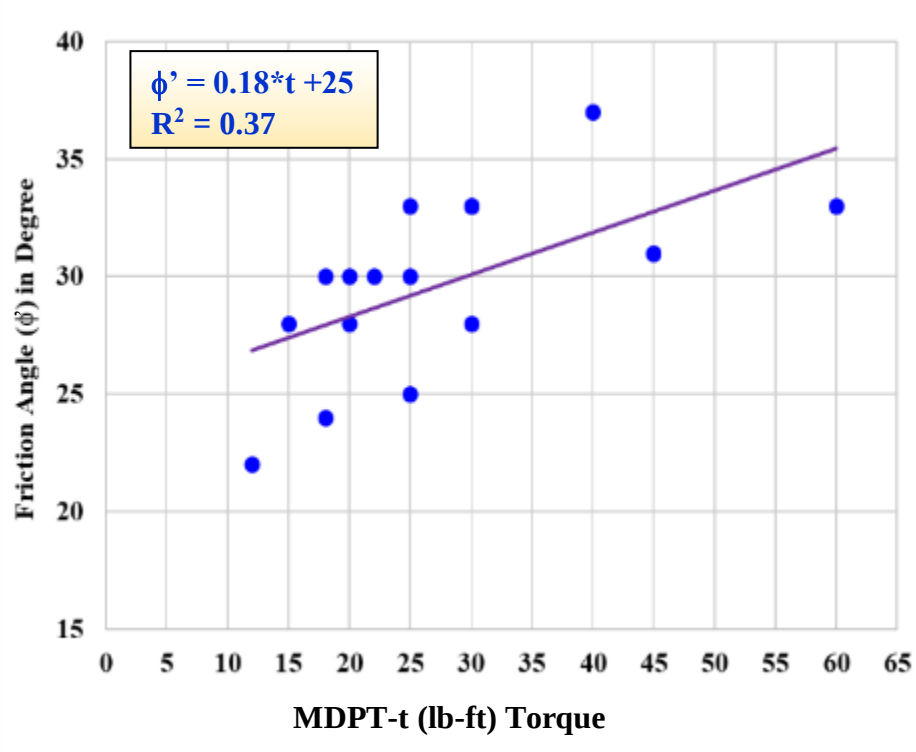

Figure 5.21 Correlation between friction angle (ϕ') and MDPT-t (lb-ft).

$$\phi' = 0.18*\text{MDPT-t} + 25 \leq 40^{o} \qquad (5.28)$$

where MDPT-t = Torque (T) (ft-lb).

Equation 5.28 should have a maximum friction angle of 40º or less, depending on the local values. The range of the acceptable friction angle must be calibrated to the local typical friction angles. See Table 5.2 for typical effective friction angles ϕ'.

5.10.2 Correlation Between the MDPT-t Measured Torque with the Effective Cohesion from Triaxial Tests

This section evaluates the relationship between the in-situ MDPT-t (lb-ft) directly with the measured cohesion (C) (psf) from the laboratory triaxial tests. Figure 5.22 shows the relationship and the linear trend line between the cohesion (psf) from the triaxial tests and the in-situ torque (lb-ft) using MDPT-t. This evaluation was performed to determine the extent of the

significance of the relationship between the MDPT-t (lb-ft) torque and the laboratory cohesion (C). From the linear regression analysis, the Pearson r (correlation coefficient) was 0.574 and the significance (F), or p-value, was 0.0317. Figure 5.22 shows the strength of the linear relationship between C and MDPT-t, with R^2 = 0.35 and r =0.574. The graph indicates a positive linear relationship between the cohesion and the MDPT-t values, possibly due to the soil type, uniformity, and layer thickness, and the distance between these tests. In addition, the reason for the weak relationship (Lower R^2) could be due to the presence of a high percentage of fine, which will affect the penetration and the blow counts. However, due to the limited number triaxial tests, it will be difficult to generalize the strength of the relationship between the undrained C and the MDPT-t measured torque.

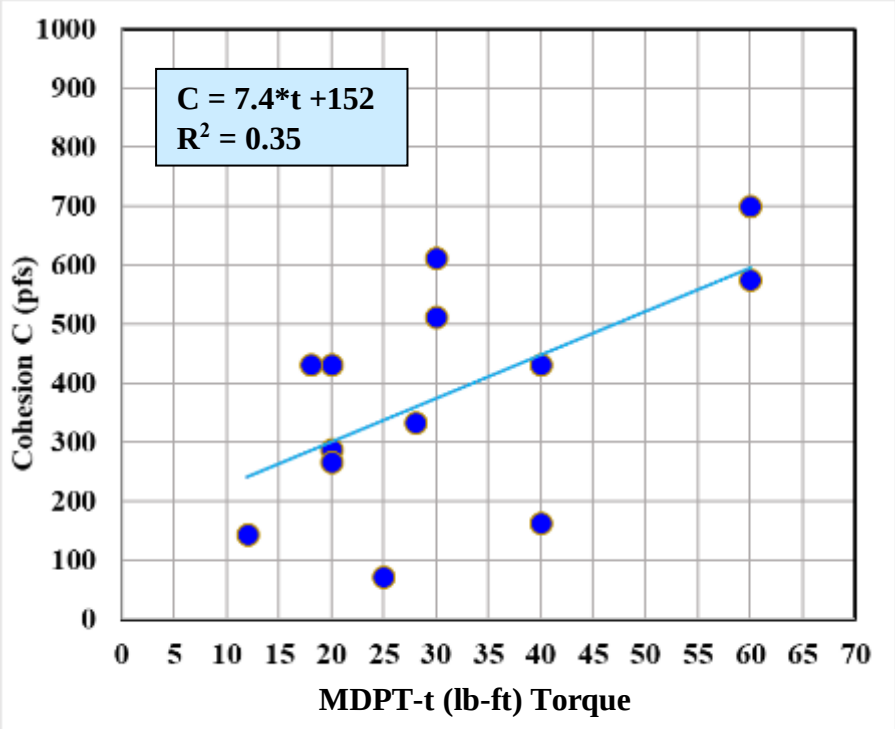

Figure 5.22 Correlation between cohesion (C) (psf) and MDPT-t (lb-ft).

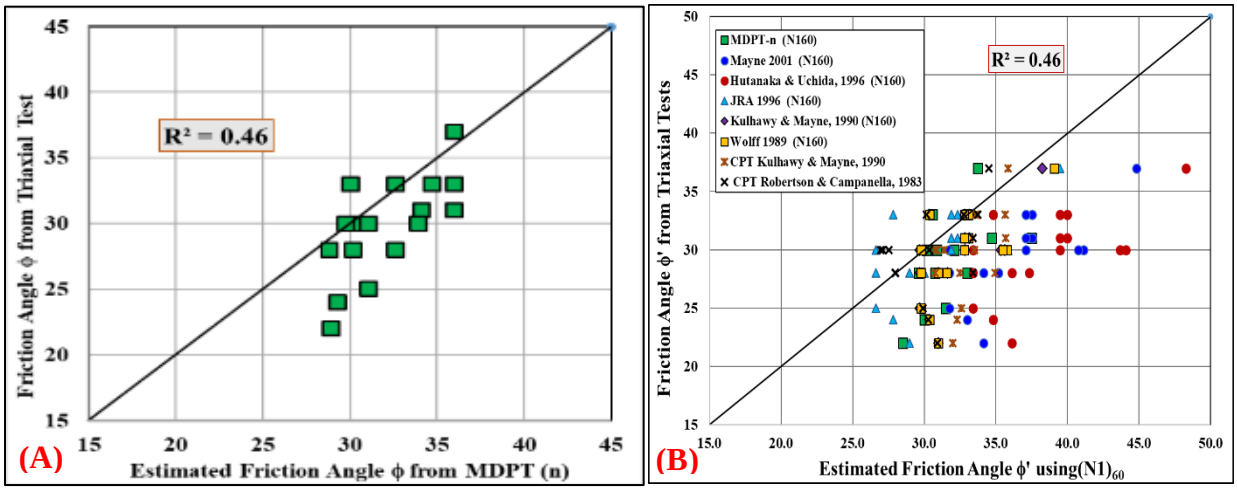

Figure 5.23 (**A**) Measured friction angle (ϕ) from triaxial tests vs. estimated friction angle (ϕ) from MDPT-n using equation from Figure 4.4 (low). (**B**) Comparing other researchers' CPT equation with MDPT-n to estimate the friction angle using actual SPT(N).

5.10.3 ϕ MDPT-t Torque and MDPT-n Versus Friction Angle ϕ from Triaxial Tests

This section demonstrates the direct relationship between the estimated friction angle using MDPT-n blows per ft and the measured friction angle (ϕ) from the laboratory triaxial tests at each location. The estimated friction angle (ϕ) was calculated using the low equation from Chapter 4 (see Figure 4.4), and the results are shown in Figure 5.23. The equation developed to estimate the friction using the MDPT-n blow counts is slightly higher than the measured friction angle from the laboratory triaxial tests. The strength of the relationship can be attributed to many factors such the location of the tests, the sample tested is not representative of the predominant soil, the laboratory test procedure, and the horizontal and vertical variability of the site. However, the trend between the estimated ϕ and the measured ϕ from the triaxial tests showed a positive relationship, and the friction angle (ϕ) will increase with the increase of the MDPT-n blows per ft. As described in the previous sections and chapters, the MDPT device can be calibrated, and it can predict the friction angle and the cohesion if sufficient data are available.

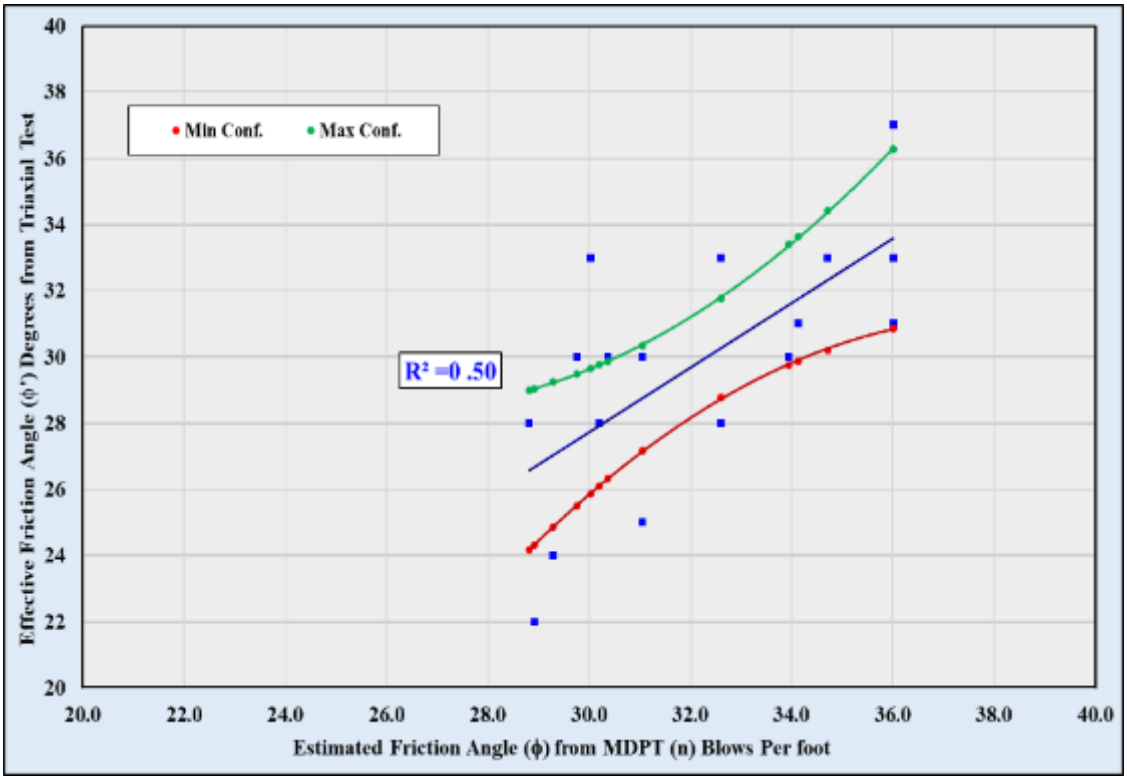

Figure 5.24 Measured ϕ from the triaxial test and the predicted ϕ using MDPT-n.

The comparison between the measured effective friction angle and the predicted friction angle using the MDPT-n blows per ft are presented in Figure 5.23. The trend lines R^2 of 0.46 and Pearson r coefficients of 0.7 were calculated using a Microsoft Excel spreadsheet. As previously described, the R^2 is a measure of how close the data are to the fitted regression line. On the other hand, the Pearson r coefficient indicated the effect size of a linear relationship between two data sets. Therefore, the r of 0.7 indicates a large positive linear relation between the measured ϕ' and the predicted ϕ. The p-values were determined using a statistics calculator; the p-value 0.0029 indicates that a significant relationship between the measured and estimated ϕ exists, because it is less than 0.05. Figure 5.24 shows the 95% confidence level for the above correlation.

5.10.4 Comparing the Empirical Correlation of the MDPT-t With Other Researchers

This section compares the results of the empirical correlation and the in-situ unit skin friction (*fs*) of the MDPT-t with that of other researchers, pile load tests, and the Texas cone penetrometer (TCP). As shown in Figures 5.25, 5.26, and 5.27, the *fs* versus SPT (N) blows per ft are plotted in three different graphs. These figures show that the empirical correlations developed for the MDPT-t measured torque are comparable with other predictions. The overall MDPT-t *fs* versus SPT (N) blows per ft shows a positive relationship. Variations in the strength of this relationship can be influenced by regional soil characteristics and the distance and depths of these tests from each other.

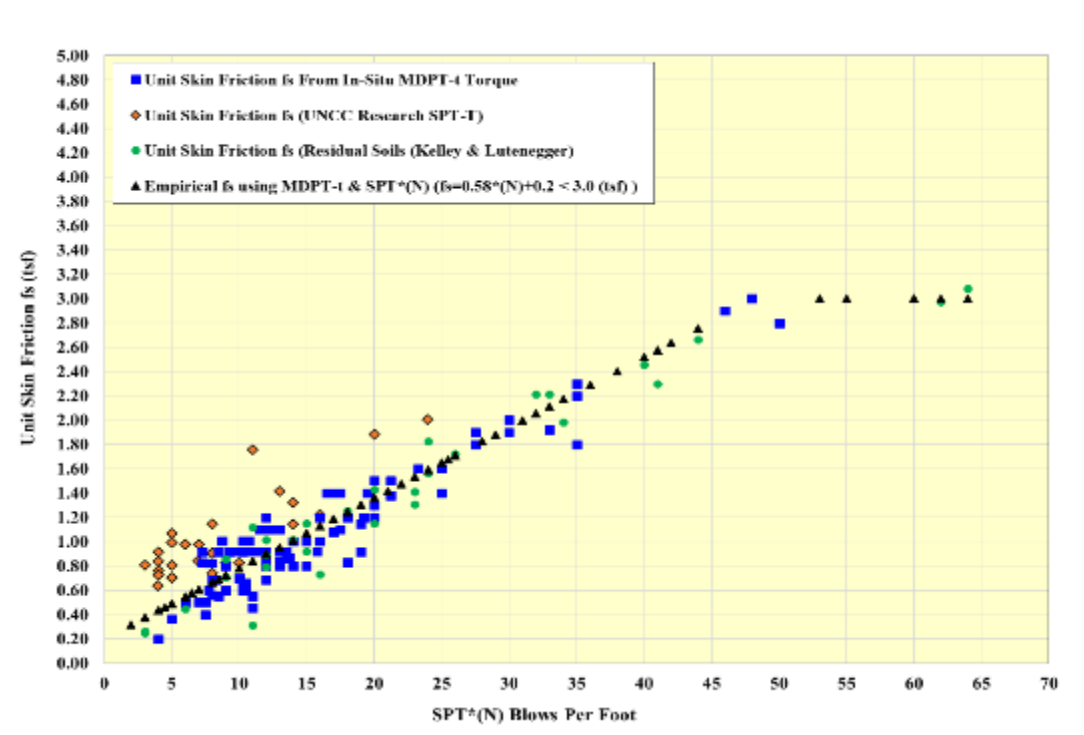

Figure 5.25 Unit skin friction *fs* (tsf) from other researchers and MDPT-t *fs* vs. SPT*(N) blows per ft.

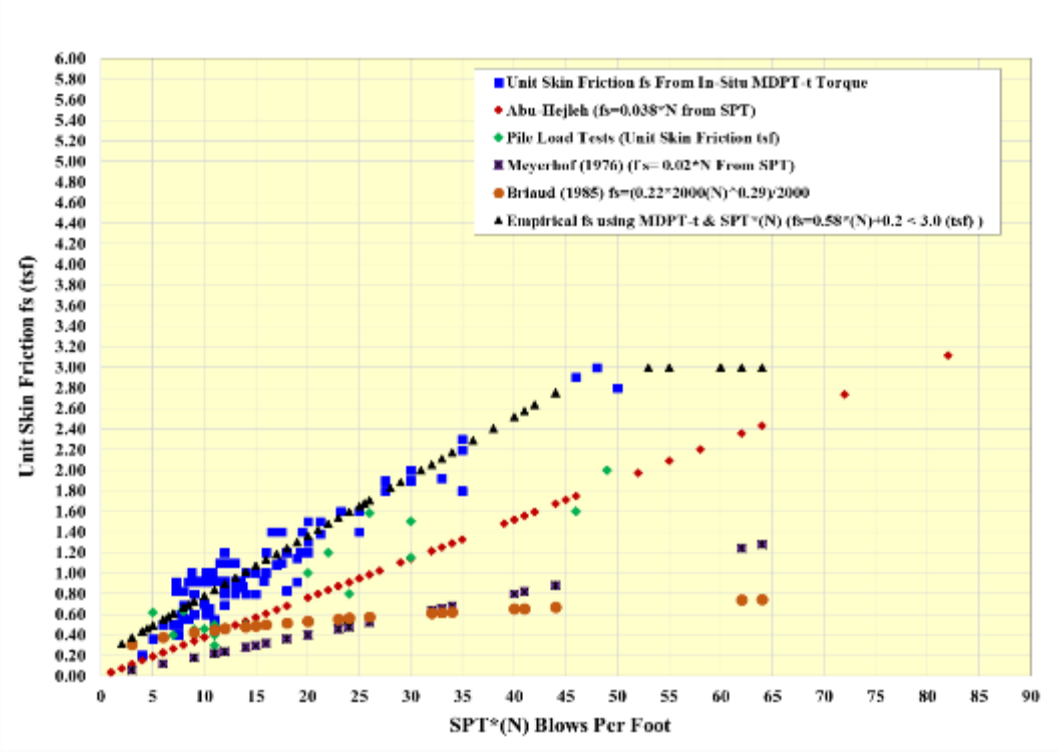

Figure 5.26 Unit skin friction *fs* (tsf) from different researchers and MDPT-t *fs*, including pile load tests unit skin friction vs. SPT* (N) blows per ft.

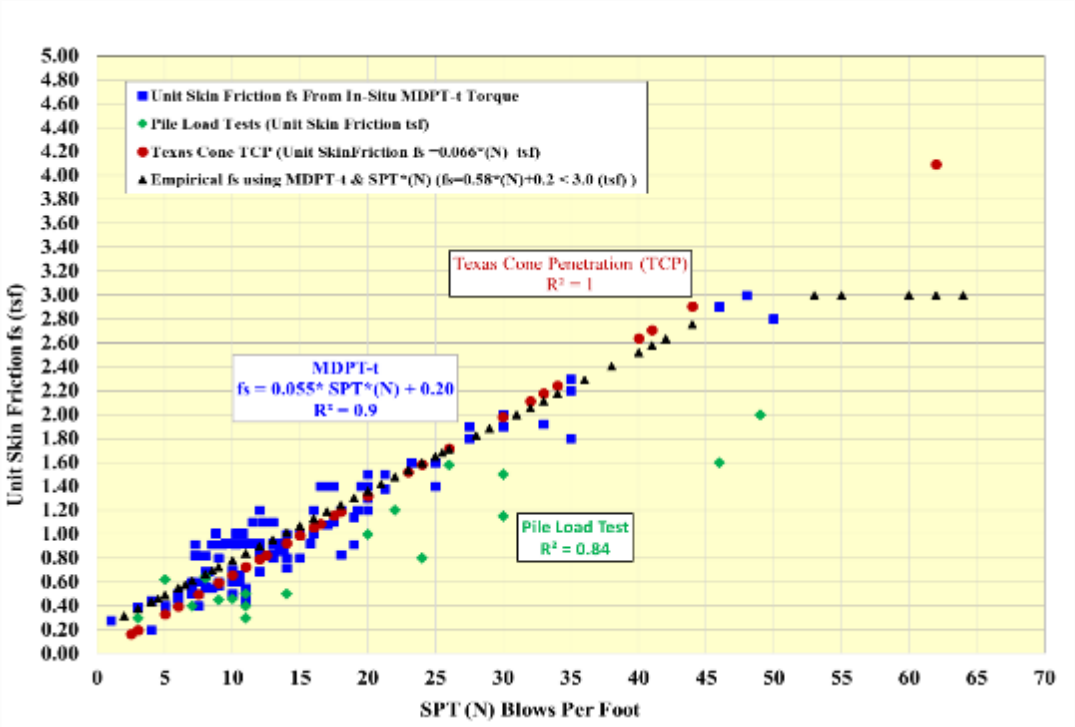

Figure 5.27 Unit skin friction *fs* (tsf) from MDPT-t, pile load tests, and Texas cone penetrometer (TCP) vs. SPT (N) blows per ft.

5.10.5 Comparing the Empirical Correlation of the MDPT-t Unit Skin Friction *fs* with Unit Skin Friction from CAPWAP™, APILE™, and Vesic Static Design Methods

This section compares the results of the empirical correlation and the in-situ unit skin friction (*fs*) of the MDPT-t with the dynamic testing (CAPWAP™) and static design methods such as Vesic and APILE™ software (Nordlund method). The *fs* versus SPT (N) was plotted on four graphs at different depths to evaluate the depths factor and to determine which method gives higher or lower values of unit skin friction at different blow counts, as shown in Figure 5.28.

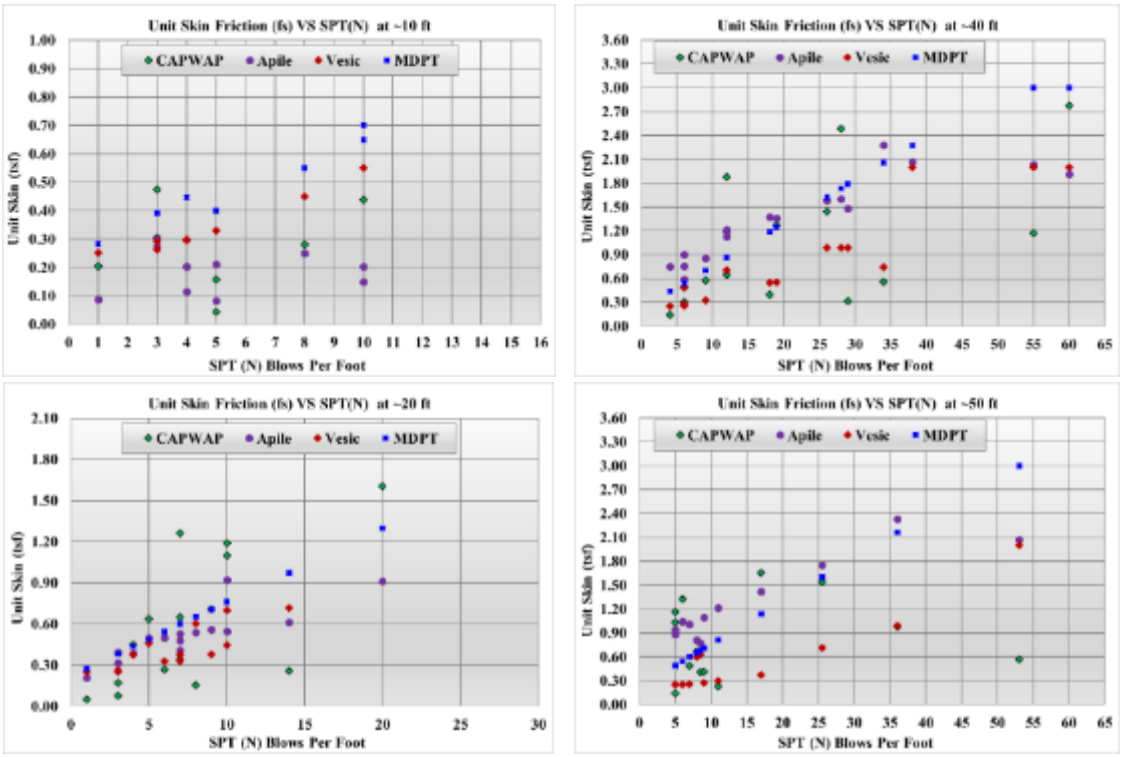

Figure 5.28 Unit skin friction *fs* (tsf) from MDPT-t, CAPWAP, APILE, and Vesic methods vs. SPT (N) blows per ft at depths 10, 20, 40, and 50 ft.

APILE is a software program that professional engineers use to compute axial capacity, including skin and tip resistance as a function of depth for a driven pile in clay, sand, or mixed-soil profiles. The following methods are used to compute pile capacity:

- American Petroleum Institute (API RP-2A).

- U.S. Army Corps of Engineers (USACE).
- U.S. Federal Highway Administration (FHWA) (uses Nordlund design method).

APILE can be used to analyze different types of piles, such as pipe, HP steel, precast concrete, tapered, timber, and Raymond.

Vesic (1977), Meyerhof (1976), and Coyle and Castello (1981) published reports describing the procedure for calculating the ultimate bearing capacity of pile, where the pile capacity depends on both tip and skin frictional resistance (skin friction).

$$Qu = Qt + Qs \tag{5.29}$$

where Qu is the ultimate load carrying capacity, Qt is the tip resistance, and Qs is the skin frictional resistance.

The Vesic pile bearing capacity was used by NCDOT geotechnical engineers to estimate pile lengths based on required pile-bearing capacity. Figure 5.28 represents the Vesic, Apile static design methods, the CAPWAP dynamic test, and MDPT-t unit skin friction *fs* (tsf) versus SPT (N) values at different depth groupings. By keeping the depth relatively constant, our prediction methods primarily rely on the SPT (N) value and the soil type. Hence, APILE and Vesic have a relatively linear trend, where the unit skin increases with increased SPT (N).

From the four graphs shown in Figure 5.28, the MDPT-t prediction is within a reasonable range of the other methods, including CAPWAP values. CAPWAP values are rather variable, possibly due to the variability from the SPT (N) and from the soil set-up (these are end-of-drive values, so restrikes may differ). We can also determine which method predicts higher or lower values at each depth. For example, APILE and Vesic predict similar skin friction at a depth of 20 ft for most blow counts; however, APILE predicts higher skin resistance than Vesic at a depth of

50 ft. Therefore, Vesic may be more conservative than APILE for long piles, while APILE may be more conservative for short piles.

The data used to generate Figure 5.28 was based on pile-driving analyzer (PDA) data for a specific project. Each PDA report was analyzed using the SPT (N) and the pile type and lengths to estimate the unit skin friction from the CAPWAP, APILE, and Vesic methods. The MDPT unit skin friction *fs* data was generated from an empirical correlation of MDPT-t and MDPT-n with conversion to SPT* (N), and from the in-situ torque test using the MDPT-t.

Step 1:

Convert the MDPT-n to uncorrected SPT (N) using Equation 4.3 in Chapter 4.

$$\text{Estimated SPT* (N)} = 0.25*\text{MDPT-n} \qquad (4.3)$$

Step 2:

Estimate unit skin friction using the equation from Figure 5.26.

$$Rs = 0.055*\text{SPT* (N)} + 0.2 \qquad (5.30)$$

Step 3:

Plot the estimated *fs* versus the estimated (N) values for different depths, as shown in Figures 5.25 - 5.27 and Figure 5.28.

5.11 Conclusion and Recommendation

The MDPT-t tests were performed in two different geological regions of North Carolina to produce empirical correlations. The results from the torque test are positive and can be cost-effective when using a portable and easy-to-use device. The main limitation of the research was the limited number of laboratory triaxial tests. NCDOT primarily performs triaxial tests for weak soil, and thus not many triaxial tests data were available. The data used in the research were

specifically collected and tested for another NCDOT sponsored research project, "Design of Temporary Slopes and Excavations in Residual Soils" by Gabr and Borden (2016).

Based on the limited data, the analysis shows a reliable correlation exists between the in-situ measured torque MDPT-t and the laboratory triaxial test effective friction angle ϕ' and effective cohesion C'. The results of this study shows that the use of a small and portable MDPT-t may serve as a quicker tool for site investigation and provide reasonable soil parameters for geotechnical engineers to use in planning, design, and analysis.

The MDPT-t unit skin friction was examined and compared with other researchers, and the results were promising. The unit skin friction produced by the MDPT-t device is within a reasonable range of the other reported values. In addition, the MDPT-t unit skin friction was examined and compared to the skin friction of other dynamic and static design methods such as CAPWAP, the Vesic design method, and APILE software, and the results were within acceptable range. However, caution must be taken when using statistical analysis to supplement engineering judgment. For example, a high R^2 correlation does not suggest a strong connection between the variables, and a low R^2 correlation may be affected by the accuracy and the size of the sample data, or other factors need to be considered in the evaluation. Overall, the MDPT-t performance was acceptable and provided promising results.

CHAPTER 6. MDPT-t TORQUE AND MDPT-n BLOWS CORRELATED TO CONE PENETRATION TEST (CPT)

6.0 Abstract

The Standard Penetration Test (SPT) is the most common in-situ test for soil subsurface investigations. However, the Cone Penetration Test (CPT) is considered more reliable and more accurate than the SPT for soil characterization. The CPT is considered to be quick and provide more accurate results than SPT. Many soil properties have been correlated to both the SPT and CPT. Most foundation design methods were developed based on the results of these tests; therefore, it is vital to correlate the MDPT to the SPT (N) and the CPT tip resistance (q_t) and the sleeve friction (*fs*), especially for the preliminary evaluation of any project.

The SPT requires a drill rig, and the CPT requires a heavy truck to push the cone. Mobilizing a heavy drill rig or specialty truck can be very costly for a rushed or unplanned project or for a small project. The Mini Dynamic Penetration Test (MDPT), supplemented with the measurement of torque (MDPT-t), can be used to obtain a direct measurement of soil unit skin friction (*fs*), after rotating the cylindrical cone with a calibrated torque wrench, more quickly and more economically than with heavy and expensive equipment. The MDPT device is portable and economical to use.

The MDPT was correlated to limited data with CPT exploration. The purpose of this study was to investigate the relationships between the MDPT and the CPT. Correlations were established between the cone tip resistance (q_t), sleeve friction (*fs*), MDPT-n blow counts, and MDPT-t torque for two locations. A positive linear relationship was found between the CPT tip stress q_t, CPT sleeve stress *fs*, and the MDPT-n and MDPT-t torque for this study. In general, CPT q_t versus MDPT-n showed higher correlation coefficients than CPT *fs* versus SPT(N); see Figures 6.4 and 6.5.

6.1 Introduction

The use of in-situ tests to estimate design parameters for deep foundations is necessary when undisturbed samples are difficult to obtain due to limitations inherent with the sampling equipment, different soils encountered, and the strength of the material. This chapter presents the development of the MDPT-t device as an alternative tool for convenient and economical in-situ testing. The results from this new test can be correlated to conventional soil testing methods, and they can be used to estimate unit skin friction and other soil properties. In addition, testing with this new device is quicker and more economical compared with other available tools.

The purpose of this section is to correlate the MDPT-t torque (lb-ft) and the MDPT-n blows per ft to the tip (q_t) and sleeve friction (*fs*) of the CPT test. The CPT test is one of the two most common penetration tests in our practice. The initial development of the CPT was by a Dutch laboratory for soil mechanics in 1955. In the static CPT test, a cone is pushed into the soil layers using the weight of the truck. During the penetration, the cone tip resistance (q_t) and the sleeve friction (*fs*) are recorded continuously. The CPT is an excellent tool for profiling strata changes and providing soil characterization. Various foundation design methods were developed based on the outcome of the CPT test, and therefore it is vital to correlate the MDPT results to the CPT due to the accuracy and the repeatability associated with CPT exploration.

The study had a limited number of CPT tests during the development and testing of the MDPT device, because the North Carolina Department of Transportation uses the CPT test for large and sensitive projects or upon request by the design engineer. CPT exploration is mainly performed between borings to enhance the stratigraphy between the SPT borings for the subsurface inventory report to be included in the contract documents. This report assists contractors with preparing their bid estimate for projects.

The number of blow counts per ft of penetration (n) obtained from the MDPT during in-situ testing can be empirically correlated to the Cone Penetration Test (CPT) q_t or sleeve friction *fs*. See Chapter 7 for more details about the MDPT device and test procedures.

6.2 History and Literature Review of CPT Correlations

Many authors have pointed out the importance of SPT - CPT correlations. Robertson (2010) reported that more studies are needed to evaluate the reliability of the CPT and SPT correlations so that CPT data can be used in foundation design. Kulhawy and Mayne (1990) discussed the advantages of having a procedure to correlate SPT (N) and CPT cone tip resistance (q_t). Both SPT and CPT are the most used in-situ soil tests worldwide, and both represent soil resistance to penetration, even though the CPT is quasi-static and the SPT is dynamic.

In early 1960s, Meigh and Nixon suggested the use of a constant value of q_t/N for different soil types. A number of researchers have proposed that the q_t/N ratio is a function of the mean grain size (D50) of the soil. Table 6.1 illustrates the ratio q_t/N decrease with the increase of fine material, and the increase with increasing grain size (D50). In addition, results from other studies indicate that the q_t/N ratio is smaller for sands with high fines content than for clean sands. Kulhawy and Mayne (1990) collected the results from a number of studies and presented them in one graph to show the relationship and the trend between the q_t/N ratio and the fines content of the soil. The SPT* (N) blow counts used in this research were estimated from the MDPT-n and were not corrected due to some limitations of the data.

Table 6.1 Reported q_t/N Ratio in (MPa).

Researchers	Soil Type	qt/N (MPa)
Meyerhof (1956)	No specified	0.4
Meigh and Nixon (1961)	Coarse Sand	0.2
Schmertmann (1970)	Sandy Gravel Sand Fine to Medium Sand	0.8 – 1.0 0.5 – 0.6 0.3 – 0.4
Danziger et al. (1998)	Sand Silty Sand Clayey Silt Clay	0.57 0.5 0.31 0.45
Akca (2003)	Sand Silty Sand Silty Clay Clay	1.0 0.5 0.3 0.2

6.3 Pile Capacity Evaluation from CPT

In general, many design engineers prefer for their analysis the in-situ mechanical behavior of soil instead of the characterization of soil based on the grain size (e.g., Ku et al., 2010).

The CPT test is more reliable for pile design purposes than the SPT test because the CPT data are more reliable and the cone penetration generates the cone tip resistance and sleeve friction similar to the pile bearing capacity. The CPT test consists of a cylindrical penetrometer with a conical tip that is mechanically pushed into the ground. It requires a heavy truck to generate sufficient force to push the cylindrical penetrometer into the ground. The CPT penetration has some similarity to the pile-loading mechanisms.

Although many researchers have studied and developed expressions to estimate soil properties based on the tip cone resistance q_t, other researchers have suggested the use of cone sleeve friction *fs* to estimate the soil adhesion. Schmertmann (1978) stated that the cone penetration test CPT can be used to measure the cone sleeve friction *fs*, which can be used to estimate the shaft resistance in cohesive soil. Schmertmann (1978) and Price and Wordle (1982) studied and recommended the use of the CPT cone sleeve friction *fs* for estimating the pile side friction, as shown in the following equation:

$$qs = R_{sfi} * fs_i \qquad (6.1)$$

where qs is the total ultimate shaft resistance, R_{sf} is an empirical ratio to convert the cone sleeve friction to shaft resistance qs, and fs_i is the average undrained cone sleeve friction for layer i.

The values of R_{sf} in Equation 6.1 is needed to convert the cone sleeve friction to shaft resistance at each layer. Table 6.2 was based on the graph developed by Schmertmann (July 1978) on page 127 of the FHWA-TS-78-209 "Guidelines for Cone Penetration Test Performance and Design."

Table 6.2 Values of the Factor R_{sf} by Schmertmann (1978).

***fs*/Pa**	**Values of Rsf**	
	Steel Piles	**Concrete and Timber Piles**
0.25	0.97	0.97
0.5	0.70	0.76
0.75	0.48	0.58
0.88	0.40	0.52
1.00	0.36	0.47
1.50	0.27	0.43
2.00	0.2	0.40
Pa = atmospheric pressure = 100 kPa = 0.1 MPa = 1 tsf.		

6.4 CPT and MDPT Data Selection

CPT and MDPT were performed in two projects at different locations in Greensboro. The data for both projects were obtained from NCDOT project U-2412B and R-2525C, located in the Piedmont region in Greensboro, Guilford County, in North Carolina.

The U-2412B site was selected because another research study sponsored by NCDOT, "The Design of Temporary Slopes Excavations in Residual Soils", which was conducted by Dr. Roy Borden and Dr. Mohammed Gabr of North Carolina State University, had retrieved 94 Shelby tubes (ST) from ten different borings between station 403+45 and station 405+70. The tubes were extracted from depths ranging 2–52 ft (0.6 m–15.5 m), and the data are used in this chapter.

CPT tip and sleeve friction was performed in four different stations, as shown in Figures 6.2 and 6.3 from U-2525C project. The selected data were obtained from soil investigations using SPT and CPT. The MDPT blow counts and torque tests were performed adjacent to the CPT test locations to establish the correlations between the MDPT and CPT. Four variables are

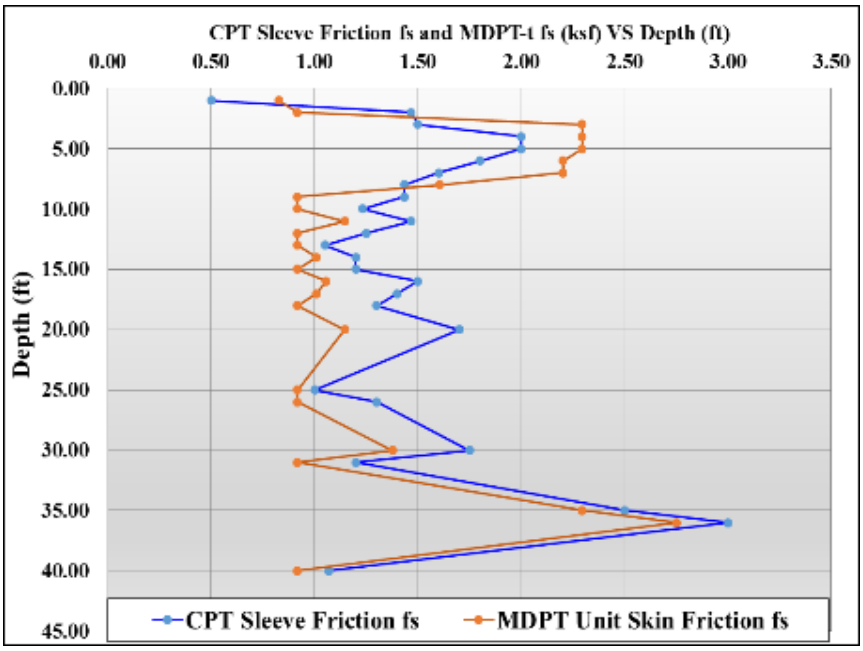

Figure 6.1 Comparison between MDPT-t unit skin friction *fs* and CPT sleeve friction *fs* with depths.

representative of the data used in this research: MDPT-n, MDPT-t, CPT tip resistance q_t (tsf) (MPa), and sleeve resistance *fs* (ksf) (kPa).

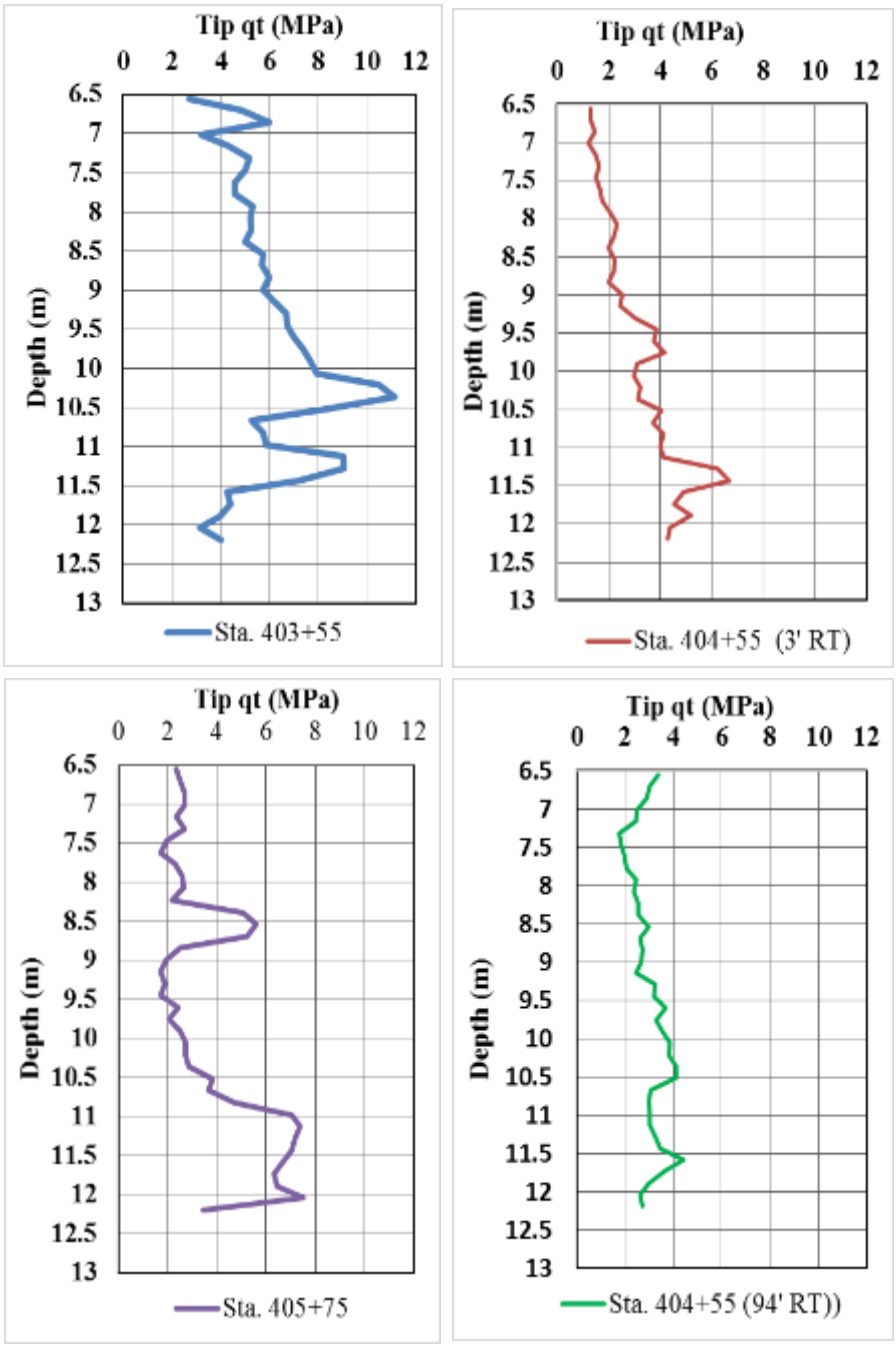

Figure 6.2 CPT tip stress (MPa) vs. depths in meters at different stations.

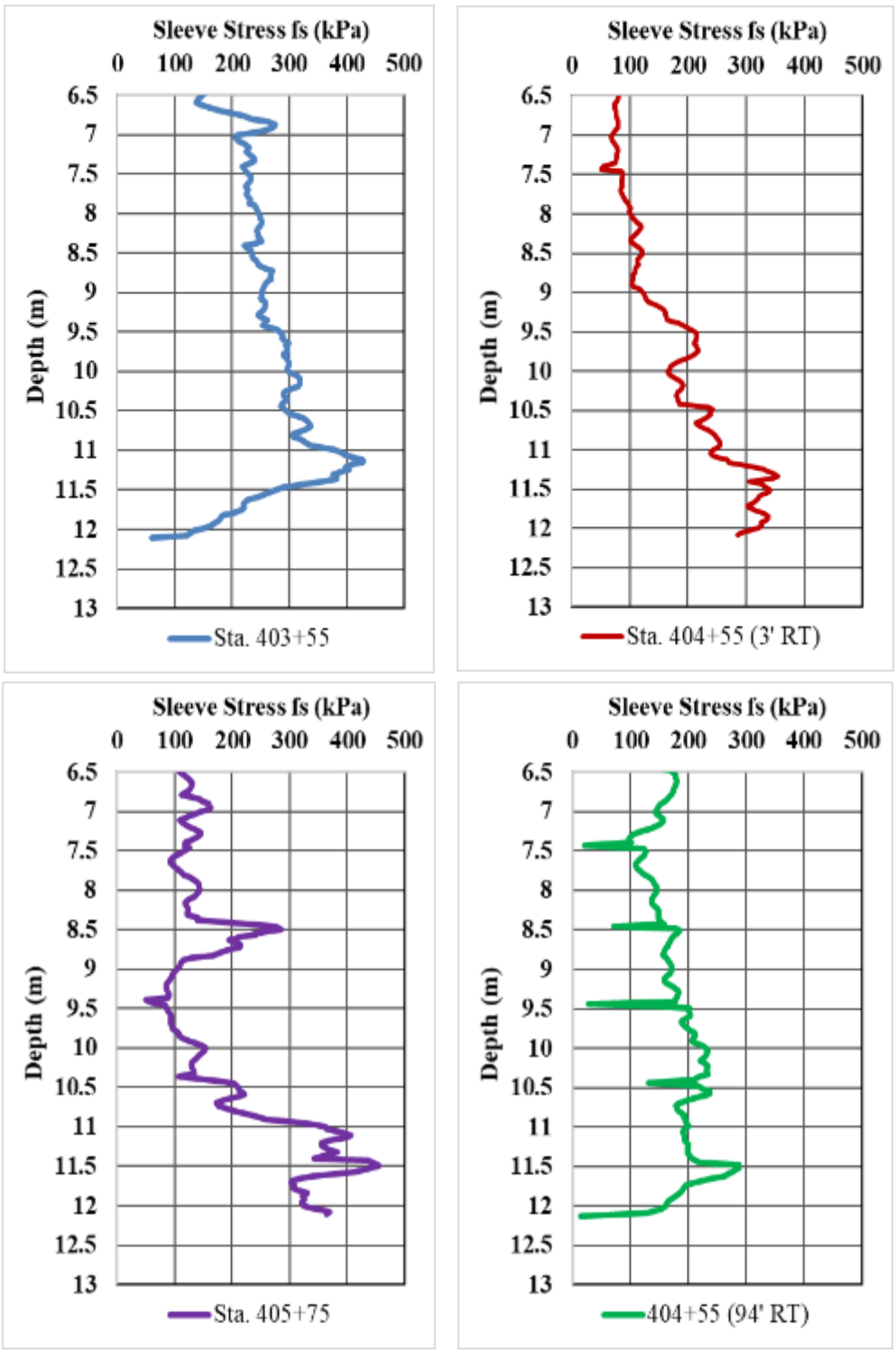

Figure 6.3 CPT sleeve stress (kPa) vs. depths in meters at different stations.

6.5 Summary and Discussion

The data was limited to the two projects due to the lack of CPT usage at NCDOT, the locations of these tests, and the cost associated with using the CPT in the projects. Many state DOT geotechnical engineers do not use CPT data in their design due to limited available resources such as charts, design manuals, or guidelines. Despite the limited data in this study, a correlation was established between MDPT-n and MDPT-t, and the CPT q_t and CPT *fs*.

6.5.1 MDPT-t Unit Skin Friction and CPT Sleeve Friction *fs*

Figure 6.1 shows that the MDPT unit skin friction generated from the torque is similar in shape to the average CPT sleeve friction *fs*. The data indicate that the sleeve friction *fs* from the CPT is larger than the MDPT *fs*. The higher values may be due to the procedure for each test (the MDPT is dynamic and the CPT is quasi-static) and site vertical and horizontal variability. It is also possible that the CPT test is more sensitive than the MDPT test. Lunne et al. (1997) reported that most of the CPT data are used to correlate the cone tip stress q_t to engineering properties and disregard sleeve friction *fs* measurements, as they are considered less reliable.

The MDPT unit skin friction was obtained from the MDPT-t torque at different depths and locations adjacent to CPT test. The *fs* was calculated using Equation 5.13:

$$fs = \frac{2\,\mathrm{T}}{\pi \mathrm{d}^2 \mathrm{L}}$$

Figure 6.4 shows the relationship between CPT sleeve stress *fs* and MDPT *fs*. A positive linear relationship was found between CPT, *fs*, and MDPT *fs* for the two projects, with the coefficient of determination R^2 of 0.66.

The linear regression in Figure 6.4 shows that the MDPT *fs* (kPa) can estimate the CPT *fs* (kPa) using the following equation:

$$\text{MDPT-t } (fs) = 0.64*\text{CPT } (fs) + 59 \qquad (6.2)$$

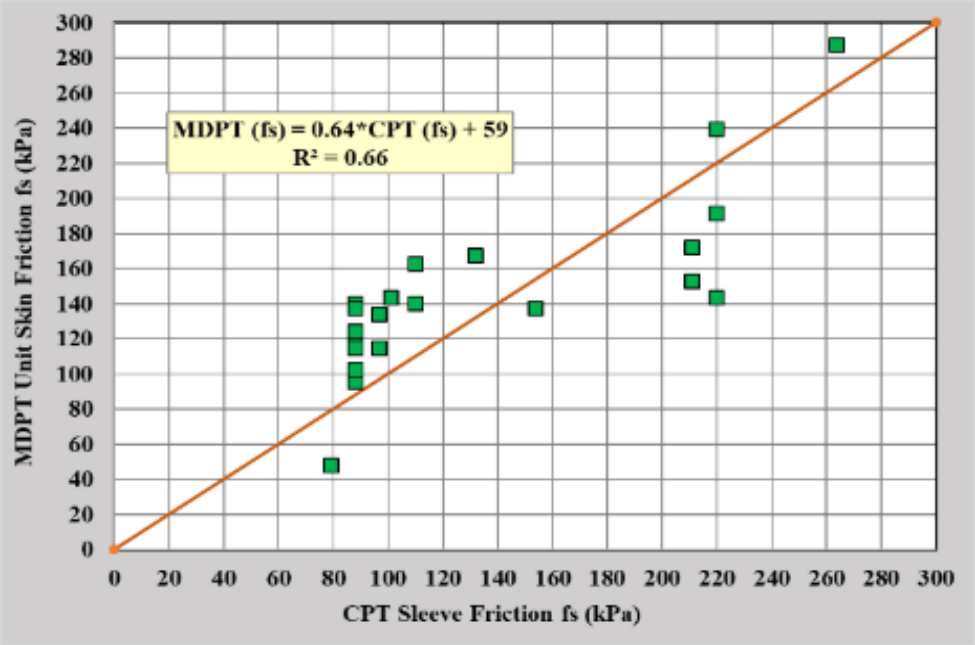

Figure 6.4 Plot of MDPT-t unit skin friction *fs* vs. CPT sleeve friction *fs* (kPa).

6.5.2 MDPT-n Blow Counts and CPT Tip Resistance q_t

The MDPT-n blows per ft were correlated to CPT tip resistance. The MDPT-n was converted to equivalent uncorrected SPT (N) blows using the average between Equation 1 and Equation 2 in Chapter 4 (Piedmont region: $N_{80} = 0.27n$ and Coastal region: $N_{80} = 0.23n$ use N= 0.25*n)) and then correlated to the CPT tip stress q_t. Figure 6.5 shows the relationship between the CPT tip stress q_t and the estimated SPT* (N) blows per ft. A positive linear relationship was found between CPT, q_t, and MDPT-n with the coefficient of determination R^2 of 0.87 with mean square error (MSE) of 0.12.

The linear regression in Figure 6.5 shows that the MDPT-n can be used to estimate the CPT q_t (MPa) using the following equation:

$$q_t = 0.23 * N + 0.2 \qquad (6.3)$$

where N is the equivalent to SPT (N) blows per ft estimated using MDPT-n, and q_t is the estimated CPT tip resistance in MPa.

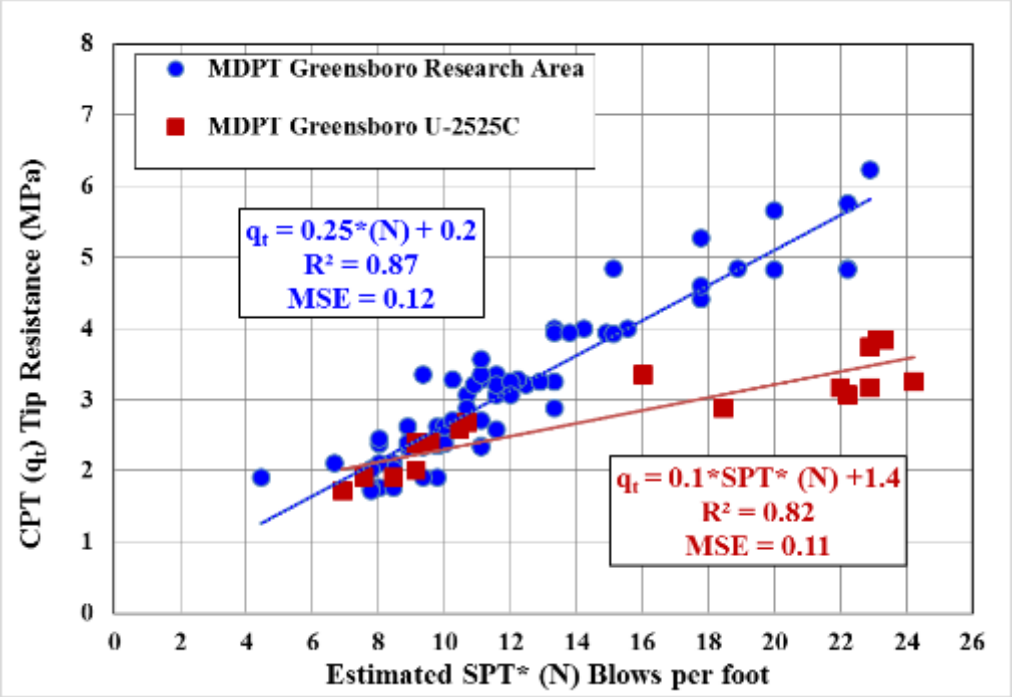

Figure 6.5 CPT (q_t) vs. estimated SPT* (N) using MDPT-n blows per ft.

Figure 6.6 shows the correlation of MDPT-n and CPT q_t along with other researchers' correlations of CPT q_t and SPT (N) blows per ft. The MDPT-n results are encouraging and comparable to other results.

6.6 Conclusion and Recommendation

The MDPT was correlated to limited data with CPT exploration. The relationship between the MDPT and the CPT was examined and the correlations were developed between the cone tip resistance (q_t), sleeve friction (*fs*), and the MDPT-n blow counts and the MDPT-t torque

for two locations. A positive linear relationship was found between the CPT tip stress q_t, CPT sleeve stress *fs*, and MDPT-n and MDPT-t for this study. In general, CTP q_t versus MDPT-n showed higher correlation coefficients than CPT *fs* versus SPT(N) (see Figures 6.4 and 6.5). The results of the regression analysis show a positive trend between the MDPT-t torque and CPT sleeve friction *fs*, and a positive trend between the MDPT-n blows per ft and the CPT tip resistance q_t. Although the correlation is promising, precautions are needed when using the information in different sites due to the limited data. Many researchers have stated that any correlation is unlikely to be unique for all soils, but the suggested relationships could be a framework for future refinements. Figure 6.6 shows a promising result of the MDPT-n and other researchers' work.

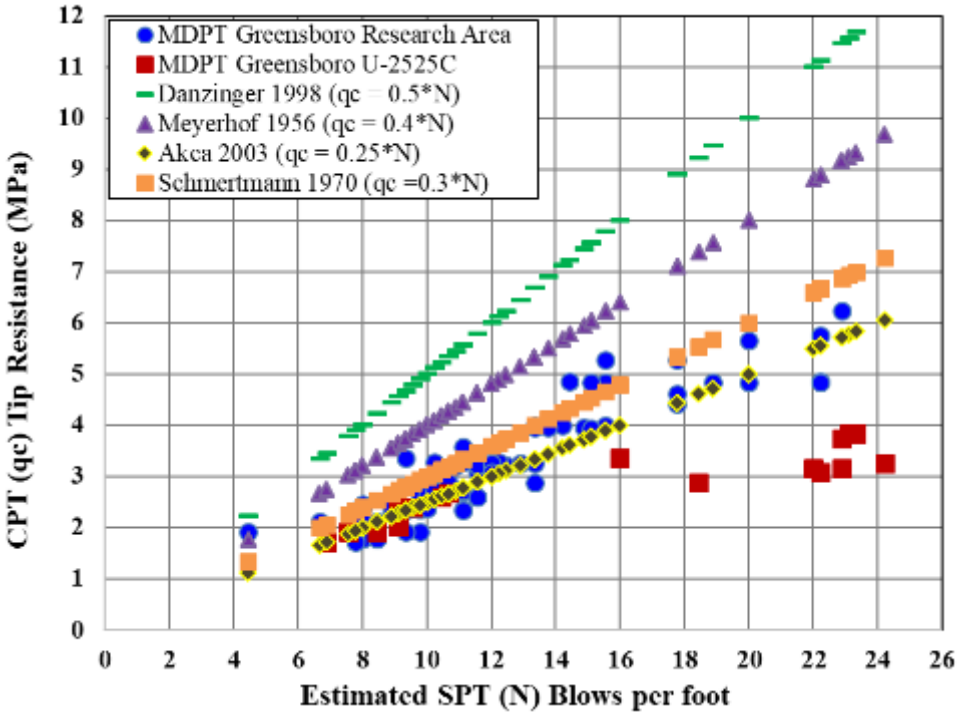

Figure 6.6 CPT (q_t) and estimates q_t from different researchers vs. estimated SPT* (N) using MDPT-n (q_t = qc).

Since the statistical and regression analyses are the main method used in this chapter, the size of the data is significant for the accuracy of the result. Additional data in the future will

increase the accuracy and the reliability of the correlations. Furthermore, it is recommended to calibrate the MDPT tests with CPT tests at each project site if possible to achieve accurate results.

CHAPTER 7. MINI DYNAMIC PENETRATION TEST MDPT VERIFYING SOIL COMPACTION AND BEARING PRESSURE

7.0 Abstract

Compaction is a process that increases soil density by using mechanical impact energy to remove air from the voids surrounding soil particles. Compaction is a very important phase in the construction of roadway embankments, building foundations, and transportation infrastructures, because the stability and the safety of the roadway embankment and the pavement depends on the compaction techniques and effort. In-situ density tests are typically used to measure the degree of compaction. The current methods for measuring compaction have significant limitations. For example, some electronic devices require constant calibration and costly maintenance; others are dangerous to operate, such as a nuclear gauge, or require costly equipment, such as intelligent compaction. This chapter discusses the newly developed Mini Dynamic Penetration Test (MDPT) device and its correlation with the dry density of soil to verify field compaction effort.

Wood laboratory boxes were built to perform control tests for soil types A-4 and A-5 with different compaction and moisture contents. The MDPT-n values were then correlated with the dry density and moisture content. The dry density γ_d and water content are typically measured with a nuclear gauge but can also be measured with a sand cone or rubber balloon, among other methods. The balloon density apparatus determines the in-place density of soil using a volume-displacement method, similar to the sand-displacement method. The sand cone method removes a sample of the material using calibrated sand to determine its dry unit weight and the volume of the hole from which the sample was removed. The MDPT test results showed a promising correlation between the MDPT-n blows per ft and the dry density with $R^2 = 0.86$, and the correlation between the MDPT-n blows per ft and the DCP blows per ft showed a strong

relationship. The statistical analysis of the data showed a strong positive trend between the DCP and MDPT. The strong correlation between the MDPT-n and DCP produced a coefficient of determination $R^2 = 0.86$ and $r = 0.92$. The bearing capacity can be estimated using the correlation between the MDPT, DCP, and the California Bearing Capacity (CBR). The MDPT is portable and quick to set up, run, and evaluate soil property on site. Due to its economy and simplicity, a better understanding of the MDPT results can reduce the time and cost for evaluating embankment compaction and the strength of pavement and subgrade soils.

7.1 Introduction

The compaction technique increases the density of soil particles by using impact equipment to provide the energy needed to remove the air voids surrounding the soil particles. Compaction is mostly used for constructing roadway embankments, building foundations, and transportation infrastructures. The stability and the safety of any embankment and pavement depends on the degree of compaction techniques, quality, and degree of compaction. The common parameters affecting the degree of compaction are:

a. Density
b. Water content
c. Soil type
d. Amount of energy applied

The minimum density and range of water content are usually specified for each project in order to meet the design requirements for embankment and pavement stability, but density could be used to evaluate the pavement quality and performance during and after construction. The advantages of proper compaction include:

a. Reduced settlement (or differential settlement)

b. Reduced permeability

c. Increased strength

d. Reduction or elimination of the bump before the bridge

Soil compaction typically can be achieved either by static or dynamic loading. Static compaction is performed by applying load slowly; dynamic compaction is performed by the repeated blows of a falling mass; and vibratory compaction is performed by vibrating equipment.

The roadway embankment equipment used for compaction includes:

1. Smooth-wheel rollers, used primarily for granular soils (uniform compaction)
2. Sheepfoot rollers, used mainly for clayey and silty soils (kneading compaction)
3. Pneumatic rubber-tired rollers used for clay soil
4. Vibratory rollers used for granular soils

The nuclear moisture density meter is most commonly used to determine soil density and water content at the same time. Despite the advantages of the nuclear method, it has many drawbacks, such as:

1. Requires correlation with other techniques or conventional methods, such as sand cone testing
2. Federal regulations for handling and storage of nuclear equipment
3. Transportation of radioactive materials
4. Operator licensure
5. Operators may be exposed to radioactive rays and must monitor their health regularly

Proper compaction of roadway embankments and pavement foundation layers is essential to achieving stability and long-lasting pavement performance. According to the NCDOT

compaction manual, “In general, embankment refers to any layer placed below the subgrade”. The subgrade is usually 8 in-thick and refers to the portion of the roadbed prepared as a foundation for the pavement structure (including the curb and gutter). The quality of the pavement foundation is controlled by the properties of the foundation material and the degree of compaction (Hancher et al., 2003). To ensure the suitability of the borrow or backfill materials, the soil is compacted at different layers to reach its maximum density. The borrow materials are usually compacted in the laboratory using the proctor test at different moisture conditions to obtain the optimum dry density and moisture content (ASTM D 698/AASHTO T99). The target value from the proctor test is used later for quality control (QT) and quality assurance (QA) during construction.

It is difficult to accurately measure proper compaction levels with the current frequency of the soil density without the use of nuclear density gauges (NDG) during construction. However, many state DOTs are trying to replace NDGs due to the following reasons:

1. Nuclear gauges use radioactive materials that may be hazardous to operators.
2. Mandatory radiation safety training for operators.
3. The licensing requirements, record-keeping, and storage of the gauges are stringent and very complicated.
4. Leak tests and annual calibration to maintain the NDGs.
5. Field verification of the NDG by using other accepted density testing methods.
6. Limited to a depth of 8 in.

Other available density devices, such as the rubber balloon and the sand cone methods, are also time- and labor-intensive. Most of these methods measure the degree of compaction

effort up to only 1 ft (305 mm) and require a longer time to run each test. The increased testing frequency may delay construction and cause contractors to file claims in response.

7.2 Problem Statement and Compaction Issues

7.2.1 Compaction and Frequency of In-situ Density Tests

Verifying the degree of compaction in-situ is a major issue for many state DOTs due to the frequency and the quality control of the compaction process. The following are examples of the NCDOT's requirements for testing frequencies:

a. Embankments: One density test every 5,000 yd^3 (4,000 m^3). A density test is recommended for every other lift of the embankment as it is being constructed (each lift is 8 in-thick).
b. Subgrade: One test every 1,000 linear ft for roads up to 28 ft (8.5 m) wide; for roads wider than 28 ft, one test every 3,000 yd^2 (2,500 m^2).
c. Chemically treated subgrade (lime or cement): One test every 2,000 lf (600 m).

NCDOT's current practice for compaction density requirements is at least 95% in accordance with AASHTO T 99, as modified by NCDOT and described in its compaction manual.

In recent years, many state DOTs have experienced unnecessary and unexpected roadway cracks and pavement failures. The compaction of the subgrade layers of the pavement has become even more critical to the success of pavement performance. Unfortunately, many pavement failures could be related to the compaction efforts, quality assurance/quality control (QA/QT) testing methods, and less frequent density testing during construction and acceptance of work. Therefore, a portable, effective, reliable, economical, quicker, and easy to use alternative for compaction control during roadway construction is great demand.

The MDPT device can be used to verify the specific density requirement in the field at any location or depth. It can estimate the dry density by calibrating the MDPT blow counts with a few density tests, and estimate the field density by using the developed empirical equation. The MDPT-n can also evaluate the dry density of soil layers to any depth quickly and economically.

The objective of this chapter is not to eliminate or to replace the use of conventional in-situ density tests, but rather to increase the frequency of density testing by using the MDPT device in addition to the typical limited-frequency density tests to expedite the density process. Figure 7.1 shows a sketch of the MDPT device parts. The hammer (weight mass) is marked with groove to distinguish the difference between the DCP hammer and the MDPT hammer.

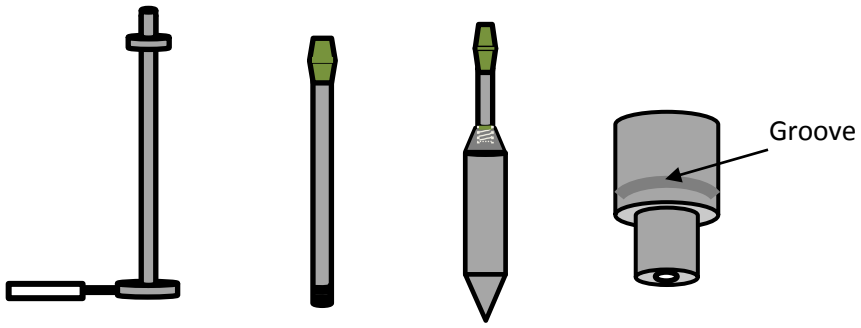

Figure 7.1 Sketch of MDPT parts.

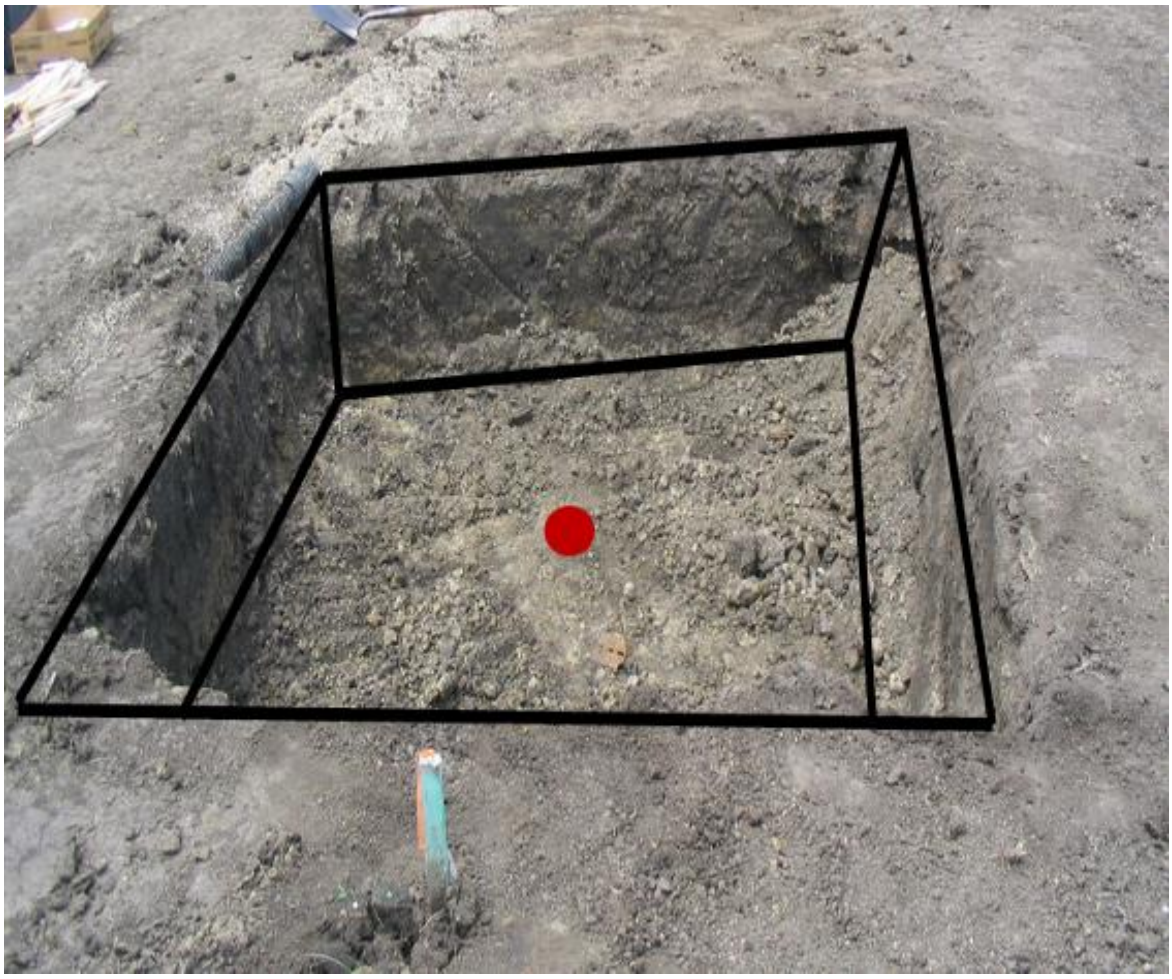

Figure 7.2 Illustration of the difficulty in verifying the bearing pressure in open cut of spread footing during construction.

7.2.2 Verifying Pavement Subgrade Strength and the In-situ Bearing Pressure for Retaining Walls and Spread Footings

This section discusses the typical in-situ methods for verifying subgrade strength or bearing pressure for shallow foundations. For soil strength verification, the in-situ bearing capacity is typically estimated or determined using plate load tests (PLT), cone penetration tests (CPT), or standard penetration tests (SPT), all of these tests are expensive, require heavy equipment, time consuming and are difficult to perform due to limited and confined space such as spread footing excavation, as shown in Figure 7.2. Similarly, the California Bearing Ratio (CBR) is typically used as strength indicator for the subgrade, subbase, or base of pavement

layers; however, it is time-consuming and expensive, and its repeatability is low. The MDPT test can be used to estimate bearing pressure indirectly by correlating the MDOT test results to DCP and CBR value based on the relationship between the DCP and the MDPT-n.

7.3 Objective

The objective of this chapter is to correlate the MDPT-n blows per ft (blows/300 mm) with the dry density γ_d of the subgrade or embankment layers and the DCP to estimate the CBR. The approach to achieve this objective requires the following tasks:

1. Study the relationship between the MDPT-n blow counts and soil dry density obtained by the nuclear gauge method or from laboratory tests.
2. Establish a relationship between the MDPT-n blow counts and the DCP to estimate the CBR in order to estimate the bearing capacity.

7.4 Literature Review

In-situ penetration tests have been widely used in geotechnical engineering for site investigation and soil characterization in support of analysis and design. The standard penetration test (SPT) and the cone penetration test (CPT) are the most common in-situ penetration tests; however, the dynamic cone penetrometer test (DCP) is used as an in-situ method for estimating the structural properties of soil or pavement.

The normal testing procedure for the DCP is performed continuously from the ground level to the desired penetration depth. The DCP was originally developed by A. J. Scala in 1956 in Australia. The current standard DCP according to ASTM D 6951-03 consists of a mass weight of 17.6 lb (8 kg), a drop height of 22.6 in (557 mm), and a 60º cone angle. Scala (1965) used the DCP with an extension to drive the cone 6 ft (1.8 m) below ground level to estimate soil strength, and he was the first to develop a correlation between the CBR and the DCP for pavement design.

Afterwards, many researchers developed and modified methods and testing equipment to investigate foundation layers for pavement design. Gawith and Perrin (1962) reported the use of the same DCP in Australia, which was used to develop the DCP-CBR correlation curve.

Sowers and Hedges (1966) built a light weight DCP device with a 15-lb (≈ 6.8 kg) weight and 20-in (508 mm) drop height. The apex cone angle was 45º to minimize the driving resistance, as shown in Figure 7.3. This lighter DCP was used to verify the bearing capacity or soil condition at spread footing locations, and most of their DCP tests were performed in augured holes.

Kleyn (1975) indicated that a road department in South Africa used the DCP with a 30º cone tip to investigate soil layers for pavement design in 1973.

Sekmeier et al. (1999) evaluated the relationship between DCP results and the degree of compaction of fills materials, such as mixture of clayey and silty sand, for the Minnesota Department of Transportation. Sekmeier et al. estimated the CBR from the DCPi penetration index values and then used published charts and formulas to estimate the resilient modulus from the estimated CBR to correlate the percent of compaction. However, the study showed no clear correlation or the relationship between the moduli and the degree of compaction.

In 2004, the ASTM D6951-03 introduced the standard test method in shallow pavement layers using the latest DCP design (ASTM, 2004).

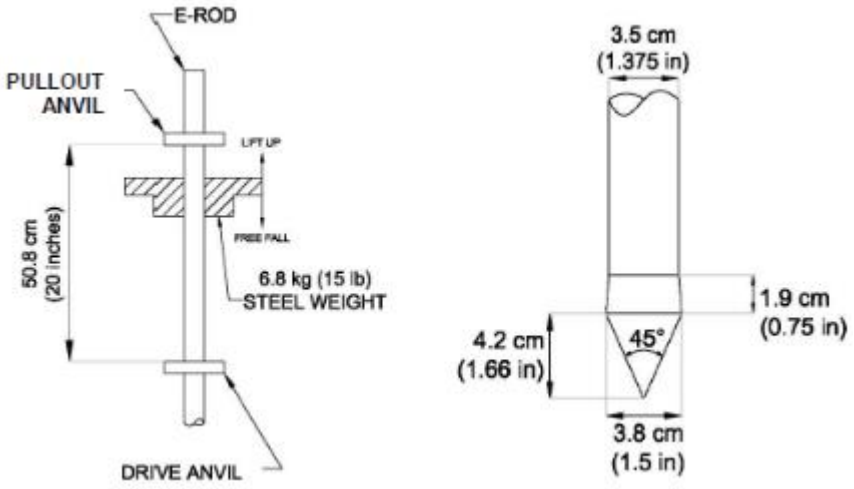

Figure 7.3 Sowers dynamic cone penetrometer (after Sowers and Hedges, 1966).

7.4.1 Correlations Between DCP Readings and CBR Values

Several researchers have studied the relationship between the DCPi penetration index and the California Bearing Ratio (CBR). The in-situ CBRs determined the DCP can be calibrated using laboratory-soaked CBRs. The base, subbase, and the subgrade soil strength can be estimated from the cone penetration resistance, which can be converted into CBR, subgrade modulus k, resilient modulus E, and soil support value (SSV). Most researchers' equations for the CBR is expressed as a function of the penetration rate (PR) (in mm/blow).

The following empirical correlations were developed by various researchers and agencies. Smith and Pratt (1983) reported the Australian Road Research Board (ARRB) had studied the relationship between the CBR and the DCP penetration rate (PR), and thus developed the following empirical relationship:

$$\text{Log (CBR)} = 2.56 - 1.15 \text{ Log (PR)} \qquad (7.1)$$

The North Carolina Department of Transportation (NCDOT) (Wu, 1987) established an empirical relationship between CBR and DCP. The relationship was based on the average of

three DCP tests and the field CBR within a distance of less than 1 ft (0.3 m) around the CBR test location:

$$\text{Log (CBR)} = 2.64 - 1.08 \text{ Log (PR)} \text{ or } \text{CBR} = 435/ \text{PR}^{1.08} \ (R^2=0.79) \qquad (7.2)$$

Livneh (1987) developed the following relationship between CBR and the PR:

$$\text{Log (CBR)} = 2.20 - 0.7 [\text{Log (PR)}]^{1.5} \qquad (7.3)$$

The U.S. Army Corps of Engineers (USACE) (Webster, Grau and Williams, 1992) developed a relationship between the CBR and the PR of the DCP, expressed by the following equation, which was used by many state DOTs and federal highway agencies:

$$\text{Log (CBR)} = 2.465 - 1.12 \text{ Log (PR)} \text{ or } \text{CBR} = 292/(\text{DCPI})^{1.12} \qquad (7.4)$$

where DCPI is the Dynamic Cone Penetrometer Index, in units of length divided by blow count.

The difference between the USACE correlation and the NCDOT correlation was based on lab CBR values and field CBR values, respectively. Since it is known that the field CBR value is generally twice the value of lab CBR value, the results of these two independent studies match very well, based on Equations 7.2 and 7.4.

Kleyn (1992) developed the following equation:

$$\text{Log (CBR)} = 2.62 - 1.27 \text{ Log (PR)} \qquad (7.5)$$

Coonse (1999) presented the following correlation:

$$\text{Log } (\text{CBR}_{\text{field}}) = 2.53 - 1.14 \text{ Log } (\text{PR}_{\text{field}}) \qquad (7.6)$$

Equation 7.4 was developed by the USACE and was adapted by many researchers, practitioners, and agencies around the world, and it was selected as one of the best correlations as noted by Livneh (1995), Webster et al. (1992) and Siekmeier et al. (2000).

Gabr et al. (2001) developed a correlation between the DCPi and the plasticity index and the saturation ratio based on laboratory tests of the Piedmont residual soils in Davidson County, NC, with more than 60% fines. Gabr et al. used these correlations to predict the dry unit weight and water content of the soil.

Abu-Farsakh et al. (2004) conducted both laboratory and in-situ testing to evaluate the use of DCP for quality control and quality assurance for pavement and embankment construction. The CBR, DCP, and the plate load tests (PLT) were performed in the laboratory on selected soils with a mixture of silty clay and clayey silt, and then compared with in-situ tests performed on subgrade pavement layers for several projects for the Louisiana DOT. Abu-Farsakh et al. concluded that the DCP was a dependable device for estimating the stiffness and the modulus of embankment, as well as for the base layers of pavement and subgrades. The results of their study indicated that the PR of 5.5 mm/blow is an acceptable value for crushed limestone base.

Wu and Sargand (2007) evaluated the use of the DCP for evaluating the construction of pavement layers for the Ohio DOT. The penetration ratio PR was measured in mm/blow, and the data were collected based on ten projects tested over a two-year period. Data from both chemically treated and untreated subgrade was collected. Wu and Sargand concluded the use of DCP during construction can significantly improve the quality control/quality assurance and the performance of the subgrade materials. They also recommended that an acceptable PR for both treated and untreated soil layers is 8 mm/blow (0.32 in/blow).

Puppala (2008) evaluated the correlation between DCPi rate values and the resilient modulus. He found that many engineers, researchers, and agencies have used the DCP to estimate the moduli and used the values in many transportation projects for compacting

subgrades and granular soil without addressing the site variability. However, Puppala provided a valid warning to users of the DCP to be very careful when estimating and using moduli from different sites, because most of the correlations are site-specific and mostly empirical, and their use for different soils requires careful evaluation and engineering judgment.

Gabr and Browning (2006) studied the effect of the cone tip apex angle on penetration resistance. The study included five different sizes of cone tip apex angles: 50º, 60º, 75º, 90º and 120º (see Figure 7.4). Based on the laboratory tests, the study concluded that increasing the cone tip apex angles increases the tip resistance.

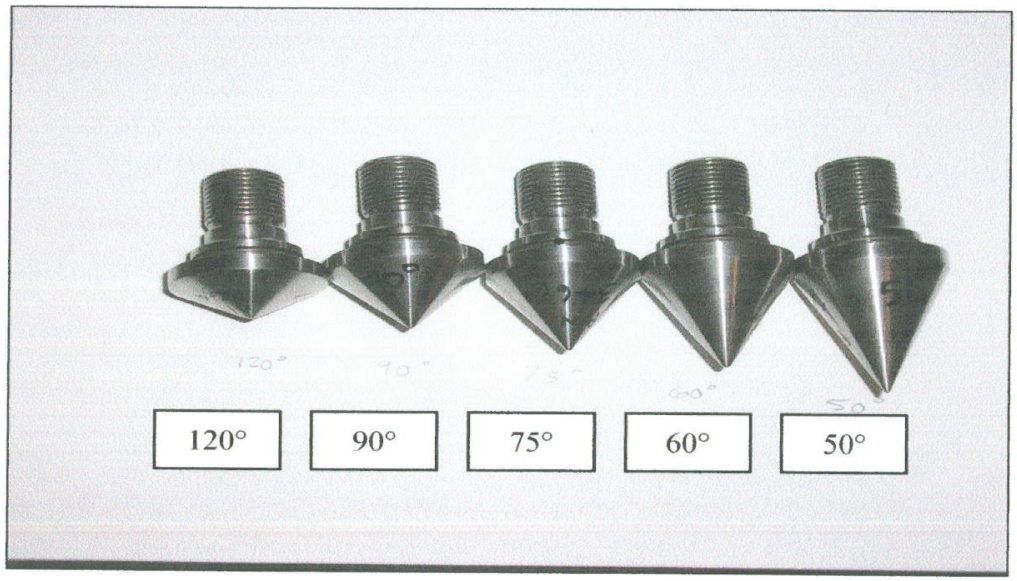

Figure 7.4 Cone tip apex angles (120º, 90º, 75º, 60º, 50º) (Browning, 2006).

Paige Green (2009) reported the following equations were previously published by the Transvaal Roads Department in Pretoria, South Africa, and can be used to estimate the CBR and the unconfined compressive strength from the DCP:

$$\text{If DN} > 2 \text{ mm/blow} \quad CBR = 410 \times DN^{-1.27} \tag{7.7}$$

$$\text{If DN} < 2 \text{ mm/blow} \quad CBR = (66.66 \times DN^2) - (330 \times DN) + 563.33 \tag{7.8}$$

$$UCS = 15 \times CBR^{0.88} \tag{7.9}$$

or $UCS = 2900 \times DN^{-1.09}$ (7.10)

where CBR is the California Bearing Ratio, DN is the DCP number (mm/blow), and UCS is the unconfined compressive strength.

Table 7.1 Correlations Between CBR and PI (after Harison, 1987 and Gabr et al., 2000).

Author	Correlation	Field or laboratory based study	Material tested
Kleyn (1975)	log (CBR) = 2.62 - 1.27· log(PI)	Laboratory	Unknown
Harison (1987)	log (CBR) = 2.56 - 1.16· log(PI)	Laboratory	Cohesive
Harison (1987)	log (CBR) = 3.03 - 1.51· log(PI)	Laboratory	Granular
Livneh et al. (1994)	log (CBR) = 2.46 - 1.12· log(PI)	Field and laboratory	Granular and cohesive
Ese et al. (1994)	log (CBR) = 2.44 - 1.07· log(PI)	Field and laboratory	ABC*
NCDOT (1998)	log (CBR) = 2.60 - 1.07· log(PI)	Field and laboratory	ABC* and cohesive
Coonse (1999)	log (CBR) = 2.53 - 1.14· log(PI)	Laboratory	Piedomont residual soil
Gabr (2000)	log (CBR) = 1.40 – 0.55· log(PI)	Field and laboratory	ABC*

*Aggregate base course

PI = PR = DCPI (Dynamic Cone Penetrometer Index in units of length divided by blow count)

The literature review indicates that most of the testing was conducted with a DCP cone (Figure 7.5) to correlate with the CBR, resilient modulus (M_R), and soil parameters.

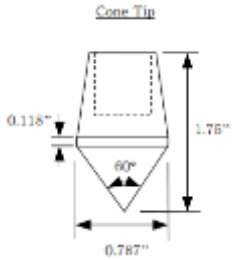

Figure 7.5 Typical DCP cone geometry.

The standard Dynamic Cone Penetrometer (DCP) (ASTM D6951) includes the following:

1. Steel rod ranging from 3.2–6.5 ft (1–2 m)
2. Standard size of hardened steel cone at the end (0.787 in) (20 mm)

3. Drop hammers: 10 lb (4.6 kg) for soft soils and 17.6 lb (8 kg) for stronger soils; in this study the 17.6 lb (8 kg) hammer was used
4. Drop height of 22.6 in (574 mm)

The soil strength and the compaction of the soil can be indirectly estimated by measuring the penetration of the cone against the number of drops of the weight. The DCP may also be used to obtain an approximate value of the California Bearing Ratio (CBR), which is an index of soil-bearing strength. The CBR and DCP have been used in practice for many decades, and many researchers have conducted tests and produced many data sets and empirical correlations between the penetration rate of a DCP rod, CBR, and soil strength. The main advantage of a DCP is that it does not require any external reaction forces—it only relies on the kinetic energy provided by a drop hammer.

7.5 Description of Mini Dynamic Penetration Test (MDPT)

The MDPT can be driven down to 45± ft (13.7± m) below ground surface with 5/8-in (15.8-mm) stainless steel rods extensions. The MDPT hammer configuration was designed to mimic the SPT tip and skin resistance behavior to produce 10% of the SPT total energy of 350 ft-lb (48.4 kg-m). The hammer consists of a steel mass of 17.5 lb (7.98 kg) falling 24 in (609 mm) to develop 35 ft-lb (4.84 kg-m). Figure 7.7 shows an actual MDPT during a field test. The SPT measured N value blows per ft (blows per 300 mm) is defined as the penetration resistance, which equals the sum of the number of blows required to drive the SPT sampler to a depth interval between 6 in–18 in (150–450 mm). The MDPT procedure will encompass the same effect of friction and other factors to reduce the delivered energy.

7.6 DCP and Bearing Capacity Correlations

The bearing capacity of shallow foundations was correlated to the DCP penetration. Packard (1973) studied and compared the bearing capacity measured at 2.5 mm deflection from the plate load test with various CBR materials at a similar deflection. The study was for the design of concrete airport pavement.

$$\text{Bearing capacity (kPa)} = 3426.8\ DN^{-1.0101} \quad (7.11)$$

where DN is the cone penetration rate (mm/blow).

However, the literature review indicates that most of these methods did not carry the test failure, nor was there a clear indication to describe whether the values are ultimate or allowable. Although the DCP is a useful tool for field verification, it has the following limitations due to the shaft friction from the extension rod:

- Augured holes (4 in–6 in) (102 mm–152 mm) are required to perform penetration tests.
- The maximum effective testing depth in augured holes range 15 ft–20 ft (4.6 m–6 m).

7.7 Data Selection From Both Laboratory and Field Testing

This section describes the data selection and field test procedure for the dry density, moisture content, and MDPT tests conducted for this study. The moisture content and the dry density tests were obtained by the nuclear gauge method used in the field (see Figure 7.6).

7.7.1 Laboratory Test: Phase I Control Testing

In Phase I of the testing procedure, the relationship between the MDPT test and the dry density test was evaluated in a controlled environment. Two wood boxes 2.5 x 2.5 x 1.5 ft (762 mm x 762 mm x 457 mm) were constructed and filled with three predominate Piedmont soil types: A-4, A-5, and A-7-5 from Winston Salem, North Carolina, as shown in Figure 7.8. The test procedure below was followed:

1. Place the soil in each box in three layers (0.5 ft, 1 ft, 1.5 ft) (152 mm, 305 mm, 495 mm) with the proper water content (wc%).
2. Measure the soil density without compaction, with walking compaction, and with tamping compaction to achieve three different compaction levels.
3. Use a nuclear gauge to measure the density and moisture content in four directions of each layer and each compaction level (rotate the nuclear device in for direction and record the results), as shown in Figure 7.6.
4. Drive the MDPT in four corners of the dry density test location and record the blow counts for each compaction level.
5. Increase the moisture content by adding more water to again measure the dry density.

7.7.2 Field Test: Phase II

The results of Phase I were encouraging, as there was a strong relationship between the MDPT-n blow counts and the dry density values. In Phase II of the testing procedure, tests similar to those conducted in Phase I were performed for the natural ground and compacted roadway embankment. The field testing included the MDPT, DCPT, and nuclear gauge. Several sites from three counties within North Carolina were selected for the field testing, as shown in Table 7.2. For the selected sites, the MDPT, DCPT, and density tests were performed at the same location, allowing for comparison between the three test results. Field tests were necessary to confirm and refine the correlation between the MDPT and the dry density.

Table 7.2 shows the number of tests and the locations of each test. The dry density and the moisture content tests were taken in four directions, as shown in Figures 7.6 and 7.7, to obtain an average value. The distance between the MDPT test and the dry density was approximately within 1 ft (305 mm), as shown in Figure 7.6.

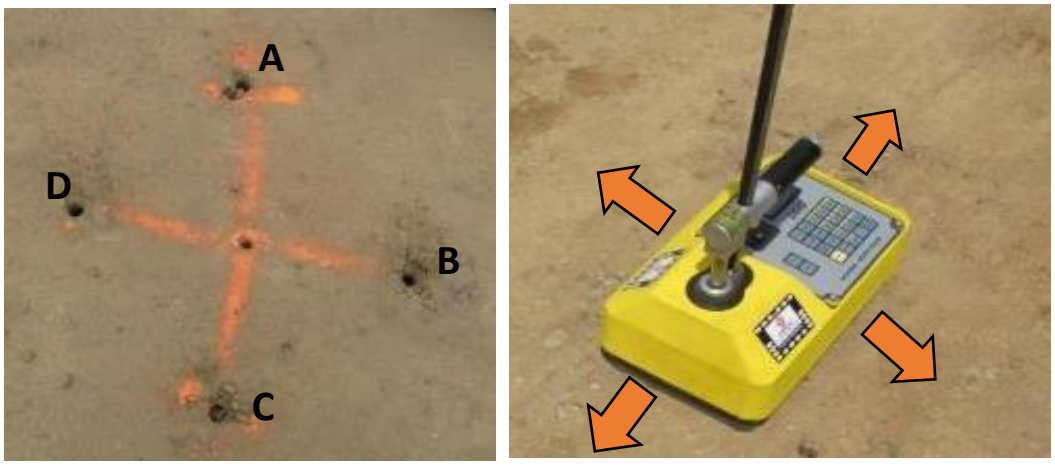

Figure 7.6 Nuclear density test in four directions and the MDPT tests at four points.

Figure 7.7 MDPT tests at different points (Wake Co. field work).

Figure 7.8 Laboratory density tests (MDPT, 0.5 in rod and DCP).

Figure 7.9 MDPT device.

Table 7.2 Number of MDPT-n, Density and Water Content at Various Locations.

Location	MDPT-n	Dry Density γd	% Water Content
Wake, NC Field	9	9	9
Wake, NC Laboratory	30	30	30
Monroe, NC	15	11	11
Anson, NC	15	15	15

Table 7.3 Sample of Data Collected from Box 1 Test at 1.5 ft After Tamping with Steel Plate.

A	MDPT (n)	% Moisture	Dry Density (pcf)
6"	6	17.1	85.6
12"	10	17.1	85.6
18"	10	17.1	85.6
B	MDPT (n)	% Moisture	Dry Density (pcf)
6"	5	16.7	83.6
12"	10	16.7	83.6
18"	10	16.7	83.6
C	MDPT (n)	% Moisture	Dry Density (pcf)
6"	5	16.1	81.5
12"	12	16.1	81.5
18"	10	16.1	81.5
D	MDPT (n)	% Moisture	Dry Density (pcf)
6"	7	17.1	84.9
12"	9	17.1	84.9
18"	10	17.1	84.9

1 in = 0.0254 m, 1 pcf = 16.0184 Kg/m^3 = 0.157087 kN/m^3

7.8 Data Analysis

This section discusses the regression analysis of the results obtained from the field and laboratory tests. Table 7.3 is an example of the data collected at each point, A, B, C, and D, around the density and water content tests. The data was compiled and organized to perform a regression analysis to evaluate the strength of the direct correlation between the MDPT-n, the

dry density, and the moisture content. The analysis results show a positive and a strong correlation between the dry density and the MDPT-n blow counts, with R^2 of 0.92.

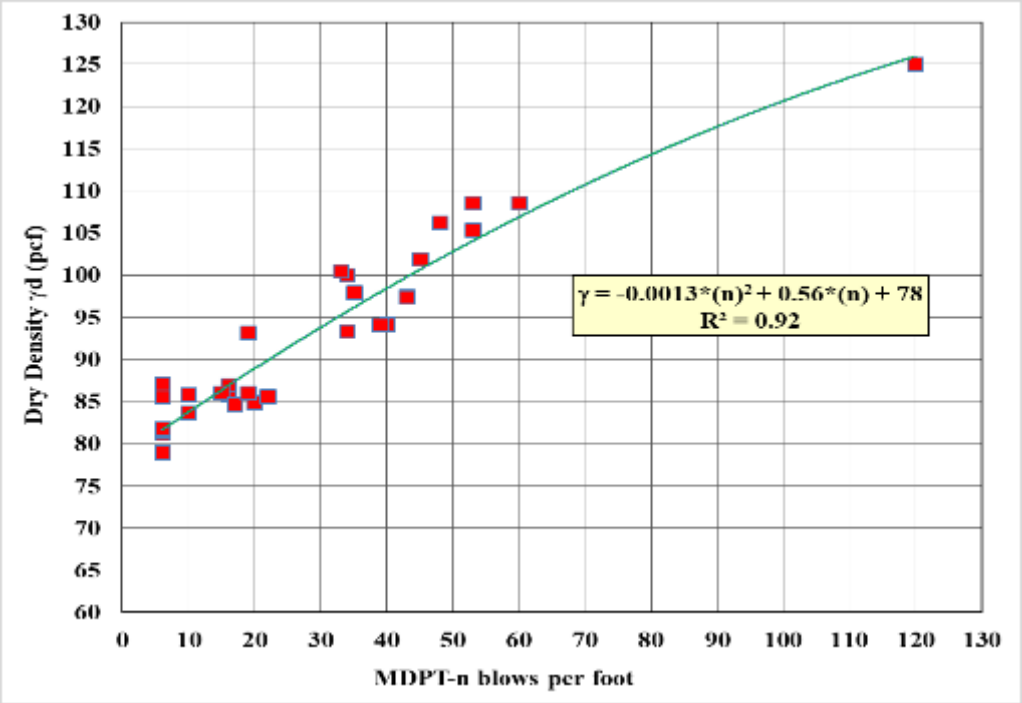

Figure 7.10 Direct correlation between dry density γd and MDPT-n.

Equation 7.12 is developed directly from the analysis between the MDPT-n and the dry density tests without converting the MDPT-n to SPT*(N), as shown in Figure 7.10.

$$\gamma_d = -0.0013*(n)^2 + 0.56*(n) +78 \qquad (7.12)$$

γ_d = Dry density in pcf (1 pcf = 16.02 kg/m^3)

Figures 7.11 and 7.12 present the correlation between the estimated SPT* (N) blows per ft from the MDPT-n blows with the dry density tests. Equation 7.3 is developed from Figure 7.12.

$$\gamma_d = -0.021*SPT*(N)^2 + 2.2*SPT*(N) +78 \qquad (7.13)$$

γ_d = Dry unit weight or dry density in pcf (1 pcf = 16.02 kg/m^3)

SPT* (N) = Estimated blows per ft from MDPT-n (1 ft = 305 mm or ~ 300 mm)

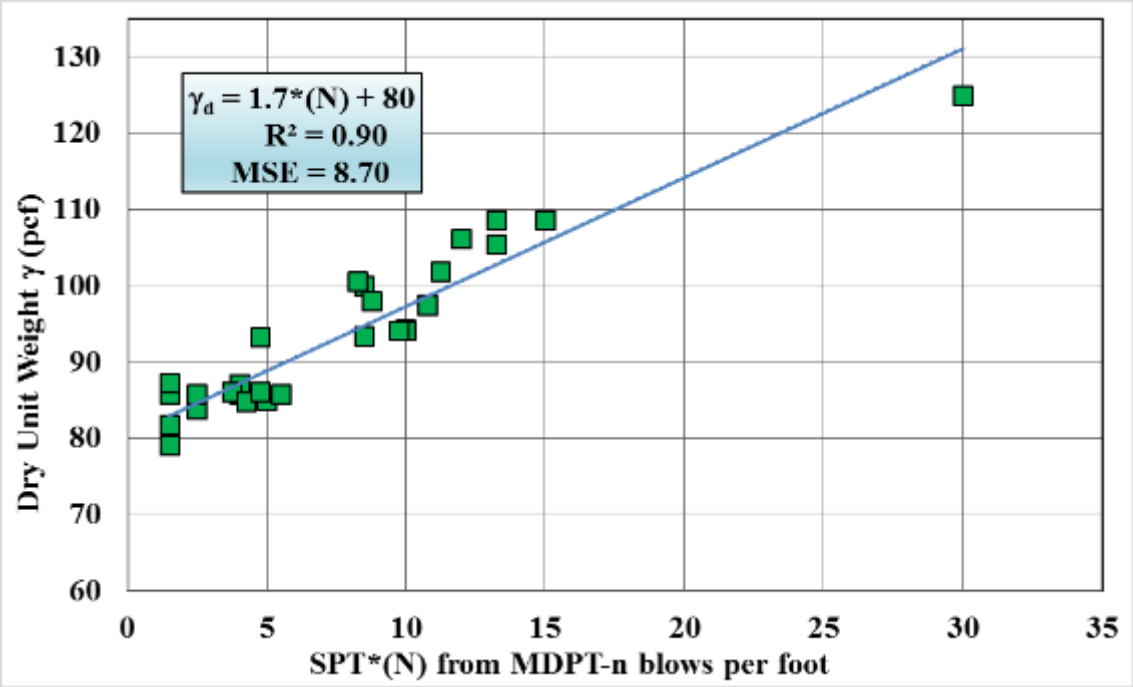

Figure 7.11 Linear trend: Correlation between dry density γd and estimated SPT*(N) from MDPT-n.

Table 7.4 summarizes the additional relationships investigated and presents corresponding Figures 7.11 and 7.12. The anaysis shows a significant positive relationship exists between the dry density and the MDPT-n blow counts. Both linear and nonlinear regression were performed to show the strength of correlations, the R^2 is 0.90 and 0.91 for linear and the non linear correlation, respectively. The MSE for the linear correlation is 8.7.

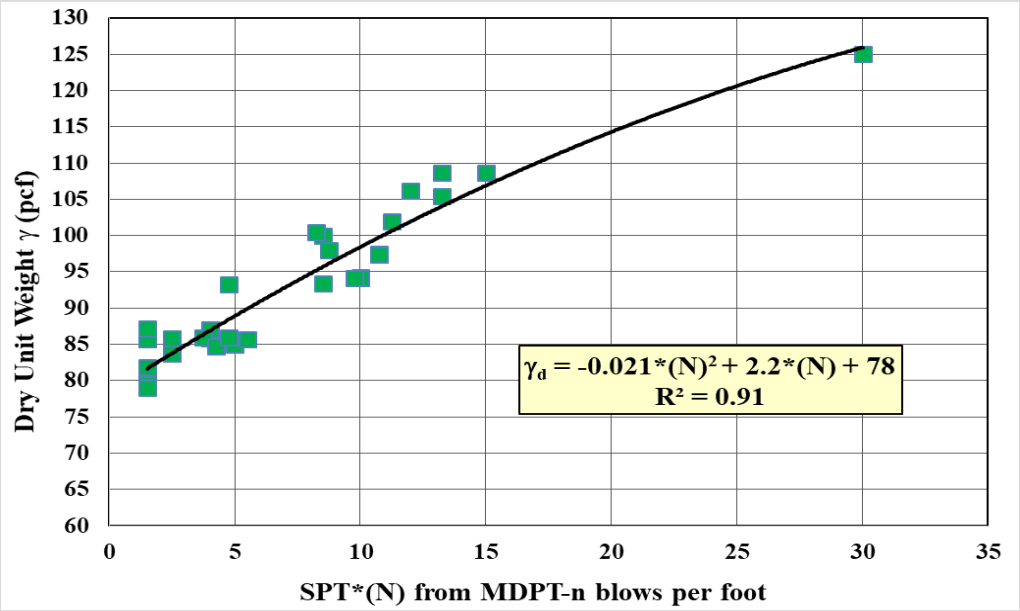

Figure 7.12 Polynomial trend: Correlation between dry density γd and estimated SPT* (N) from MDPT-n.

Table 7.4 Summary of the Regression Analysis for the Correlation Between Dry Density γd and SPT*(N) from MDPT-n Blows.

Regression	Trend Equation	R^2	r Coeficient	P-value	Standard Error
Linear Figure 7.12	$\gamma_d = 1.7*(N) + 80$	0.90	0.94	0.000	3.99
Polynomial Figure 7.13	$\gamma_d = -0.021*(N)^2 + 2.2*(N) + 78$	0.91	0.95	0.000	3.73

The steps from Chapter 4 were used to convert the MDPT-n to SPT* (N) to genertae Figures 7.11 and 7.12 and to develop the equations listed in Table 7.4. The results shows the significant relationship between the dry density and the MDPT-n blows per ft for the both the linear and nonliner correlations, with R^2 of 0.90 and 0.91, respectively. Figure 7.13 shows the 95% confidence interval for the correlation between the estimated SPT* (N) using MDPT-n and the dry density. The results are shown in the two red and green curves drawn next to the blue regression line. These curves represent a 95% confidence interval for the regression line. This interval includes the true regression line with 95% probability.

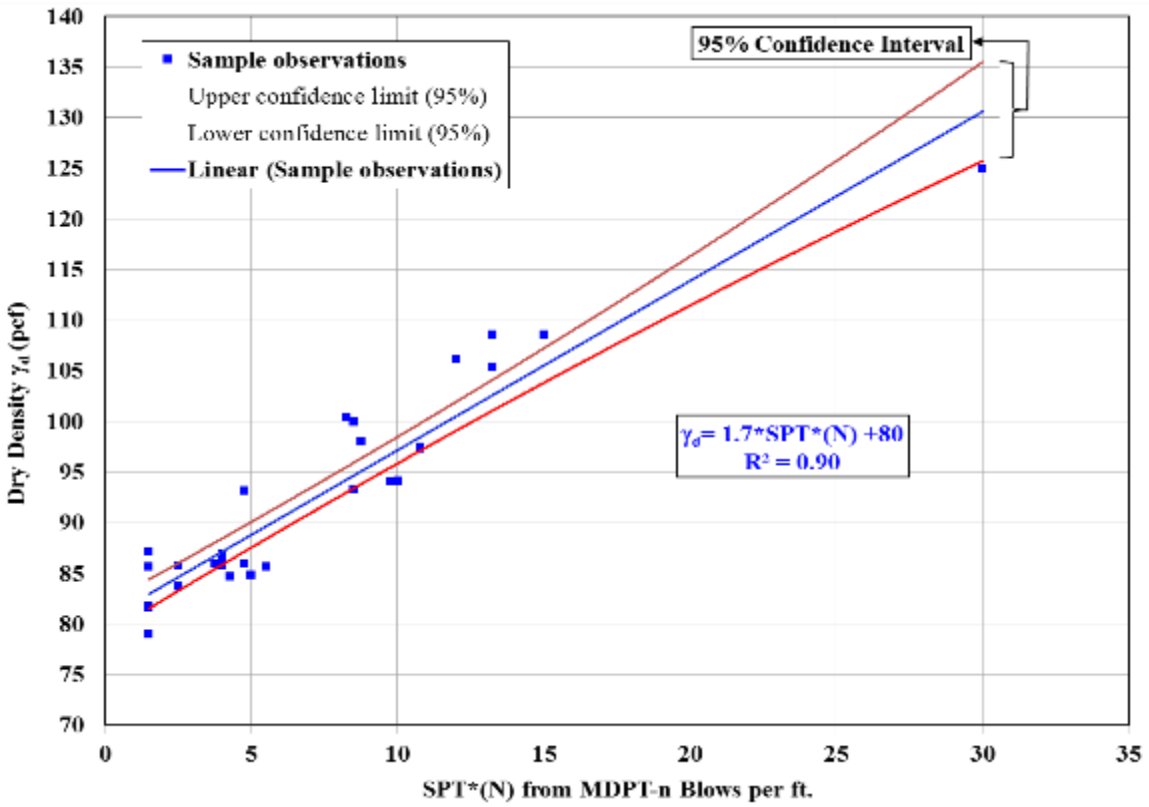

Figure 7.13 Linear regression and 95% confidence limits between γ_d and SPT* (N).

7.8.1 Relationship Between Water Content (WC%) and MDPT-n and Dry Density γ_d

This section describes the relationship between the water content and the MDPT-n blow counts and the dry density. Compaction is a major aspect of roadway construction, pavement, runways, earth dams, and retaining walls. Compaction is a process that increases soil density or unit weight by decreasing the air volume. There is usually no change in water content; however, the degree of compaction is estimated by the dry density and depends on both the percentage of water content (wc%) and the applied energy (e.g., number of drop impacts, number of roller passes). The maximum dry density of soil occurs at an optimum water content. The laboratory and the field tests were conducted with a nuclear gauge to estimate the dry density and the water content and the MDPT-n blow counts, and the data were compiled and analyzed using statistical analysis to determine the strength of the relationship. Figure 7.14 illustrates the negative

relationship between the dry density and the water content. The field test was compacted to an optimum water content of 15%-17%; the higher the water content, the lower the dry density.

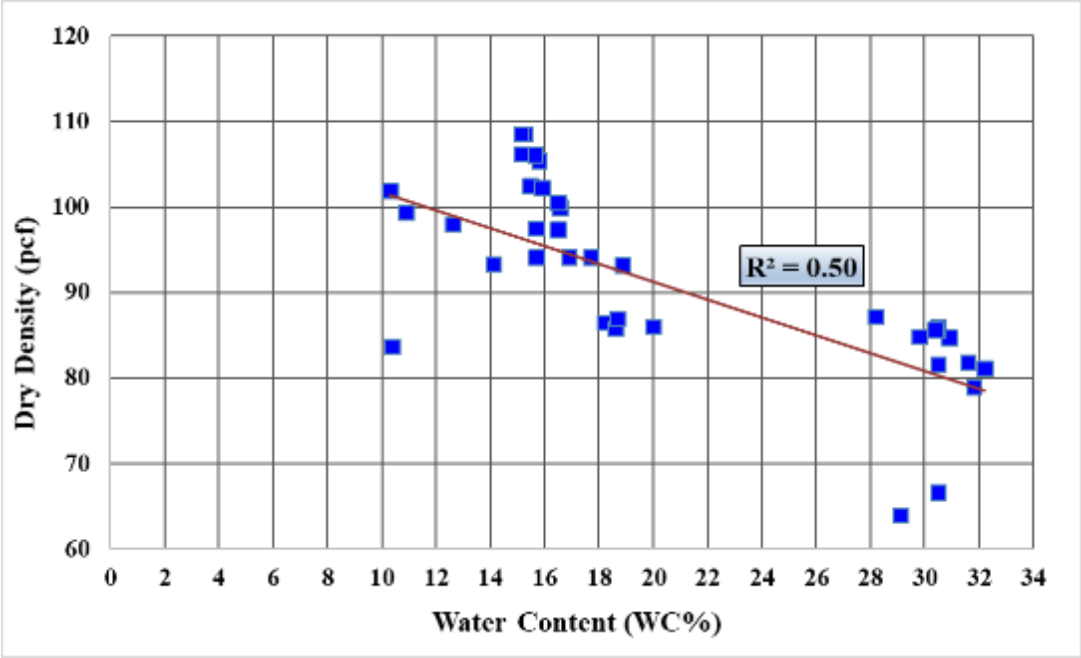

Figure 7.14 Dry density γd vs. percentage of water content (wc%).

Similarly, Figure 7.15 illustrates the negative relationship between the MDPT-n blows per ft and the percentage of water content. There is a negative trend with R^2 of 0.35; therefore, 35% of the variation in MDPT-n is due to the water content. The higher the water content, the lower the MDPT-n blows, and this relationship considered low strength. Also, see Table 7.5 for the multiple regression analysis and the results between the dry density and both the water content and the SPT* (N).

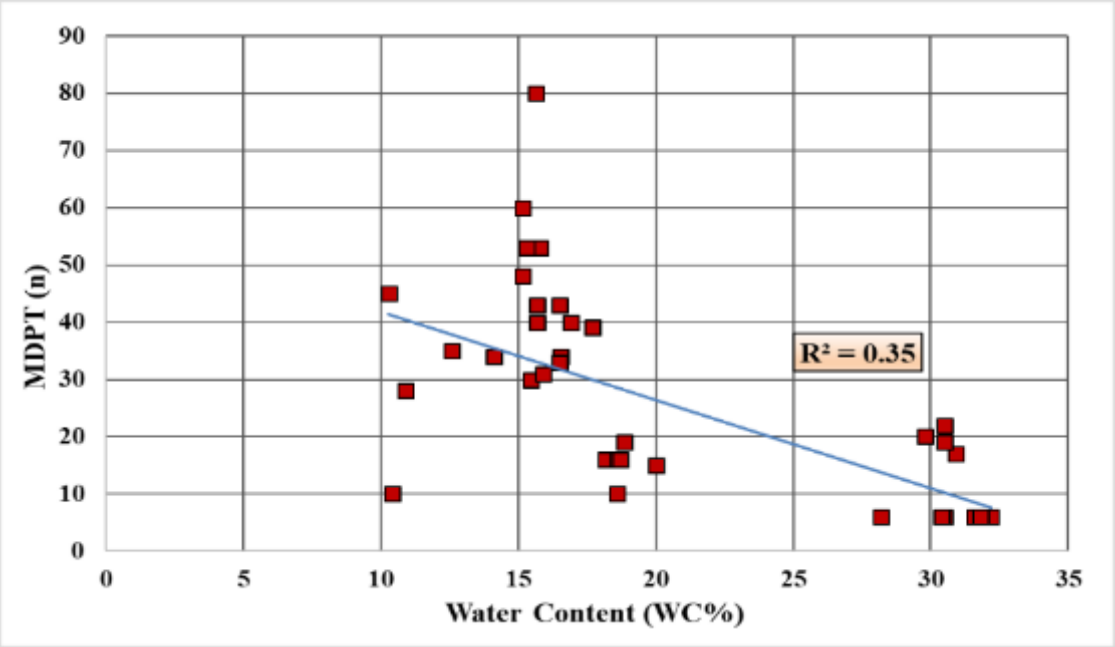

Figure 7.15 MDPT-n blows per ft vs. percentage of water content (wc%).

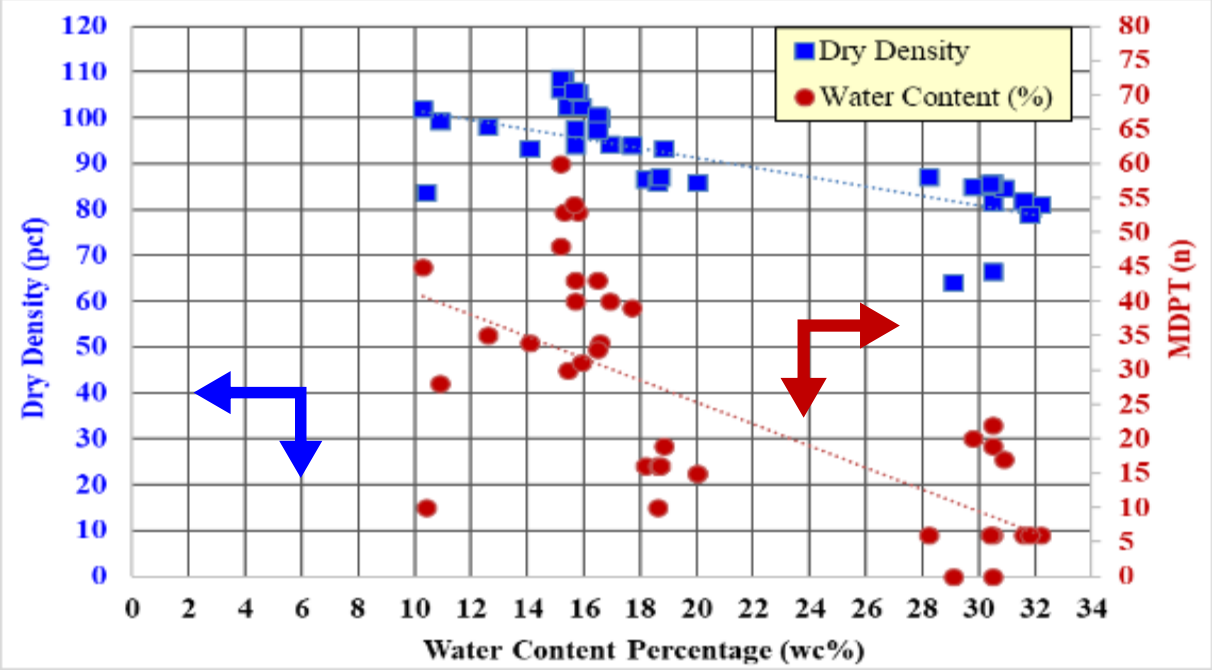

Figure 7.16 Dry density γd and MDPT-n blows per ft vs. percentage of water content (wc%).

Figure 7.16 illustrates the three variables (dry density, MDPT-n in relation to water content) to show the trend and the direct relationships between these variables.

Figure 7.17 shows the relationship between the dry density, estimated SPT* (N), and the water content. The blue arrow indicates the relationship between the SPT (N) and the dry density. The red arrow indicates the relationship between the dry density and the water content. The $R^2 = 0.91$ is the same as in Figure 7.12, presenting the correlation between the dry density and the estimated SPT* (N).

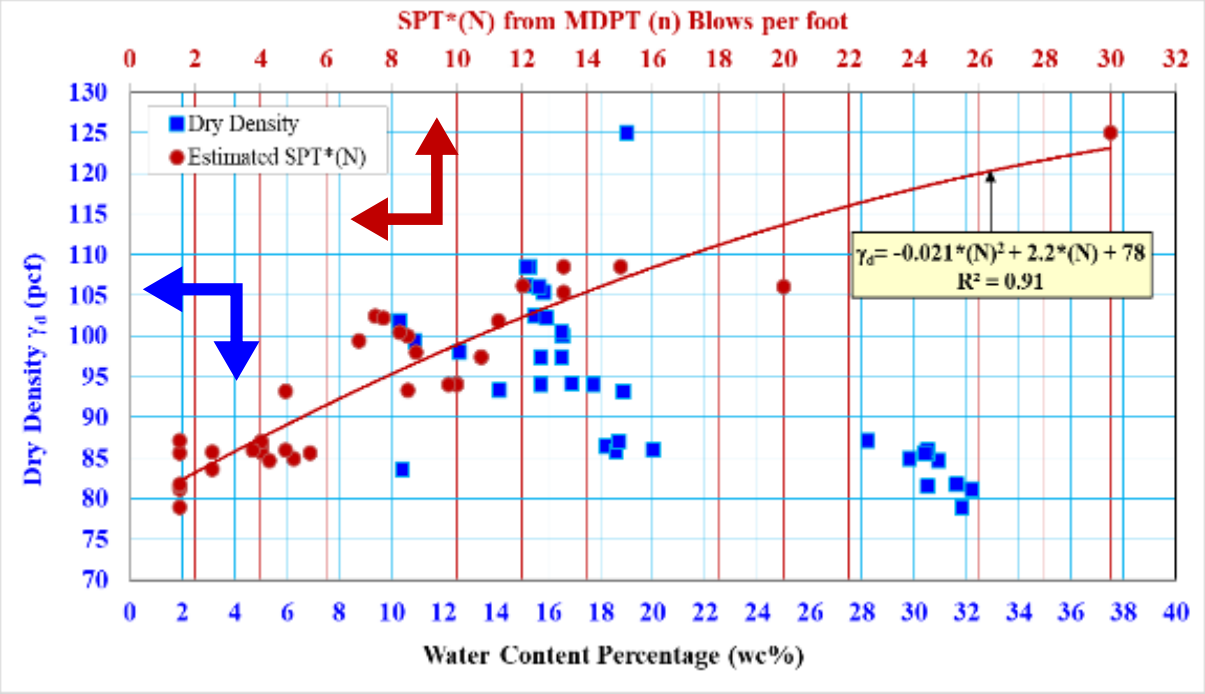

Figure 7.17 Illustration of relationship between the γd and (N) and between γd and water content (wc%).

7.8.2 Multiple Regression Analyses

Correlation and multiple regression analyses were conducted to examine the relationship between the dry density, estimated SPT* (N), and the water content. Table 7.5 shows a summary of the multiple regression between the dry density, SPT*(N), and water content. The results clearly indicate there is a significant relationship between the dry density and the SPT*(N) and the water content. The multiple regression model with two predictors (water content and SPT* (N)) produced $R^2 = 0.92$, p-value < .001. The relationship can be shown in the following equation:

$$Y = \beta 0 + \beta 1X1 + \beta 2X2 \qquad (7.14)$$

where Y is the dry density (pcf), X1 is the SPT (N) blows per ft, and X2 is the water content percentage (example 30%).

$$\text{Dry density} = 85.6 + 1.6*\text{SPT* (N)} - 0.22*\text{ water content \%} \qquad (7.15)$$

7.8.3 Validation of Equation 7.13 and 7.15

This section seeks to validate Equations 7.13 and 7.15. The SPT* (N) estimated based on equations developed in Chapter 4 (estimated 1 SPT*(N) ~ 4 MDPT-n). Both the SPT* (N) and measured water content are used to estimate the predicted dry density, and the results are summarized in Table 7.6 using Equations 7.13 and 7.15.

Statistical analysis was conducted for both the measured and the predicted data, and the results are shown in Figure 7.18 and Table 7.6. The results for this specific data produced $R^2 = 0.92$ and p-value <0.001, which indicates significant correlation between the predicted dry density model and the measured dry density.

Equation 7.15 was validated, and the results are shown in Table 7.6 in comparison with Equation 7.13. The results of the validations are shown in Figure 7.18. The correlations between

the dry density and the both the water content and the MDPT-n produced slightly higher R^2=0.92 for Equation 7.15 and R^2=0.91 for Equation 7.13.

Table 7.5 Summary of the Output of the Multiple Regression Analysis for Dry Density γd.

SUMMARY OF THE OUTPUT (γd to SPT*(N) and water content (WC%))

Regression Statistics	
Multiple R	0.96
R Square	0.92
Adjusted R Square	0.91
Standard Error	2.95
Observations	37.00

ANOVA

	df	SS	MS	F	Significance F
Regression	2.0	3217.5	1608.7	185.1	0.0
Residual	34.0	295.6	8.7		
Total	36.0	3513.0			

	Coefficients	Standard Error	t Stat	P-value	Lower 95%	Upper 95%
Intercept	85.6	2.18	39.30	0.00	81.17	90.02
Estimated SPT (N)	1.6	0.10	15.57	0.00	1.36	1.77
Water Content (%)	-0.22	0.08	-2.58	0.01	-0.38	-0.05

SPT*(N) is the equivalent SPT(N) by converted MDPT-n blows per ft to SPT* (N).

Table 7.6 Measured and Predicted Dry Density Using Equations 7.13 and 7.15.

				Eq. 7.15	Eq. 7.13
MDPT-n	SPT* (N) from MDPT (n)	Water Content (WC%)	Measured Dry Density	Predicted $\gamma_{d,N}$ & wc%	Predicted $\gamma_{d,N}$ only
18	5	20.2	89.5	89.2	88.5
38	10	21.2	97.1	96.9	97.9
22	7	20.1	93.5	92.4	92.4
32	8	21.2	93.7	93.7	94.3
24	6	21.2	92.2	90.5	90.4
36	9	20.2	95.3	95.6	96.1
18	4	22.7	87.2	87.0	86.5
28	7	22.2	91.2	91.9	92.4

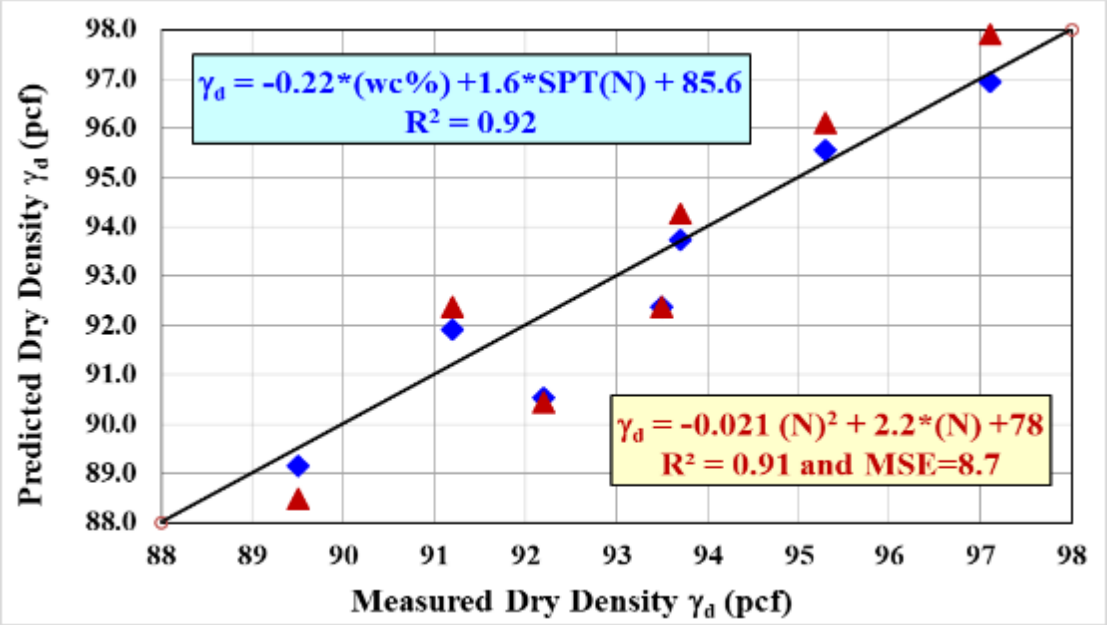

Figure 7.18 Results of the validation of Equations 7.13 and 7.15.

7.9 Bearing Pressure Verification

This section describes the valuable benefits of using the MDPT device during construction to verify the design assumption in the field before and during the construction of shallow foundations. Field verification of the bearing pressure for shallow foundations is one of the most important basic parameters to be determined and verified before the construction of any foundations for structure, spread footings, and retaining walls.

The typical conventional methods for estimating the field bearing pressure parameter is becoming relatively expensive and time-consuming for small projects and projects with difficult access. Heavy trucks or drill rigs are very difficult to use in open cut as shown in Figure 7.2. The MDPT is a multipurpose device that can be used to obtain the field bearing capacity. While this study did not fully focus on the direct and reliable correlations between the MDPT and the field bearing pressure or bearing capacity, there are two proposed methods for verifying the field bearing pressure using the MDPT device. The first method is to correlate the MDPT-n to the Dynamic Cone Penetrometer (DCP) n-value, because many researchers conducted studies

correlating the bearing capacity and the CBR to the DCP. Field tests were performed for both the DCP and MDPT adjacent to each other for the Piedmont soil to develop an imperial correlation between the MDPT and (DCP) (blows/300 mm). The data for the DCP was limited to shallow foundations.

Lacroix and Horn (1973) proposed a correction process for the nonstandard SPT penetration resistance (N) which allows engineers to correlate the standard penetration resistance (N) to a solid cylindrical shape with a conical point. Lacroix and Horn stated the required energy to drive the sampler or cone shape to a specific depth (L) was directly proportional to both the square of the outside diameter (D^2) and the distance of penetration (L) and inversely proportional to the energy per blow.

$$N_{Espt} = N_f\,(2\text{ in}/D_f)^2 \text{ x } 12\text{ in}/L_f \text{ x } W_f/140\text{ lb} \text{ x } H_f/30\text{ in} \quad (7.16)$$

$$N_{Espt} = \frac{2\,N_f W_f H_f}{175 D_o^2 L_f} \quad (7.17)$$

where N_{Espt} is the SPT – equivalent blow count, N_f is the measured blow count by other equipment, W_f is the hammer mass (lb), H_f is the Fall distance (in), Do is the outer diameter of non-standard sampler, and L_f is the driving distance (penetration) (12 in).

7.9.1 MDPT and DCP Correlation

This section describes the relationship between the MDPT blows and the DCP blows to estimate the CBR using published empirical equations. The standard ASTM D6951 DCP was used in the correlation of this study (NCDOT DCP). Due to the depth limitation of the DCP, the correlation was limited to 6 ft (1.8 m). Several sites were tested using the standard DCP and MDPT adjacent to each other to obtain better correlations.

Figure 7.19 shows the field testing results of the MDPT blows and the DCP blows. The results obtained from these sites are very promising, and it is clear that the MDPT blows are

higher than the DCP. The drop height and the mass weight for both the DCP and MDPT are almost similar, and the MDPT conical diameter (1 in) (25 mm) is slightly bigger than the DCP cone diameter, which is typically 0.787 in (20 mm). The DCP cone side is enlarged to minimize side resistance (skin) during penetration and thus the major driving resistance will be generated from the tip. On the other hand, the MDPT driving resistance will be generated from both the side and tip resistance. The higher blows of the MDPT could be due to the skin friction and size of the cone.

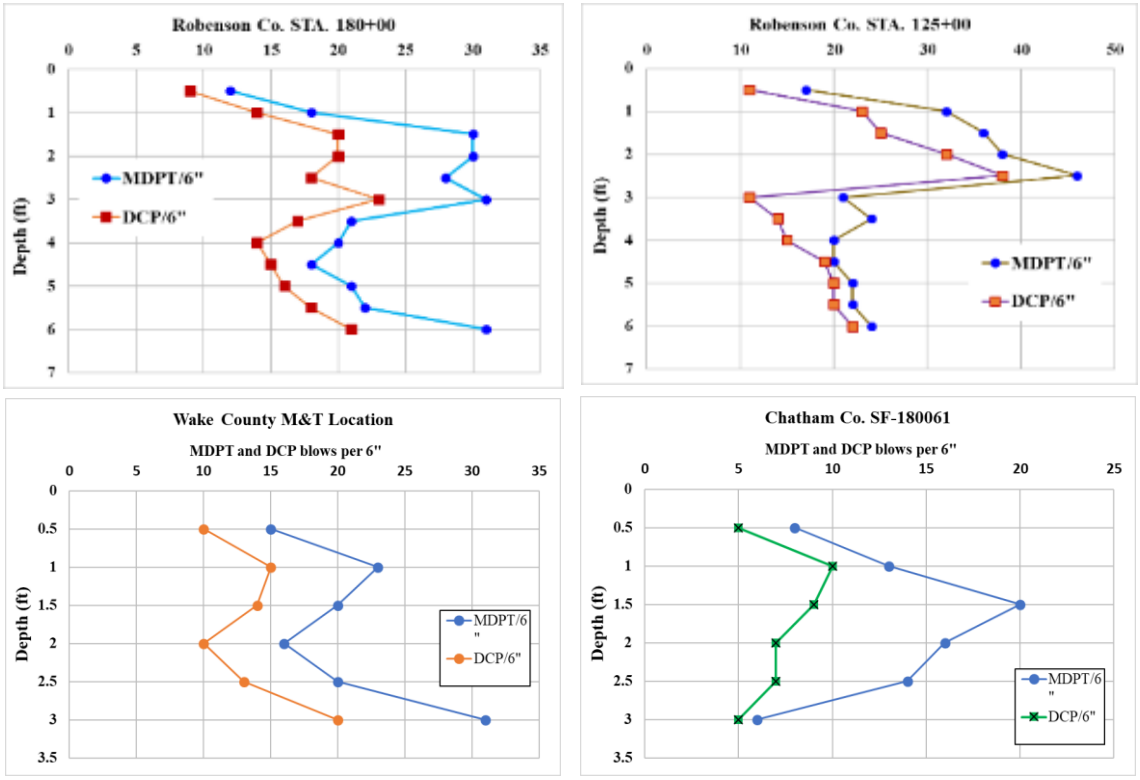

Figure 7.19 Field tests comparing the MDPT blows/6 in to DCP blows/6 in MDPT.

The regression analysis between the MDPT and DCP blows per ft indicated that MDPT has a strong correlation with the DCP blows per ft by achieving a coefficient of determination R^2 of 0.88 and MSE = 11.8, as shown in Figure 7.20.

The correlation between the MDPT-n and DCP blows per ft is shown in the following equation:

$$\text{DCP blows per ft} = 0.74*(n) - 2 \qquad (7.18)$$

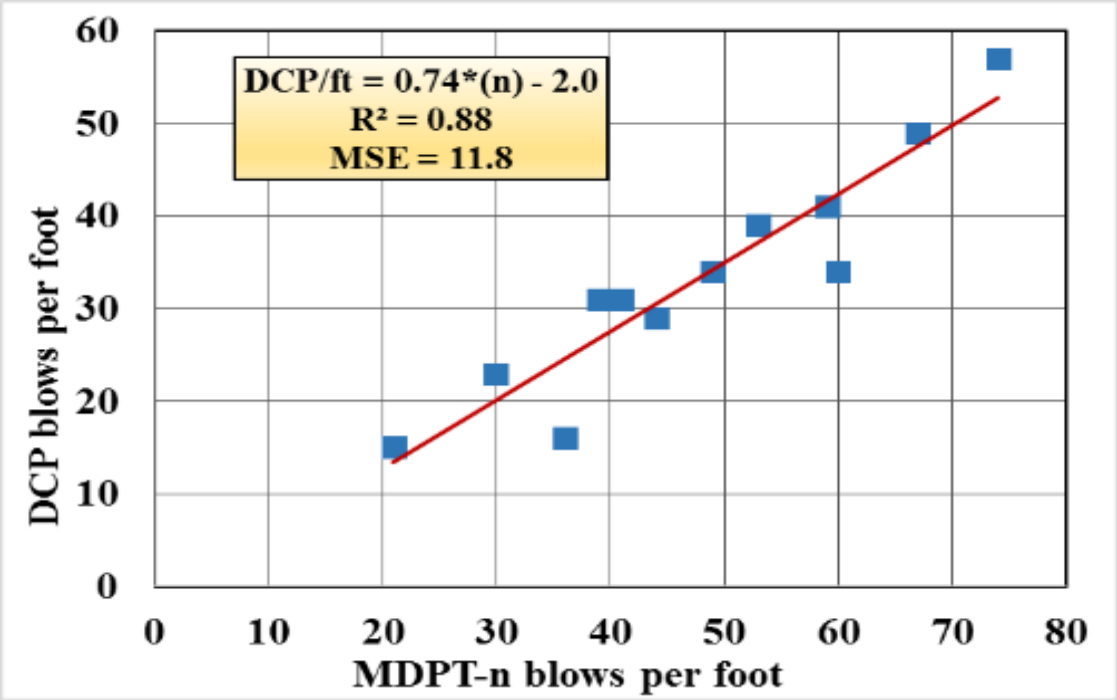

Figure 7.20 Correlation between standard DCP blows and MDPT-n blows per ft.

As described earlier in this chapter, many correlations have been developed by other researchers between the standard DCP (refer to ASTM D 6951 Section Five for Dynamic Cone Penetrometer (DCP) equipment specifications) and the CBR to estimate the bearing pressure. Therefore, Equation 7.18 should be used to estimate the DCP and then convert the blows per ft to blows per drop to use any equation that will work with similar material.

With proper calibration, the MDPT can provide results essentially equivalent to that of the nuclear density device (see Figure 7.6) or any other density test. In addition, the MDPT is small, portable, and easier and more convenient to use in many settings, is not bound by any federal regulations, and it does not expose operators to radioactive rays.

7.10 Summary and Conclusions

The dry density γ_d and water content were measured using the typical tools in the field during construction. Field and lab tests were performed to correlate the dry density to the MDPT-n, as shown in Table 7.2 and 7.3. The MDPT-n has shown promising results in predicting the dry density in the field. The MDPT test results showed a promising correlation between the MDPT-n blows per ft and the dry density, with R^2 of 0.90 and MSE=8.7 as shown in Figure 7.11.

Using the MDPT as a quick, portable, and economical test device will improve the frequency of compaction testing during construction without delaying contact time. Increasing the testing frequency is essential to the stability and safety of pavement structures and roadway embankments.

Field MDPT and DCP tests were performed at four sites in the Piedmont region of North Carolina. For each test location, soil density and moisture content were measured in-situ using a nuclear gauge at different depths and directions, as shown in Figure 7.6. The relationship between the MDPT-n and the DCP blows per ft were examined. The data analysis shows that a strong, positive trend appears to exist between the DCP and MDPT. Figure 7.20 shows a strong correlation between the MDPT-n and DCP and produced a coefficient of determination $R^2 = 0.88$, r = 0.94, and MSE =11.8.

Due to the limitation of the data and the available resources, this study did not consider soil types other than Piedmont soil. The results of the statistical analysis of the specific soil and sites between the DCP and the MDPT-n are shown in Figure 7.20. The correlation developed in this chapter will provide a useful tool for estimating the CBR while at the same time checking the compaction effort during construction instead of running two separate tests. The relationship between the dry density, DCP, and the MDPT should be used with caution because it is derived

from limited data. The MDPT and DCP are subjected to considerable uncertainty, and thus the penetration tests should be calibrated using other conventional tests to reduce the uncertainty in the predictions.

The MDPT penetration test does not require pre-auguring holes and can be driven up to 45 ft.; therefore, the MDPT performance is quicker and overcomes the penetration depth. Site-specific correlations will provide better results, improve the confidence level, and enhance the quality of the data. To refine the developed relationships in this study, further study is needed to gather adequate data to improve the model.

CHAPTER 8. CONCLUSIONS, CONTRIBUTION TO STATE OF THE ART, AND RECOMMENDATIONS FOR FUTURE WORKS

8.0 Conclusions

To reduce the need for heavy and expensive equipment, it was necessary to develop a portable, quick, efficient, and economical device such as the MDPT for investigating low-volume roads and smaller projects. This study presents the development of new portable mini dynamic penetration and torque tests (MDPT and MDPT-t) and procedures to estimate soil strength and engineering properties. Based on the work of this study, the following conclusions can be made:

- The MDPT must be calibrated for each project in order to obtain accurate results and provide field quality control.
- The calibration process can be incorporated with the subsurface investigation plan in locations where the soil engineering properties are necessary for design and construction. The calibration should include laboratory tests such as triaxial shear, unconfined compression, and consolidation tests, if needed.
- The MDPT device is not proposed as a replacement for the SPT, CPT, DCP, or vane tests, but simply as another tool that may be used in many geotechnical tasks.

8.1 MDPT-n Correlation to SPT (N) to Use the Established Correlations Between the SPT (N) and Shear Strength

- The MDPT was tested in 14 counties from the Coastal region (CR) and the Piedmont region (PR) of the state of North Carolina. Analyses of the data show a clear linear relationship between the measurements from the SPT N-value and MDPT n-value. In-situ test results from the MDPT indicate the soil properties can be estimated using the MDPT device without the use of costly drill rigs or trucks. The MDPT can also be used to

evaluate subgrade and soil-layer strength and estimate soil properties using correlations with other in-situ testing methods.

- MDPT correlations results show that the MDPT-n will produce three to five blows/ft for each one SPT (N) blow/ft. On average, MDPT-n = SPT(N)*4 or estimated SPT* (N) = 0.25*MDPT-n.
- The empirical correlations of MDPT(n) to SPT and friction angle:

  $\phi = -0.0042(N1_{60})^2 + 0.46(N1_{60}) + 25$ Low

  $\phi = -0.0041(N1_{60})^2 + 0.46(N1_{60}) + 28$ Average

  $\phi = -0.0041(N1_{60})^2 + 0.45(N1_{60}) + 30$ High

  $\phi = 0.3(90 + 0.25n)$
- Both the correlation coefficient (R) and the coefficient of determination (R^2) indicate a strong positive linear relationship between the SPT (N) values and the MDPT-n values for the Piedmont and Coastal regions.
- In general, the MDPT was found to be a reliable method for assessing soil strength, and it yields soil properties without the use of heavy drill rigs and costly equipment.
- The MDPT correlations could be improved with additional field testing data.

8.1.1 MDPT-t Torque Measurement of Unit Skin Friction and Correlation with Soil Properties

- The MDPT-t device was tested in both the Coastal and Piedmont regions of North Carolina as an economical alternative for estimating the unit skin friction, the friction angle ϕ', and the cohesion in different soil layers.

- MDPT-t can be used to determine the skin friction between steel and soil using the following equation: $fs = \frac{2\,T}{\pi d^2 L}$ (T = torque)
- The correlation between the measured torque from MDPT-t and the blow counts from the MDPT-n for both the Coastal and the Piedmont regions produced a coefficient of determination R^2 of 0.94 and 0.90 for the Piedmont and Coastal regions, respectively. Regression analysis was carried out to calculate the least squares fit for the given data points and the R^2 values were calculated to determine the accuracy of the correlations. The R^2 for soil type A-4 is 0.85, for soil type A-5 the R^2 is 0.79, and for soil type A-7-5 the R^2 is 0.99.
- The above difference for the coefficient of determination R^2 was based on the soil characteristics for each region.
- The number of the triaxial tests was limited to 17 due to construction schedules and limited access to the site; therefore, the correlation was impacted by the sample quality and lower number of tests.

8.1.2 Correlation Between the MDPT-t Measured Torque with the Effective Friction Angle ϕ' From Triaxial Tests

- The MDPT-t torque (lb-ft) was evaluated to predict the effective friction angle (ϕ') for three predominant soils: A-4, A-5, and A-7-5. The analysis showed there is a definite trend between the measured torque and the effective internal friction angle ϕ'. The regression analysis shows the correlation between ϕ' determined from the triaxial tests and the in-situ measured torque produced linear regression. The Pearson r (correlation coefficient) was 0.61 and the significance (f), or p-value, was 0.0099. Comparing the

R^2 = 0.37 and the r =0.61, it can be concluded there is a weak positive relationship between the friction angle (ϕ') and the MDPT-t values. The following equation was developed from the above regression analysis to show the relationship between the MDPT-t torque and ϕ':

ϕ' = 0.18*MDPT-t +25 $\leq$ 40º, where MDPT-t = Torque (t) (ft-lb) (8.1)

However, due to the limited number of triaxial tests, it is very difficult to generalize this relationship.

8.1.3 Correlation Between the MDPT-t Measured Torque with the Effective Cohesion From Triaxial Tests

- The linear relationship between C and MDPT-t produced R^2 = 0.35 and r =0.574. This result may be caused by the soil type, uniformity, layer thickness, and distance between these tests.
- Many researchers have suggested that the weak relationship (Lower R^2) could be due to the presence of a high percentage of fine, which impacts the penetration and the blow counts. However, the number of triaxial tests will determine the strength of the relationship between the C and the MDPT-t measured torque (i.e., the higher the test number, the stronger the relationship).
- The relationship can be shown as C = 7.4 MDPT-t + 152 (psf), where t is the torque from the MDPT-t.

8.1.4 Comparing the Empirical Correlation of the MDPT-t with Other Researchers

- The correlation of the MDPT-t unit skin friction (*fs*) with other researchers' empirical equations was promising. The author developed the following equation:

Unit skin friction *fs* (tsf) = 0.055*SPT* (N) + 0.2 with R^2 = 0.9 (8.2)

Equation 8.2 is similar to equation 5.30.

- The overall MDPT-t (*fs*) results versus SPT (N) blows per ft show a positive relationship compared with the results from other researchers.
- The variation of the relationship can be influenced by the regional soil characteristics and the distance and depths of these tests from each other.
- The MDPT-t unit skin friction was examined and compared with the unit skin friction of dynamic and static design methods, such as CAPWAP, Vesic, and APILE programs, which determined that both the unit skin friction and the results were reasonable and promising.

8.1.5 MDPT-T Torque and MDPT-n Blows Correlated to the Cone Penetration Test (CPT)

- The MDPT was correlated to limited data with CPT exploration to evaluate the relationship between the CPT and MDPT. The collected data showed a strong correlation between the estimated SPT* (N) from MDPT-n with the coefficient of determination of R^2= 0.87.
- The relationship between the MDPT and the CPT can be expressed by the equation of the equivalent CPT, q_t (MPa) = 0.25*(N) + 0.2, based on the available data. The correlation was examined with that from other researchers and the results were very promising, as shown in Figure 6.5.
- The results of the statistical analysis between the MDPT and the CPT show that a positive trend line relationship exists between the CPT *fs* and MDPT *fs*, based on the data obtained from two project sites, with the coefficient of determination R^2 of 0.66. The MDPT-t *fs* (kPa) can estimate the CPT *fs* (kPa) using the following equation:

$$\text{MDPT-t } (fs, \text{ in kPa}) = 0.64*\text{CPT } (fs) + 59 \qquad (8.3)$$

Equation 8.3 is similar to equation 6.2.

8.1.6 Mini Dynamic Penetration Test (MDPT) Verifying Soil Compaction and Bearing Pressure

- The MDPT correlation to the dry density was strong, with the coefficient of determination $R^2 = 0.91$ and developed equation $\gamma_d = -.021*(N)^2 + 2.2*(N) +78$.
- The MDPT test can be used to indirectly estimate the bearing pressure by using the developed correlation between the MDPT-n, SPT, CPT, and DCP.
- Unlike DCP penetration tests, the MDPT penetration test does not require pre-auguring holes and can be driven to twice the depths of the DCP test; the MDPT is faster and can be driven deeper than the DCP. However, it is realized that site-specific correlations will provide better results, improve the confidence level, and enhance the quality of the data.

8.2 Contribution to the State of the Art

There is a need for the development of portable devices and procedures to provide this valuable information before, during, and after construction. The development of the MDPT proves to be useful, economical, portable, and simple to use, and thus it can be an alternative to conventional methods of in-situ soil strength determination such as SPT and CPT. The MDPT provides quick and accurate in-situ verification of the bearing capacities of shallow foundations and estimation of soil properties, and it can be used without heavy drilling rigs or trucks. In addition, the development of a non-electronic, portable. manual device will greatly reduce the breakup time and malfunction.

Foundations are a critical and important part of structure construction. If the foundation material does not adequately support the design loads, excessive settlement or structure failure may occur; therefore, adequate in-situ testing is necessary for the success of the foundation

design. The design engineer must be able to check and perform in-situ testing as needed, and the MDPT will fulfill this need. Some projects have limited and difficult access to the site for investigation, and thus cutting the access road or drilling through the bridge deck will increase the time and cost of the investigation. Similarly, verifying the bearing capacity for spread footing or retaining wall foundations can also be difficult to access during construction (see Figure 7.2 on page 126). Figures 8.1 and 7.2 show good examples of the difficulty and the excessive cost of using conventional investigation equipment for small projects.

Figure 8.1 Example of low-head space required for drilling from the bridge deck (top of bridge).

The MDPT is an exceptionally promising device that can be used for many geotechnical tasks. It gives a continuous evaluation of the soil layers, unlike the SPT test, which provides soil evaluations every 5 ft (1.5 m) and risks missing valuable information about the soil characteristics by skipping 5-ft (1.5-m) increments.

The MDPT device can be operated by one person and used for many tasks, such as:

- Estimating the rock or refusal elevation without mobilizing the drill rig and three crew members at a cost of $3,500/day compared with $500/day for the MDPT.
- Estimating the pile embedment for unknown foundation bridges.
- Estimating the unit skin friction to assist the design engineer with pile foundation design.
- Evaluating the California Bearing Ratio blow counts versus depth for pavement design.
- Evaluating or verifying the bore holes completed by SPT more quickly and economically.
- Improving safety when using smaller equipment.
- Using the developed relationships between the MDPT test results and other commonly used foundation parameters.

Table 8.1 Comparison Between the MDPT Device and Other In-situ Test Equipment.

Task	MDPT	SPT	CPT	DCP
Daily Rate (Cost)	$500	$3,500	$5,000	$1,000
Equipment Cost	$1,000	>100,000	>100,000	$2,500
Dynamic Test	Yes	Yes	No	Yes
Static Test	No	No	Yes	No
Soil Type	S, C, L	S	S, C, L	S, C, L
Estimate Soil Stiffness	Yes	Yes	Yes	No
Skin Resistance	Yes	Yes	Yes	No
Tip Resistance	Yes	Yes	Yes	Yes
Portable and Economical	Yes	No	No	Yes
Depth of Investigation **>20'**	Yes (up to 13.7 m)	Yes	Yes	No (limit to 2 m)

Table 8.1 illustrates the comparison between the MDPT device and other in-situ equipment. It also shows that the MDPT device can provide valuable in-situ information quickly and economically.

8.3 Recommendations for Future Works

1. Improve and validate the correlation between the MDPT torque unit skin frictions and shear strength (triaxial tests) for the Piedmont, Coastal, and Mountain regions in North Carolina by testing more sites and creating a larger database to provide useful and valuable correlations.
2. Develop a robust data acquisition system that can count the blow counts and indicate the penetration depths that can handle the shock wave (hammer impact).
3. Evaluate the effect of overburden on the MDPT blow counts.
4. Improve the correlation between the MDPT and CPT by using more data.
5. Improve the relationship between the MDPT blow counts, dry density, and moisture content to improve compaction in other regional areas.
6. Conduct further testing to develop a standardized test procedure for use of the MDPT, and then develop an ASTM standardization of the MDPT-t torque and the soil test shear strength.
7. Improve laboratory and field-testing processes to compare reliable data.
8. Develop MDPT-t torque versus time correlations for different soil types.

REFERENCES

Abu-Farsakh, M. Y., K. Alshibli, M. Nazzal, and E. Seyman, (2004). Assessment of In-Situ Test Technology for Construction Control of Base Courses and Embankments, Technical Report, Louisiana Transportation Research Center, Baton Rouge, LA 70808, FHWA/LA.04/385.

Abu-Farsakh, Murad Y., Munir D. Nazzal, Khalid Alshibli and Ekram Seyman, (2005). "Application of Dynamic Cone Penetrometer in Pavement Construction Control", Transportation Research Record, 1913, TRB, National Research Council, Washington, D.C., pp. 52–61.

AASHTO - LRFD Bridge Design Specification, seventh edition, 2014 article 10.

AASHTO, "Manual on Subsurface Investigations," 1988 ASCE, "Use of In-Situ Tests in Geotechnical Engineering," ASCE Special Technical Publication No. 6, 1986.

Akca, N. "Correlation of SPT-CPT data from the United Arab Emirates." Engineering Geology, volume 67, 2003: 219-231.

ASTM D3689 "Standard Test Method for Individual Piles under Static Axial Tensile Load", 1995. 6.

ASTM D422, "Standard Test Method for Particle Size-Analysis of Soils", 2000.

ASTM D4253, "Standard Test Method for Maximum Index Density and Unit Weight of Soils Using a Vibratory Table", 2000.

ASTM D4254, "Standard Test Method for Minimum Index Density and Unit Weight of Soils and Calculation of Relative Density", 2000.

ASTM D854, Standard test method for specific gravity of soil solids by water pycnometer", 2005.

ASTM. (1996) "Standard practice for determining the normalized penetration resistance of sands for evaluation of liquefaction potential."

ASTM. (2000). "Standard practice for classification of soils for engineering purposes ~Unified Soil Classification System." ASTM-D 2487-00, West Conshohocken, PA.

ASTM-D 6066-96, West Conshohocken, Pa. ASTM. (1999). "Standard test method for penetration test and split-barrel sampling of soils." ASTM-D 1586-99, West Conshohocken, PA.

Ayers, M. E. (1990). "Rapid Shear Strength of In-situ Granular Materials Utilizing the Dynamic Cone Penetrometer." Ph.D. Dissertation, University of Illinois, Urbana, IL, 1990.

Bowles, J. E., (1977). Foundation Analysis and Design, McGraw-Hill, Inc., New York.

Bowles, J. E., (1979). Physical and Geotechnical Properties of Soils, McGraw-Hill, Inc.

Bratt, T., J. Twardowski, and R. Wahab (1995). "Dynamic Cone Penetrometer Application for Embankment/Subgrade Inspection." Proceedings, International Symposium on Cone Penetration Testing – CPT'95, Linkoping, Sweden, pp 421–427.

Briaud, J. L. (1992). The pressuremeter. London, UK: Taylor & Francis.

Browning, John Adam (2006), Cone Tip Apex Angle Effects on Cone Penetration Testing. North Carolina State University.

Bullock, P. J., Schmertmann, J. H., (2003). "Determining the effect of stage testing on the dimensionless pile side shear setup factor." Research Report BC354, RPWO#27, Florida Department of Transportation.

Chandler R. J. (1968). The shaft friction of piles in cohesive soils in terms of effective stress. Civ Eng Public Works Rev 60(708):48–51.

Chin, Chung-Tien, Shaw-Wei Duann, and Tsung-Chung Kao (1998). "SPT-CPT correlations for granular soils." 1st Int'l Symposium on Penetration Testing, 1988: Vol. 1 pp. 335–339. Edinburgh Gate, Harlow.England: Pearson Education Limited, 2011. Danziger, F. A. B., C. F. Politano, and B. R. Danziger. "CPT-SPT correlations for some Brazilian residual soils." Geotechnical site characterization: Proceedings of the First International Conference on Site Characterization - ISC'98. Atlanta, Georgia.

Clayton, C. R. I. 1995. The Standard Penetration Test (SPT): Methods and use. Report 143. UK: Construction Industry Research and Information Association.

Coduto, D. P. (2001). Foundation Design: Principles and Practices. Upper Saddle River: Prentice Hall. [22] Courtesy of Google Maps, 2013.

Coonse, J. (1999). Estimating California Bearing Ratio of Cohesive Piedmont Residual Soil Using the Scala Dynamic Cone Penetrometer, Master's Thesis (MSCE), North Carolina State University, Raleigh, N.C.

Cottingham, Marcus Allen. In situ determination of residual soil shear strength parameters using the standard penetration test with torque. Diss. The University of North Carolina at Charlotte, 2010.

Coyle, H. M., and Castello, R. R. (1981). "New Design Correlations for Piles in Sand." Journal of the Geotechnical Engineering Division, ASCE, Vol. 107, No. GT17. July pp. 965–986.

Danziger, F. A. B., C. F. Politano, and B. R. Danziger (1998). "CPT-SPT correlations for some Brazilian residual soils." Geotechnical site characterization: Proceedings of the First International Conference on Site Characterization - ISC'98. Atlanta, Georgia.

Decourt, L. (1992). SPT in non classical materials - U.S. - Brazil Geotechnical Workshop on "Applicability of classical soil mechanics principles to structured soils", Belo Horizonte.

Decourt, L., and Filho, A. R. Q. (1994). "Practical applications of the standard penetration test complemented by torque measurements, SPT-T; present stage and future trends." Proc., 13th Int. Conf. on Soil Mechanics and Foundation Engineering, Balkema, Rotterdam, The Netherlands, 1, 143–146.

Decourt, L. (1998). A more rational utilization of some old in situ tests. Proc. Geotechnical Site Characterization. Balkema. Atlanta. USA, 913-918.

Decourt, L (1999). Behavior of foundations under working load conditions. In: Proceedings of the 11th Pan-American conference on soil mechanics and geotechnical engineering, Foz DoIguassu, Brazil, 4, pp. 453–488.

Department of the Navy, "Soils Mechanics Design Manual 7.1," NAVFAC DM-7.1, Naval Facilities Engineering Command, (1986).

Douglas, B. J. and Olsen, R. S. (1981). "Soil classification using electric cone penetrometer," Symposium on Cone Penetration Testing and Experience. Proceedings of the ASCE National Convention, St. Louis, 209–227.

FHWA, "Cone Penetrometer Test," FHWA- SA-91-043, 1991.

FHWA, "Soils and Foundations Workshop Reference Manual," NHI Course No. 132012, FHWA NHI-00-045, August 2000.

FHWA, "Subsurface Investigations –Geotechnical Site Characterization," Reference Manual for NHI Course No. 132031, FHWA-NHI-01-031, 2002.

Gabr M. A., Coonse, J., and Lambe, P. C. (2001). "A Potential Model for Compaction Evaluation of Piedmont Soils using Dynamic Cone Penetrometer (DCP)", ASTM Geotechnical Testing Journal, Vol. 24, Issue 3, 2001, pp. 308-313.

GAWITH, A. H. and Perrin, C. C. 1962. Developments in the design and construction of bituminous pavements in the State of Victoria, Australia. Proc 1st Int Conf Structural Design of Asphalt pavements, Ann Arbor, Michigan, 1962.

Hancher, D. E., Goodrum, P. M., & Thozhal, J. J. (2003). Constructability Issues on KyTC Projects. Lexington, Kentucky Transportation Center.

Hassan, A. B. (1996). "The Effects of Material Parameters on Dynamic Cone Penetrometer Results for fine-grained soils and granular materials", Ph.D. dissertation, Oklahoma State University, 1996, 134 pages.

Holtz, Robert D., and William D. Kovacs. An Inroduction to geotechnical Engineering. Englewood, New Jersey: Prentice-Hall, Inc., 1981.

Jamnongpopatkul, P., Kiatkajornkul, C., and Vasinvarthana, V. (1987). "Some practical interpretations of cone penetration tests for Bangkok subsoils." 9th Southeast Asian Geotechnical Conf., Southeast Asian Geotechnical Society, Asian Institute of Technology, Engineering Institute of Thailand, Bangkok, Thailand, 3, 83–92.

Jardine, R., Chow, F., Overy, R., and Standing, J. (2005). ICP design methods for driven piles in sands and clays, Thomas Telford, London.

Kasim, A. G., Chu Ming-Yau, and J. N. Curtis. "Field Correlation of Cone and Standard Penetration Tests." ASCE Journal of Geotechnical Engineering, 1986: 368–372.

Kelley, S. P., and Lutenegger, A. J. (1999). "Enhanced site characterization in residual soils using the SPT-T and drive cone tests." Behavioral characteristics of residual soils, B. Edelen, ed., Geotechnical Special Publication No. 92, ASCE, New York, 88–100.

Kessler Soils Engineering Products. 2010. K-100 Models with quick user's manual. Kessler Soils Engineering products, VA.

Kishida, H., and Uesugi, M. (1987). "Tests Of The Interface Between Sand And Steel In The Simple Shear Apparatus." Geotechnique, 37(1), 45–52.

Kleyn, E. G. (1975), the Use of the Dynamic Cone Penetrometer (DCP), Transvaal Roads Department, Report No. L2/74, Pretoria. 90.

Kovacs, William D., Lawrence A. Salomone, and Felix Y. Yokel. Energy measurement in the standard penetration test. U.S. Dept. of Commerce, National Bureau of Standards (Washington, D.C.), 1981. Kulhawy, F. H., and P. W. Mayne. Manual on Estimating Soil Properties for Foundation Design. Palo Alto, California: Electric Power Research Institute, 1990.

Kruizinga, J. (1982). "SPT-CPT correlations." Proc., 2nd European Symp. on Penetration Testing, Balkema, Rotterdam, The Netherlands, 1, 91–94.

Kulhawy, F. H., and P. W. Mayne. 1990. Manual on Estimating Soil Properties for Foundation Design, Report EL 6800, 360 pp. Palo Alto: Electric Power Research Inst.

Littlechild, B., Plumbridge, G., Hill, S., and Pratt, M. (2000). "Innovation in South East Asia." DFI2000NYC—A Global Perspective on Urban Deep Foundations, 25th Annual Meeting

and 8th Int. Conf. and Exhibition, R. E. Sandiford, ed., Deep Foundations Institute, Englewood Cliffs, N.J., 115–125.

Livneh, M. (1987). "The Use of Dynamic Cone Penetrometer in Determining the Strength of Existing Pavements and Subgrades". Proc., 9th Southeast Asian Geotechnical Conference, Bangkok.

Livneh, M. (2000). "Friction Correction Equation for the Dynamic Cone Penetrometer in Subsoil Strength Testing", Transportation Research Record 1714, TRB, National Research Council, Washington, D.C., pp. 89–97.

Lunne, T., and K. H. Andersen (2007). "Soft clay shear strength parameters for deepwater geotechnical design." Proceedings 6th International Conference, Society for Underwater Technology. London: Offshore Site Investigation and Geotechnics, 2007. 151–176.

Lunne, T., Robertson, P. K., and Powell, J. J. M. (1997). *Cone Penetration Testing in Geotechnical Practice*, Blackie Academic and Professional, Chapman and Hall, London, 312 p.

Lutenegger, A. J., and Kelley, S. P. (1998). "Standard penetration tests with torque measurement." Proc. 1st Int. Conf. on Site Characterization—Geotechnical Site characterization, Robertson P. and Mayne P., eds., Balkema, Rotterdam, The Netherlands, 2, 939–945.

Lutenegger, A. J. and Kempker, J. H., April 2009. History Repeats, Screw Piles Come of Age – Again, Structural Engineer Magazine.

Lutenegger, A. J., and Kelley, S. P. (2001). "Estimating pile skin friction in clay and sand using SPT-torque tests." In-situ 2001 Int. Conf. on In-situ Measurement of Soil Properties and Case Histories, P. P. Rahardjo and T. Lunne, eds., Graduate Program, Parahyangan Catholic Univ., Bandung, Indonesia, 495–499.

Mair, R. J. and Wood, D. M. 1987. Pressuremeter testing method and interpretation, Construction Industry Research and Information Association Project 335. Publ. Butterworths, London. ISBN 0-408-02434-8.

Maksoud, M. A. F. (2006). "Laboratory determining of soil strength parameters in calcareous soils and their effect on chiseling draft prediction." Balkin Agricultural Engineering Review, 9, 1–13.

Mayne, P. W., Niazi, F. S., Woeller, D. J. (2010). Drilled shaft response in Piedmont residuum using elastic continuum analysis and seismic piezocone tests. In: Proceedings of Geo-Shanghai 2010 deep foundations and geotechnical ln-situ testing (GSP 205). ASCE, Reston, Virginia, pp 200–205.

Meigh, A.C., and I. K. Nixon (1961). "Comparison of in-situ tests of granular soils." Proceedings of 5th international Conference on Soil Mechanics and Foundation Engineering. Paris.

Meyerhof, G. G. (1956). "Penetration tests and the bearing capacity of cohesionless soils." J. Soil Mech. Found. Div., 82-1, Paper 866, 1–19.

Meyerhof, G. G. (1976). Bearing capacity and settlement of pile foundations. J Geotech Eng Div 102:195–228.

Niazi, Fawad S., and Paul W. Mayne. "Evaluation of EURIPIDES pile load tests response from CPT data." International Journal of Geoengineering Case Histories 1.4 (2010): 367–386.

Lutenegger, Alan J. "Estimating driven pile side resistance from SPT-torque tests." Contemporary Topics in In-situ Testing, Analysis, and Reliability of Foundations. 2009. 9–17.

Ohya, S., T. Imai, and M. Matsubara 1982. Relationships between N value by SPT and LLT pressuremeter results. In Proceedings of 2nd European symposium on penetration testing Vol. 1, 125–130. Amsterdam.

Packard, R.G. 1973. Design of Concrete Airport Pavements. Portland Cement Association.

Paige-Green, P. and Du Plessis, L. 2009. The use and interpretation of the dynamic cone penetrometer (DCP) test. CSIR Build Environment, Pretoria.

Parker, F., M. Hammons, and J. Hall (1998). "Development of an Automated Dynamic Cone Penetrometer for Evaluating Soils and Pavement Materials", Final Report, Project No. FLDOT-ADCP-WPI #0510751, Florida Department of Transportation, Gainesville, Florida.

Peck, R. B., Hanson, W. E. and Thornburn, T. H., (1974). Foundation Engineering, 2nd Edition, John Wiley & Sons, New York. Ayers, M. E., M. R. Thompson, and D. R. Uzarski (1989)." Rapid Shear Strength Evaluation of In-Situ Granular Materials", In Transportation Research Record 1227, TRB, National Research Council, Washington, D.C., 1989, pp. 134–146.

Peixoto, A. S. P., and Carvalho, D. (1999). ''Standard penetration test with torque measurements SPT-T! and some factors that affect T/N ratio.'' 9th Panamerican Conf. on Soil Mechanics and Geotechnical Engineering, Associaca˜o Brasileira de Mecaˆnica dos Solos e Engenharia Geote´cnica ~ABMS!, Sociedad Argentina de Meca´nica de Suelos ~SAMS!, Sociedad Paraguaya de Geotecnı´a ~SPG!, Foz do Iguassu, Brazil, 1605–1612.

Peixoto, A. S. P., de Albuquerque, P. J. R., and Carvalho, D. (2000). "Utilization of SPT-T, CPT and DMT tests to predict the ultimate bearing capacity of precast concrete pile in Brazilian unsaturated residual soil." Advances in unsaturated geotechnics, C. D.

Shackelford, S. L. Houston, and N. Y. Chang, eds., Geotechnical Special Publication No. 99, ASCE, New York, 32–39.

Phoon, K. K., Kulhawy, F. H., Grigoriu, M. D., 1995, "Reliability-Based Design of Foundations for Transmission Line Structures," Report TR-105000, Electric Power Research Institute, Palo Alto, CA.

Phoon, K. K., and Kulhawy F. H. 1999b. Evaluation of geotechnical property variability. Canadian Geotechnical Journal 36(4): 625–639.

Piovan, T. T. C. & Peixoto, A. S. P. Influence of Angular Thrust in the Measurement of Torque in the SPT-T. Proc. 15th Pan-American Conference on Soil Mechanics and Geotechnical Engineering (XV PCSMGE) Buenos Aires. From Fundamentals to Applications in Geotecnics. Amsterdan: IOS Press BV, 2015. 1: 430-437.

Poulos, H. G. (1989). "Pile behavior: Theory and application." Geotechnique, 39~3, 365–415.

Price G, Wardle IF (1982). A comparison between cone penetration test results and the performance of small diameter instrumented piles in stiff clay. In: Proceedings of the 2nd European symposium on penetration testing, Amsterdam, 2, pp 775–780.

Puppala, A. J. (2008). "Estimating Stiffness of Subgrade and Unbound Materials for Pavement Design", NCHRP Synthesis 382, Transportation Research Board, 139 pp., ISBN 978-0-309-09811-3.

Rahim, A. M., and K. P. George (2002). "Automated Dynamic Cone Penetrometer for Subgrade Resilient Modulus Characterization", Transportation Research Record, Transportation Research Board of the National Academies, ISSN 0361-1981, Volume 1806, pp. 70–77.

Randolph, M. F., Dolwin, J., and Beck, R. (1994). "Design of driven piles in sand." Geotechnique, 44(3), 427–448.

Ranzini, S. M. (1988). T. SPT-F. Solos e Rochas, v. 11, n. único, p. 29-30.

Reuter GR (2010). Pile capacity prediction in Minnesota soils using direct CPT and CPTu methods. In: Proceedings of the 2nd international symposium on cone penetration testing (CPT'10). Huntington Beach, CA, Omni press.

Robertson, P. K., and (Robertson) K. L. Cabal (2010). Guide to Cone Penetration Testing for Geotechnical Engineering, 4th edition. Signal Hill, California: Gregg Drilling & Testing, Inc., 2010. Robertson, P. K., and R. G. Campanella. "Interpretation of Cone Penetration Tests: Part I: Sand." Canadian Geotechnical Journal, Vol. 20, No. 4, 1983: 718–733.

Robertson, P. K., and R. G. Campanella (1986). Guidelines for Use and Interpretation of the Electrical Cone Penetration Test, 3rd ed. Gaithersburg, MD: Hogentogller & Co.

Robertson, P. K., Campanella, R. G., and Wightman, A., (1983). "SPT-CPT Correlations", ASCE Journal of Geotechnical Engineering, Vol. 109, No. 11, pp. 1449–1459.

Robertson, P. K., Campenalla, R.G., Gillespie, D. and Grieg, J. (1986). "Use of piezometer cone data", Proceedings of the ASCE Specialty Conference In Situ 86: Use of In-situ Tests in Geotechnical Engineering, Blacksburg, VA. pp. 1263–80.

Roy, B. (2007). New Look at DCP Test with a Link to AASHTO SN Concept. Journal of transportation engineering, 264–274.

Sabatini, P. J., Bachus, R. C., Mayne, P. W., Schneider, T. E., Zettler, T. E. (2002), FHWAIF-02-034, 2002, Evaluation of soil and rock properties, Geotechnical Engineering Circular No. 5.

Salgado, R. (2006). The role of analysis in non-displacement pile design. Mod Trends Geomech, In: Springer proceedings in physics, 106, pp 521–540.

Salgado, R., & Yoon, S. (2003). Dynamic cone penetration test (DCPT) for subgrade assessment. Joint Transportation Research Program.

Sampson, L. R. (1984). "Investigation of the Correlation between CBR and DCP", National Institute for Transport and Road Research, CSIR, Pretoria, South Africa, Technical Note TS/33/84, December 1984.

Sanglerat, G., The Penetrometer and Soil Exploration, Elsevier Publishing Company, New York, N.Y., 1972.

Sargand, S., Issam, K., Jayson, G., & Anwer, A.-J. (2014). Incorporating Chemical Stabilization of the Subgrade in Pavement Design and Construction Practices. 2014: Ohio Department of Transportation (ODOT).

Scala, A. J. (1956). "Simple method of flexible pavement design using cone penetrometers", Proceedings of the 2nd Australian and New Zealand Conference on Soil Mechanics and Foundation Engineering, pp. 73–83.

Schmertmann, J. (1979). "Statics of SPT." J. Geotech. Eng. Div., Am. Soc. Civ. Eng., 105~5, 655–670.

Schmertmann, J. H. (1978). Guidelines for cone penetration test, performance and design. U.S. Department of Transportation, Washington, DC, Report No. FHWA-TS-78-209, 145 p.

Schmertmann, J. H. (1978). "Use the SPT to Measure Dynamic Soil Properties Dynamic Geotechnical Testing," ASTM STP 654, American Society for Testing and Materials, 341–355.

Schmertmann, J. H. (1970). "Static cone to compute static settlement over sand", In ASCE, Journal of the Soil Mechanics and Foundations Division. 1011-1035,Vol. 96, No. SM3.

Schmertmann, J. H. (1967). Guidelines for use in the Soils Investigation and Design of Foundations for Bridge Structures in the State of Florida, Florida Department of .Transportation, Research Report 121-A.

Siekmeier, J. A., Young, D., and Beberg, D. (1999). Comparison of the Dynamic Cone Penetrometer with Other Tests During Subgrade and Granular Base Characterization in Minnesota,î Nondestructive Testing of Pavements and Backcalculation of Moduli: Third Volume. ASTM 1375, S. D. Tayabji and E. O. Lukanen, Eds., American Society for Testing Materials, West Conshohocken, PA.

Siekmeier J., Young D. and Beberg D., 2000, "Comparison of the Dynamic Cone Penetrometer with other tests During Subgrade and Granular Base Characterization in Minnesota," Nondestructive Testing of Pavements and Backcalculation of Moduli: 3rd Volume, ASTM SPT 1375., S. D. Tayabji and E. O. Lukanen, Eds.

Sharma, M S Ravi, and K Ilamparuthi. "Offshore In-situ Test using Electric Piezo Cone and its Correlation with Standard Penetration Test." Journal of the Institution of Engineers (India). Civil Engineering Division, 2005: 62–66.

Soni, P. and Salokhe, V. (2006). "Theoretical Analysis of Microscopic Forces at the Soil-tool interfaces: A Review." Agricultural Engineering International: the CIGR Ejournal. Manuscript PM 06 010, 7, 1–25.

Sowers, G. and Hedges, C. (1966). "Dynamic Cone for Shallow In-Situ Penetration Testing". Vane Shear and Cone Penetration Resistance Testing of In-Situ Soils, ASTM STP 399, American Society of Testing and Materials, p. 29–35.

Subba Rao, K. S., Allam, M. M., and Robinson, R. G. (2002). "An apparatus for evaluating adhesion between soils and solid surfaces." Journal of Testing and Evaluation, 20(1), 27–36.

Technical Report, Louisiana Transportation Research Center, Baton Rouge, LA 70808, FHWA/LA.04/385.

Terzaghi, K., and Peck, R. B. (1948). Soil Mechanics in Engineering Practice, John Wiley and Sons, New York.

Tsubakihara, Y., Kishida, H., and Nishiyama, T. (1993). "Friction between cohesive soils and steel." Soils and Foundations, 33(2), 145–156.

Ting, Chien. Prediction of Shear Strength as a Function of Matric Suction for North Carolina Residual Soils. 2016.

Vesic, A. S. (1977). "Design of Pile Foundations, Synthesis of Highway Practice" 42, Res. Bd., Washington D.C.

Vesic, A. S. (1970). Tests on Instrumentation Piles, Ogeechee River Site SMFD, ASCE, 96 (SM2 March 1970.

Vesic, A. S. (1964) Investigations of bearing capacity of piles in sand. In: Proceedings of the conference on deep foundations, Mexico City 1, 197 p.

Wang, Y., and T. D. O'Rourke. 2007. Interpretation of secant shear modulus degradation characteristics from pressuremeter tests. Journal of Geotechnical and Geoenvironmental Engineering 133(12): 1556–1566.

Webster, S. L., Grau, R. H., and Williams, T. P. (1992). Description and Application of Dual Mass Dynamic Cone Penetrometer, Final Report, Department of Army, Waterways Experiment Station, Vicksburg, MS.

Winter, C. J., Wagner, A. B., and Kormurka, V. E. (2005). "Investigation of Standard Penetration Torque Testing (SPT-T) to Predict Pile Performance." Submitted to the Wisconsin Department of Transportation. Wisconsin Highway Research Program #009204-09.

Woodward R. J., Lundgren R., Boitano J. D. (1961). Pile loading tests in stiff clays. In: Proceedings of the 6th international conference on soil mechanics and foundation engineering, Paris, pp. 177–184.

Wu, S., Sargand (2007). Ohio Research Institute for Transportation and the Environment. Athens, OH. "Use of Dynamic Cone Penetrometer in Subgrade and Base Acceptance." Ohio Department of Transportation. Columbus, OH.

Yin, H. M., Luo, Z. R. (2009). Investigation of the nuclear gauge density calibration method, Road Materials and Pavement Design, 10, 625–645.